RELIABILITY ANALYSIS OF PILE DESIGNS FROM EUROCODE 7

Master Thesis

Student: M. Hehenkamp

Chair: A.P. van den Eijnden

1st Supervisor: T. Schweckendiek

2nd Supervisor: R.C. Lanzafame

TU Delft - Deltares

June 2022

ABSTRACT

Risk-based and probabilistic reliability design methods are starting to be integrated into the daily geotechnical engineering practice, as shown by the current draft of EN1997 (Eurocode 7), which explicitly allows Reliability-based verification of limit states. The semi-probabilistic design methods in EN1997 are a compromise between ease of use and accuracy of the achieved reliability levels. In contrast, EN1990 (Eurocode 0) requires accurate full probabilistic design targets. An assessment to investigate if the semi-probabilistic methods from EN1997 comply with the EN1990 reliability targets is therefore necessary since the link between the norms is not explicitly established.

In this study, pile foundations serve as an example to assess compatibility between the EN1990 and EN1997. The deterministic Dutch pile design approach by van Mierlo & Koppejan (1956), a CPT-based design method, is adapted to the semi-probabilistic model pile recipe in the EN1997 draft. This thesis assesses what reliability levels are achieved by the model pile design method in draft EN1997 considering the axial bearing capacity and how these compare to the reliability targets in EN1990.

Methodology: To assess the performance of the model pile method from EN1997, the design outcome from the semi-probabilistic model pile method is compared to fully probabilistic quantification methods of the resistances and loads. Two probabilistic quantifications are used in the assessment, a Bayesian and a Student-T model. The achieved reliabilities are assessed with both the First Order Reliability Method (FORM) and Monte Carlo Simulation (MCS). Additional insight into the influence of different parameters is provided with sensitivity analysis and the calibration of partial factors. The assessment was applied in two case studies located in the Netherlands.

In both case studies, the EN1997 designs resulted in reliability levels in good agreement with the reliability targets stated in EN 1990. This suggests an agreement between the semi-probabilistic and the full probabilistic models if sufficient CPTs are used. In both case studies, EN1997 designs accounted for more model uncertainty than the probabilistic models suggest, thus partial model factor (γ_{Rd}) in EN1997 may be conservative. EN1997 covers spatial variability and uncertainty due to limited observations with the correlation factor (ζ), a factor that transforms calculated to representative values, and the partial resistance factor (γ_{Rc}). The coverage of uncertainty with these two factors seems to be rather low, especially for situations with few CPTs available (less than 10), although the results seem to depend strongly on the degree of spatial variability in the CPT field. In the case of homogeneous soil conditions between observations, EN1997 design methods led to over-conservative designs for low numbers of observations. If the variability between limited observations (less than 10 CPTs) was high, designs are assessed to be less reliable than EN1990 requires.

Overall, the results suggest good agreement of the semi-probabilistic design methods from EN1997 with the reliability targets defined in EN1990, for designs based on sufficient observations. The sensitivity analysis and isolation of the resistance uncertainty showed for the two cases that the uncertainty of the resistance has the dominating influence on the reliability of the piles, suggesting a low impact of complex stochastic load models. The latter finding suggests that probabilistic treatment of the resistance may be sufficient for assessing pile reliability in practice, while design values could be used for the loads. Furthermore, the case studies showed that if limited (less than 10) observations (CPTs) are available, informative priors in a Bayesian updating model can still lead

to robust results for assessing and potentially designing pile foundations.

TABLE OF CONTENTS

1. INTRODUCTION

1.1 PROBLEM DEFINITION

Over the last century, Geotechnical engineering was a necessity for the construction and maintenance of build structures all around the world. The discipline closely tied to structural engineering shows a rich history of theories and practices trying to integrate the latest knowledge and theories of soil and rock behaviour into the analysis and design of geotechnical structures. (Das & Sobhan, 2016),

While the theoretical basis of soil mechanics and geotechnical engineering remains fundamentally the same as developed in the early to mid-20th century, for example, Taylor (1948) and Terzaghi (1925), the geotechnical engineering practice is still evolving with changes in design philosophy and methods. These changes in current design practices are introduced into the “daily engineering practice” via national and international norms, that require certain safety standards and methods to be fulfilled when designing geotechnical structures.

While in Europe the national norms still exist and are authoritative for most countries, the European Union standardized a baseline of design requirements and practices in the structural Eurocodes (EN 1990 – 1997). These norms define the minimum standard of structural engineering practice within the European Union (Joint Research Center, 2022).

A fundamental shift within the safety philosophy in engineering practice was the emergence of reliability theory applied to structural design, first developed within the discipline of aerospace engineering which was dominated by the idea of redundancy. Historically the safety of structures was described with the help of an equilibrium state of forces and resistance, the safety was therefore expressed in a deterministic and binary manner, thus safe or not safe (Muller & Albertini, 2015). The probabilistic design philosophy in turn is centred around limit state design. Within the limit state function, the properties of the asset are described with statistical models which leads to a final design result that is expressed as a probability of failure and reliability index or level (Rheinfurth & Howell, 1998). The reliability level expresses the uncertainty assigned to the used models and parameters (Watson, 1994). This philosophy was introduced into the structural engineering practice in recent decades and was integrated into EN1990, where the safety target for structural design is defined in terms of reliability, based on the properties of the asset (CEN, 2019).

In geotechnical engineering, the classic perspective of equilibrium states between load and resistance dominates the design practices today, while the safety requirements in the baseline for structural design (EN1990) are defined with target reliability. To maintain the current design practice, based on equilibrium states, EN1997 compromises by using the historically established design formulations and introduces partial factors to account for uncertainty in the design method or parameter descriptions. This hybrid method is defined as the semi-probabilistic design approach and tries to optimize between usability and accuracy of the methods proposed in the Eurocode (Marekk & Kvedaras, 2012). The recommended partial factors in EN1997 used to integrate the statistical element into the design of geotechnical structures should be calibrated and evaluated based on historical empirical observations and tests to achieve the target reliability level defined by EN1990 (Köhler, Sørensen, & Baravalle, 2019).

This creates tension between the underlying safety philosophy and the historically grown practice in the field of geotechnical engineering, which finds its expression in the lack of transparency and differences in design outcomes and safety evaluations as shown in studies by Queiroz (2016) and Masih et al. (2008).

The West of the Netherlands is characterized by soil deposits of the northern sea. Therefore, the soil profile for construction is characterized by soft soil layers such as clay and peat. These soft layers are interrupted by sand depositions, which offer sufficient bearing capacity for the construction of modern structures. This led the Dutch builders to use pile foundations to provide additional bearing capacity. (TNO, 2022) This importance of pile foundations led to historically grown design approaches such as van Mierlo & Koppejan (1952), which use Cone Penetration Tests (CPTs) to characterize the soil conditions.

This opens the question of the model pile method from EN1997 based on the approach by Mierlo & Koppejan (1952), which is derived historically from engineering experience, is complying with the probabilistic safety standards from EN1990.

1.2 RESEARCH AIMS AND QUESTION

The recommendations of the partial and correction factors from EN1997 are based on observations, while the reliability levels defined in Eurocode 1990 are rooted in the idea of risk design. This results in an adaptation of historically grown design approaches to account for newly defined design goals. From the following question rise:

What reliability levels are achieved by the model pile design method in draft EN 1997, and how do these compare to the reliability targets in EN 1990?

To answer the main research question, three sub-questions are formulated to investigate a certain aspect of the

1. *How does the EN1997 model pile design recipe account for spatial variability and uncertainty due to limited information in the parameter estimation and how does this compare to fully probabilistic methods?*

2. *How does the EN1997 model pile design recipe cover the model uncertainty in the design process and how does this compare to fully probabilistic methods?*

3. *What is the difference between assessed reliability in the fully probabilistic and the semi probabilistic uncertainty quantification?*

After all, sub-questions are answered, a conclusive statement about the main question can be drawn.

1.3 SCOPE OF THE THESIS

To answer the questions, the focus of this thesis is to investigate the axial resistance of the bearing capacity of a group of foundation piles. This structure offers a unique insight into the design processes of EN1997. The model pile method covers the uncertainty of three main sources: The number of observations, the spatial variability, and the model uncertainty.

Following up on the study (Ćosić, Šušić, Folić, & Bancila, 2016) which showed a probabilistic evaluation of Eurocode design methods for pile foundation focusing on the prediction of future axial resistance with CPTs (van Mierlo & Koppejan, 1952), this thesis focuses on the extent to which the partial factors and the quantification of the statistical uncertainty recommended in Eurocode influence both the deterministic design outcome and the final reliability of the assessment, similar to studies done by (Baars, Rica, Nijs, Nijs, & Riemens, 2018). This thesis focuses on the impact of the number of observations by analyzing and assessing the reliability of the pile foundations based on multiple CPTs.

To do that two case studies are conducted at different places in the Netherlands, Amsterdam, and Almere, for which sufficient CPT data is available to perform a proposed reliability assessment. Based on that data the corresponding EN1997 design will be evaluated with two different probabilistic quantification models.

Additional insight into the influence of uncertainties and their treatment in EN1997 is provided by sensitivity analysis and the calibration of partial factors based on the reliability analyses.

1.4 THE LAYOUT OF THE THESIS

First, the background of the theory which is used in the case studies is presented in Chapter 2 of the report. A more detailed explanation of the methodology which is applied in the case studies is given in Chapter 3. After the approach is explained the results of the case studies are analyzed and conclusive statements of the results are formulated in Sections 4 and 5.

Finally, a chapter with conclusions and further research recommendations is presented in section 6.

Further details about the methods and additional results for the cases are presented in the Appendix. The corresponding section in the main test refers to the specific Appendix if more information is desired.

2. THEORETICAL BACKGROUND

This chapter of the thesis introduces the theoretical background for the quantification models, design and evaluation methods used for reliability assessment. Furthermore, the background of the reliability requirements defined by EN1990 is presented.

2.1 CATEGORIES AND QUANTITATIVE ESTIMATIONS OF UNCERTAINTY IN ENGINEERING

Both the deterministic and probabilistic design approaches have methods to cover different kinds of uncertainties in the design calculations. Uncertainty in the engineering field can generally be divided into main two categories.

The first category is the Aleatoric uncertainty. These uncertainties refer to the natural variability and the imperfection of information. In geotechnical engineering, these uncertainties are for example the heterogeneity of the ground conditions, thus the spatial variability of material properties. Generally, a good quantification of these uncertainties is necessary to accurately model the information provided. Data modelling and the right assumptions are necessary to describe the given parameter of interest with sufficient accuracy. The uncertainty due to the natural randomness of the variable is called natural/spatial variability. The tools to deal with these kinds of uncertainties are uncertainty quantification models. These are good representations of the empirical observations to account for natural variability and statistical uncertainty (Frangopol, 2008).

The second category of uncertainty is Epistemic uncertainty. This uncertainty describes the imperfection introduced by describing and modelling the physical world. All engineering calculation models are an imperfect representation of the real world (Frangopol, 2008). This includes the uncertainty due to limited sampling/ information provided. The introduction of epistemic uncertainty can be due to a lack of knowledge of the contributing mechanisms or due to simplifications that make the problem solvable. Epistemic uncertainties in the models are mostly covered by the model factors.

2.2 DIFFERENT LEVELS OF RELIABILITY ANALYSIS AND SENSITIVITY ANALYSIS

This short section is a general introduction to the different methods and algorithms of reliability calculations. These methods can be categorized into three levels (Pham Quang, Vrijling, van Gelder, & Thu, 2010) Additionally, a method to determine and describe the influence of the variables in the different, the probabilistic sensitivity analysis, is introduced.

LIMIT STATE FUNCTION AND PROBABILITY OF FAILURE

The limit state function is a description of the conditions that lead to the failure of the structure in question. It is an expression of the expected resistance of the structure subtracted by the calculated load. The general definition of the state function and the failure probabilities are:

$$\mathrm{Z} = \mathrm{R} - \mathrm{S} \ (1)$$

$$\mathrm{P_f} = \mathrm{P}\{\mathrm{Z} \leq 0\} \ (2)$$

Where:

- $\mathrm{P_f}$ is the probability of failure
- if $\mathrm{Z} \leq 0$ a failure of the structure occurs
- R is the strength or resistance of the structure
- S is the load on the structure

SEMI PROBABILISTIC APPROACH (LEVEL 1)

The semi-probabilistic method is a reliability-based design and evaluation tool for which probabilistic distributions are translated to design values based on partial factors and characteristic values to make designing simple and convenient.

Partial (safety) factors are included in the design in semi-probabilistic approaches to guarantee a predefined margin of safety. Therefore, the partial factors defined by these methods quantify the epistemic and aleatoric uncertainty indirectly.

The characteristic values are defined such that they are significant for the mechanism in question, mostly this translates to the 5% percentile, to ensure that the probability of a worse value for the parameter is not greater than 5% (CEN, 2019). This can differ for design methods if defined otherwise.

This method is referred to as a Level 1 reliability analysis since the uncertainties and distributions are only represented by point (characteristic) values and the partial (safety) factor which is meant to be calibrated such that the target reliability index (β-value) is met. This leads to a useability-friendly design process, but consequently, simplifications about the uncertainties of the parameters and models are made.

CALIBRATION AND CALCULATION OF THE PARTIAL (SAFETY) FACTORS IN THE EUROCODE

The semi-probabilistic design methods proposed in the Eurocode work with characteristic values are transformed into Design values with the help of the partial factors. While the Eurocode provides recommendations for these partial factors it is also offering a calibration and calculation method to determine these factors. The general thought behind these factors is to account for the Aleatoric and Epistemic uncertainty within the model.

The partial factors are used as a correction for the relation between characteristic values and design values as presented in EN1990 (C4.3):

$$\gamma_R = \frac{R_{char}}{R_d} \quad \text{and} \quad \gamma_S = \frac{S_d}{S_{char}} \quad (3)$$

Where:

- γ_R and γ_S are the partial factor(s) corresponding to the characteristic and design resistance
- $R_{char}$and S_{char} are the characteristic resistance as defined in the Eurocode design model
- R_d and S_d are the design resistance and load as defined in the Eurocode model

These equations further translate to the following, if the assumption of normally distributed resistance and loads is valid (EN1990 – C4.4):

$$\gamma_M = \frac{R_{char}}{\mu_R - \alpha_R \beta_t \sigma_R} \text{ and } \gamma_S = \frac{\mu_S - \alpha_S \beta_t \sigma_S}{S_{char}} \quad (4)$$

Where:

- μ_M and μ_S are the mean value of the characteristic resistance and the design load
- α_R and α_S are the influence factors of the resistance and load
- β_t is the target reliability
- σ_R and σ_S are the standard deviations of the characteristic resistance and load

In EN1990 (C4.3) the partial factors for the resistance side are defined as follows:

$$\gamma_M = \gamma_{Rc} * \gamma_{Rd} \ (5)$$

Where:

- γ_M is the partial safety factor for the resistance such that: $R_d = R_{char}/\gamma_M$
- γ_{Rc} is the partial factor for the uncertainty in the calculated resistance
- γ_{Rd} is the partial factor for the model uncertainty for the calculated model

With Eq. 5 the partial factors for the resistance can be calibrated using the following Equation (EN 1990 – Sections 4.3 and 4.4) given below, under the assumption that the resistance variables are estimated to be normally distributed:

$$\gamma_{Rc} = \frac{R_{rep}}{\mu_{Res} - \alpha_{Res}\beta_t\sigma_{Res}} \text{ and } \gamma_{Rd} = \frac{\mu_m - \alpha_m\beta_t\sigma_m}{\mu_m} \ (6)$$

Where:

- γ_{Rc} is the partial factor correcting for the safety margin of the reliability target for the resistance model
- R_{rep} is the representative or characteristic value of the resistance model
- μ_{res} is the excepted value of the resistance model
- α_{Res} is the sum of the squares of the influence factors in the resistance model, excluding the model uncertainty
- β_t is the reliability target for a 50-reference period defined in EN1990 (3.8 for CC2)
- σ_{Res} is the standard deviation of the resistance model
- γ_{Rd} is the partial factor to account for the model uncertainty
- μ_m is the expected value of the model factor
- α_m is the influence factor of the model factor
- σ_m is the standard deviation of the model factor

These calculations presented a possibility to calibrate the model to findings from probabilistic quantification of the site data for the resistance side.

Approximate full - probabilistic approach - FORM (Level 2)

With a level 2 reliability approach the probability distributions of the given parameters and model factors are full implemented into the calculation method. The distributions are linearized to normal standard space. This means that the distribution functions of the parameters are transformed into standard normal space or Gaussian normal distributions. To derive a probability of failure the limit state function is therefore also linearized. A common method to do this is a Level 2 analysis is the First Order Reliability Method (FORM) for which the limit state function is linearized in the design point. the point of the limit state function close to the origin, thus with the highest probability density. Figure 1 below shows the connection between the design point, the linearized and nonlinear limit state function, and the reliability index (β) (TAW, 1997).

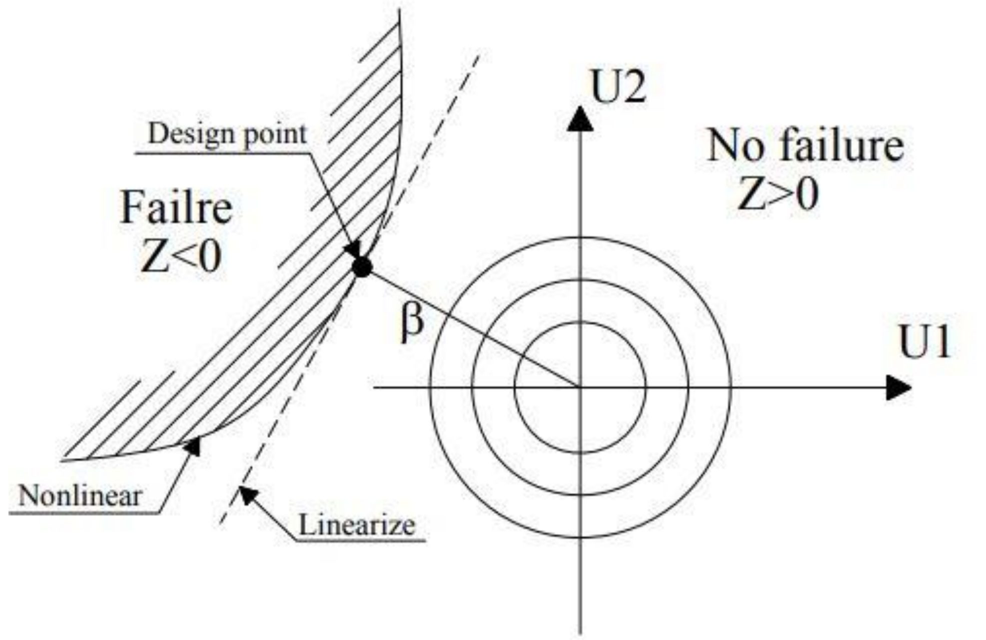

FIGURE 1 - RELIABILITY INDEX, LIMIT FUNCTIONS AND DESIGN POINT (PHAM QUANG, VRIJLING, VAN GELDER, & THU, 2010)

As Figure 1 shows, the design point is the point where the border with the failure plane is closest to the origin. The reliability index (β) corresponds to the distance of the design point to the origin. Further is visible that the limit state function is linearized in the design point. The failure probability and the reliability index are therefore only dependent on the derivative and the position of the design point.

DETERMINATION OF THE INFLUENCE FACTOR WITH THE FORM METHOD

In the FORM method, the influence factor is directly determined from the derivative of the limited state function corresponding to the parameter and the contribution of all the derivatives of the involved parameter quantifications in the standard normal space, such that (Brinkmann, 2021):

$$\alpha_i = \frac{\frac{dz_i}{du_i}}{\left|\frac{\overrightarrow{dz}}{du}\right|} \quad (7)$$

Where:

- α_i is the influence factor corresponding to the i-th parameter
- $\frac{dz_i}{du_i}$ is the derivative of the calculated limit state corresponding to the i-th variable
- $\left|\frac{\overrightarrow{dz}}{du}\right|$ is the calculated vector of the derivative to all variables

FULLY PROBABILISTIC METHOD – MONTE CARLO SIMULATIONS (LEVEL 3)

The distributions of all parameters and the model factors are fully integrated into the Level 3 calculation methods. An example is the Monte Carlo Simulation (MCS) method. With this method linear and non-linear distributions are solvable. Commonly the Monte Carlo Simulation method is used such that the parameters model factors are drawn from the corresponding distribution by chance. With the quantified distributions, many samples and simulations are generated and evaluated. (Pham Quang, Vrijling, van Gelder, & Thu, 2010). The resulting failure probability can be calculated with:

$$P_f = \frac{\sum_{i=1}^{N} Z_i}{N} \quad (8)$$

Where:

- P_f is the failure probability
- Z_i is the logical vector such that $Z_i = 1$ the limit state function is lower than 0, else $Z_i = 0$
- N is the number of samples for the Monte Carlo simulation

Since the Monte Carlo method directly estimates and evaluates the probability of failure, a simplification or linearisation of the limit state function is not necessary. While highly accurate the MCS approach is computationally intense since a multitude of cases needs to be generated and evaluated to calculate the probability of failure with sufficient confidence.

DETERMINATION OF THE ACCURACY ERROR IN THE MONTE CARLO METHOD

Due to the nature of the Monte Carlo simulation method, the accuracy of the method highly depends on the number of samples run per calculation. **The percentage error in** the probability of failure can be approximated with Equation 10 (Koehler, Brown, & Haneuse, 2009).

$$CoV_{MCS}(M, P_f) = \sqrt{\frac{1 - P_f}{M * P_f}} \quad (10)$$

Where:

- CoV_{MCS} is the coefficient of variation of the found failure probability, this is defined as the square root of the variance of the Monte Carlo simulations
- M is the number of simulations samples per calculation
- P_f is the probability of failure determined by the Monte Carlo simulation

THE RELATIVE INFLUENCE OF THE LOAD AND THE RESISTANCE MODELS

To determine the relative influence of the load and the resistance models in the probabilistic assessment a distinction between load and resistance variables is made. The total model influence can then be determined with:

$$\alpha_{model} = \sqrt{\sum_{i=1}^{N} \alpha_i^2} \quad (11)$$

Where:

- α_{model} is the influence factor for the load or resistance model
- α_i is the influence factor for the resistance or load variable i
- N is the total number of influencing variables in the load or resistance model

Equation 11, shows that dominant variables, thus the variables with the highest absolute values, are heavier weighted when assessing the relative sensitivity of the load and resistance model. The square of all sums of the influence factors is by definition 1.

2.3 UNCERTAINTY QUANTIFICATION AND SENSITIVITY

In this section, a short introduction to the 2 approaches of uncertainty quantification in this study is given. The two approaches are classical statistics and the Bayesian approach

CLASSICAL STATISTICS

The classical statistics approach for the estimation/investigation of site data in geotechnical engineering is based on the frequentist approach. Therefore, a big enough sample is assumed to lead to an accurate representation of the population of interest. In geotechnical terms that translates to the number of measurements done from the area of interest (Johannesson, 2019).

The main way to evaluate the accuracy and significance of the resulting models is via a p-value test or goodness-of-fit-test. These types of tests make statements about the probability that a certain value is derived by chance from a random sample instead of being representative of the estimated population (Baecher, 2017). This leads to testing and evaluating the data based on estimated population distribution, which is often based on spatial interpolation and averaging of local point measurements. Therefore, the quantification of the spatial and measurement uncertainties of interest is often based on engineering experience or estimates (Otake & Honjo, 2013). The information about the parameters of interest is then described with parametric distributions which are suited to describe the population.

BAYESIAN INFERENCE APPROACH

In the Bayesian approach to statistics, the population distribution, as well as the estimation of the defining parameters, are represented as degrees of belief of the analyst. Therefore, they are integrated into the model as uncertainties themselves. These beliefs lead to a prior estimated solution either based on estimations or available global information. This solution is then updated if new information is available based on the likelihood that the new information is represented by the prior distribution (Baecher, 2017).

With that updating process, a posterior distribution is created. This distribution combines the prior distributions with the new observed information and maximizes the likelihood based on the observed data. This leads to a more flexible and straightforward way of quantifying uncertainties that confront the beliefs of the underlying distributions with the available or limited information and can be updated (Johannesson, 2019). This method is well suited for cases where only limited information is available. This updating of the posterior distribution is based on the Bayes theorem which states:

$$\mathrm{P}(\mathrm{M}|\mathrm{D}) = \frac{\mathrm{P}(\mathrm{D}|\mathrm{M}) * \mathrm{P}(\mathrm{M})}{\mathrm{P}(\mathrm{D})} \quad (12)$$

Where:

- $\mathrm{P}(\mathrm{M})$ is the prior probability distribution for the model M given the prior information
- $\mathrm{P}(\mathrm{D})$ is called evidence, thus the probability that the data is observed given the prior information
- $\mathrm{P}(\mathrm{D}|\mathrm{M})$ is the likelihood of observing the data given the model and the prior information
- $\mathrm{P}(\mathrm{M}|\mathrm{D})$ is the posterior probability distribution for the model given the data and the prior information

In geotechnical engineering global data in the form of regional databases, for example, TNO (2022), are often available but the acquiring of local data is usually linked to high costs. A Bayesian statistic approach is, therefore, a powerful tool to make precise models based on the limited local data and estimating the amount of information necessary to derive them (Baecher, 2017)

2.4 RELIABILITY LEVELS FROM EN1990

EN1990 (CEN, 2019) defines target values for the reliability level of all structures/elements based on the consequence classes of said structure/elements.

The first considerations for the consequence class are the possibility of a loss of human life or personal injury. The second consideration is the economic, social, and environmental consequences of the failure of the structure or elements. The more severe criterion of the consideration defines the consequence class for the object of interest (Table 4.1 – EN1990).

Related to the consequence classes are target values for the reliability of non-seismic ultimate limit states. The reliability index and the probability of failure, referring to the 50 years return period, are used as standard metrics to express the structural reliability of the structure (β) (CEN, 2019). Table 1 below is a merge of tables 4.1 and C3.2 from EN1990. It is describing the consequence classes and the reliability targets for the assigned structures. The reliability index is given for the 50-year reference period as defined in Eurocode 1990.

TABLE 1 - CONSEQUENCE CLASSES AND RELIABILITY TARGETS FROM EUROCODE 1990

Consequence class	**Indicative qualification of consequences**		**Reliability Index (β)**
	Loss of human life or personal injury	Economic, social, or environmental consequences	
CC4 – Highest	Extreme	Huge	Individually defined
CC3 – Higher	High	Very great	4.3
CC2 – Normal	Medium	Considerable	3.8
CC1 – Lower	Low	Small	3.3
CC0 – Lowest	Very low	Insignificant	Not defined

For most structures, a Consequence Class (CC) 2 is assumed to be applicable. Therefore, the reliability target of β= 3.8 for the design lifetime of 50 years is chosen as the minimum requirement for the different cases for the pile foundations which are analyzed.

3. METHODOLOGY

This section of the report gives an overview of the used methods to derive the reliability levels of the analyzed pile foundations. The chapter starts with a general introduction of the assessment setup, which explains the workflow for the cases. A more detailed description of the different methods for the cases follows.

3.1 GENERAL RELIABILITY ASSESSMENT SETUP

The procedure to determine the reliability levels of the structure is generalized for different geotechnical structures. It aims to compare the design obtained by the semi-probabilistic design approach in EN1997 with fully probabilistic uncertainty quantification models to analyze if the applied characteristic values and the partial safety factors adequately cover the uncertainties encountered in the design process and if the designs achieve the desired reliability targets. A visualization of the reliability assessment procedure, its different components and information flow is given in Figure 2 below.

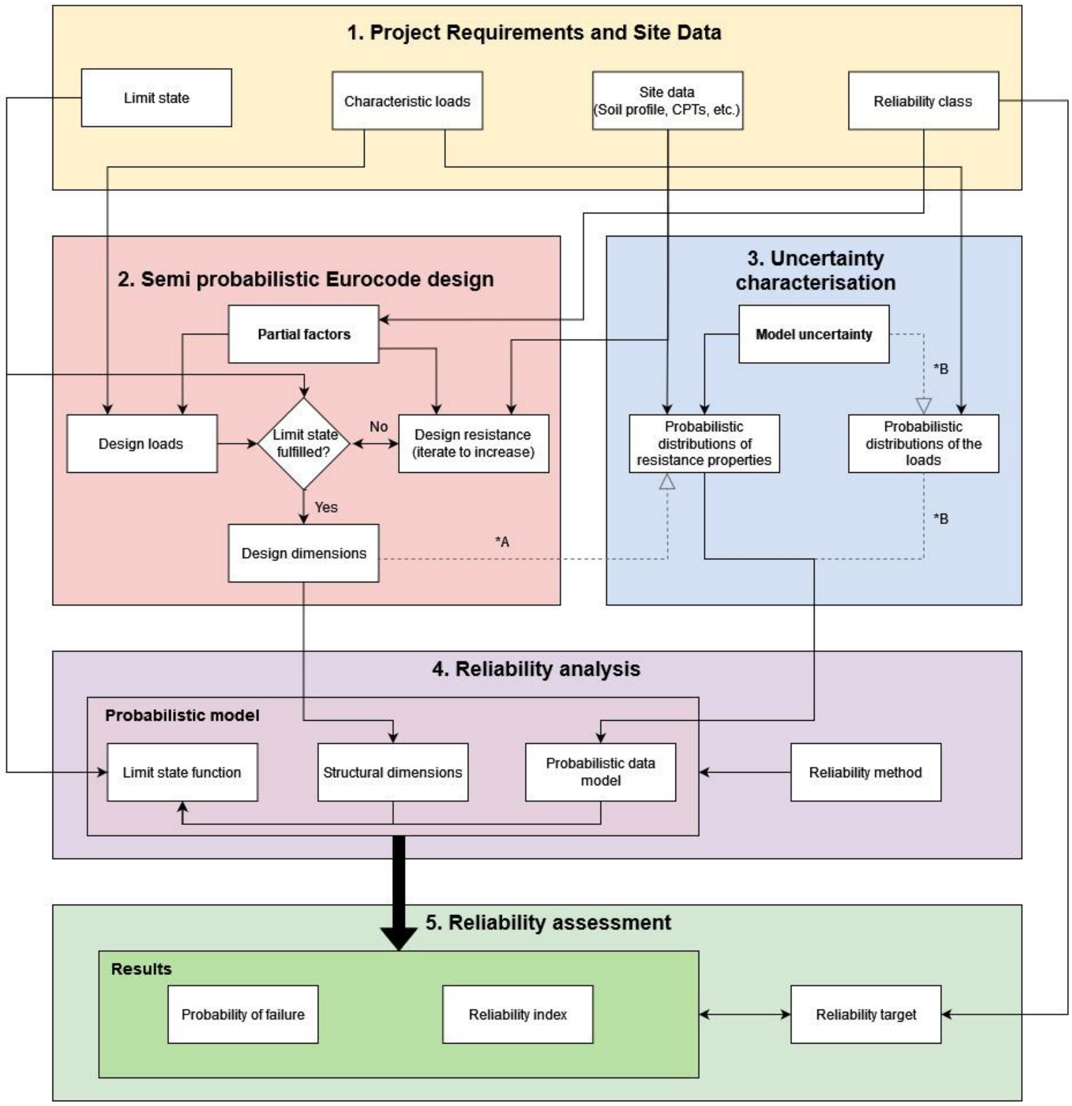

FIGURE 2 - RELIABILITY ASSESSMENT SETUP

***A** the resistance property estimation depends on the design dimension

***B** the fully probabilistic load model is not included in every combination of setup components

The setup consists of the following elements:

1. The **project requirements** (defined by the project and by EN1990/EN1997) and the geotechnical site data.
    - The target reliability class defined by EN1990
    - The characteristic loads applied to the geotechnical structure
2. The **semi-probabilistic design** from EN1997 is used to derive the design dimensions for the structure based on a limit state provided by the design recipe.
    - The design loads are derived based on the determined characteristic loads
    - The Site data are used to derive the expected design resistance
    - The reliability class can influence the partial factors which are chosen.
3. The **probabilistic model** quantifies the uncertainty within the model as distributions. Multiple options are implemented, which include a Student-T and a Bayesian model to estimate the design parameters. Optional a probabilistic load model can be integrated into the quantification.
    - The site data is used to derive probabilistic models for the geotechnical design parameters
    - The probabilistic load model is generated according to the characteristic loads
4. The **reliability analysis** is based on the design dimension (2) and the uncertainty quantification (3). These are used to simulate resistances and loads in a Monte Carlo or FORM analysis using the limit state function to derive the reliability of the structure as described in section 2.2.
    - The limit state function is then created from the probabilistic data model and the structural dimensions
    - The reliability method can be chosen per assessment (FORM, SORM, MC, etc.)
5. The **reliability assessment** compares the results of the reliability analysis are compared with the predesign defined target reliabilities from EN1990

The following section describes the different components in more detail.

3.2 AXIAL RESISTANCE OF PILE FOUNDATIONS

The main method that is used to determine the axial bearing capacity of foundation piles in the Netherlands is the so-called 4D/8D, Dutch or Koppejan method (van Mierlo & Koppejan, 1952). The method is the common practice in the Netherlands and is now also integrated into EN1997 by the addition of the model pile method. The calculation methods of van Mierlo & Koppejan (1952) are therefore used to quantify the point estimates for EN1997 design and the probabilistic quantification models.

The total axial resistance of foundation piles in axial compression consists of two main components. The Pile Base resistance (R_s), and the pile base resistance (R_b) (van Mierlo & Koppejan, 1952). This is visualized in Figure 3.

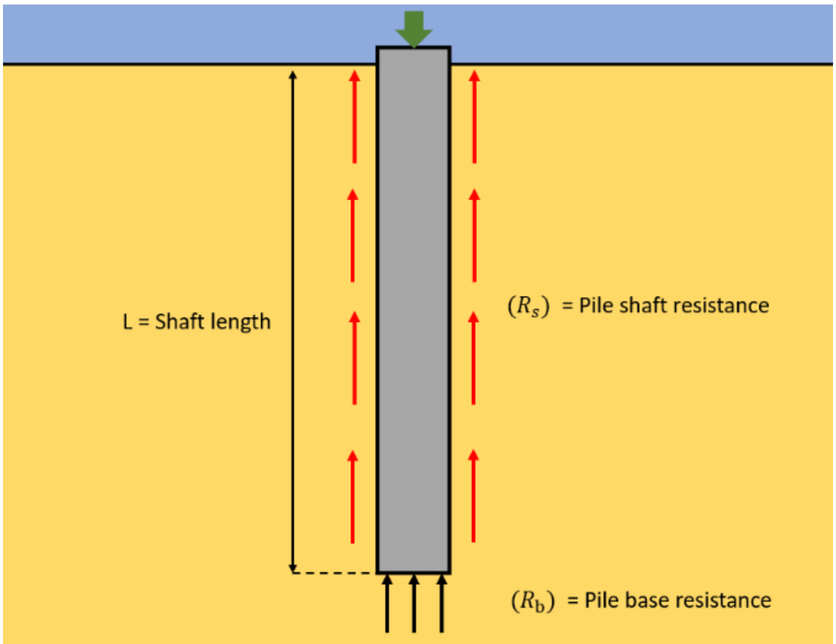

FIGURE 3 - VISUALIZATION OF THE COMPONENTS OF THE AXIAL COMPRESSIVE RESISTANCE

Thus, following EN1997 the total Pile resistance for a pile in compression is calculated with equation 13:

$$R = R_b + R_s \quad (13)$$

For which:

- R is the total axial compressive pile resistance
- R_b is the pile base resistance
- R_s is the total pile shaft resistance

More details are given in the following section.

SHAFT FRICTION

The Pile Shaft Resistance is determined by the average measured cone resistance over the length of the pile. The corresponding equation to calculate the pile shaft resistance from Eurocode 1997 and (NEN, 2019) is given below.

$$R_s = \sum_{i=1}^{n} R_{s,i} \quad (14)$$

$$R_{s,i} = \alpha_{s,i} * C_s * L_s * q_{s,i} \; (15)$$

Where:

- $\alpha_{s,i}$ is the pile class factor determined by the type of soil present in the i-th layer (EN1997 – Table C.3)
- n is the number of layers
- $R_{s,i}$ is the shaft resistance of the i-th layer, measured as averages over 0.1m
- L_s is the design shaft length in the layer [m]
- C_s is the circumference in [m]
- $q_{s,i}$ is the average cone resistance measured in the layer [Pa]

It is assumed that the fluctuations over the pile length average out, and thus the average cone resistance can be used to calculate the pile resistance. The average cone resistance per layer is calculated as the average of 0.1m vertical segments (correlation length) in the layer to average rapid measurement fluctuations. More details on the application of the correlation length and the quantification of the shaft friction (q_s) are presented in Appendix A-3.

PILE BASE RESISTANCE

Following the method from (van Mierlo & Koppejan, 1952) and EN1997 (Model pile design), the Pile Base Resistance is calculated following the Koppejan method. The resistance is calculated by:

$$R_b = A_b * \frac{1}{2} * \alpha_p * q_K \ (16)$$

For which:

- R_b is the base resistance of the pile
- α_p is the pile class factor EN1997 for translating the cone resistance to base resistance (EN1997 - Table C.2)
- A_b is the area of the pile base
- q_K is the quantified Koppejan resistance

The Koppejan resistance (q_K) is a combination of the measured cone resistance over the 3 different influence zones. The resulting factor is a combination of mean and minimum values found in the 3 zones as shown in Figure 4 below.

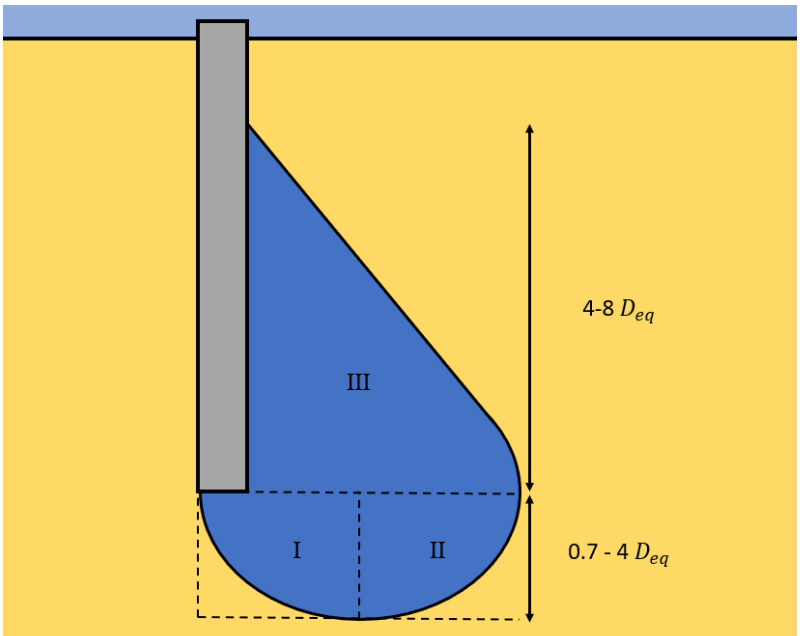

FIGURE 4 - KOPPEJAN ZONES

The Koppejan method is established as a reliable way to accurately estimate the base resistance as shown by Baars et al. (2018). Details on the calculation method and an algorithmic description of the method are present in Appendix A-4.

3.3 SEMI PROBABILISTIC EUROCODE DESIGN

The design model from EN1997 that is used in the reliability assessment is the model pile method proposed (MPM) in clause 6.6 (CEN, 2019). The Eurocode method is based on a Level 1 approach for which uncertainty is integrated via characteristic/calculation values and partial factors. The recipe aims to create a design that conforms to target reliabilities set in EN1990. The shaft friction ($\mathrm{q_s}$) and the Koppejan resistance are quantified as the expected values from Eqs. 15 and 16.

TOTAL PILE RESISTANCE

The total pile resistance, here equivalent to a characteristic value, in the model pile recipe is dependent on the calculated resistance ($\mathrm{R_{cal}}$), and the correlation factor (ζ). The statistical uncertainty is thus integrated into the process via the correlation factor (ζ). The representative resistance (R_{rep}) is equivalent to the characteristic values in other design methods. The factor is dependent on the heterogeneity of the data (CoV) and the number of observations (CPTs). The CoV referred to for ζ is defined as the variation of the total calculation resistance from Equation 13 per CPT. Table 2 shows the values of ζ obtained from Eurocode 1997 – Table 6.5.

TABLE 2 - CORRELATION FACTOR FROM EN1997 - TABLE 6.5

Correlation factor	Coefficient of variation (CoV)	Number of tests or profiles (CPTs)								
		1	2	3	4	5	7	10	20	>49
$\zeta_{\mathbf{min}}$	n/a	1.4	1.27	1.23	Use ζ_{mean} alone					
$\zeta_{\mathbf{mean}}$	<12%	Use ζ_{min} alone		1.30	1.28	1.28	1.27	1.26	1.25	1.25
	15%			1.40	1.39	1.38	1.37	1.36	1.36	1.35
	20%			1.67	1.64	1.63	1.61	1.60	1.59	1.58
	25%			1.98	1.95	1.93	1.90	1.89	1.87	1.85
	>25%	Sub-divide the Geotechnical Design Model to reduce the CoV								

Furthermore, EN1997 compensates for the installation methods and the design method of the piles via partial factors (γ_{Rc} and γ_{Rd}). The design resistance ($\mathrm{R_d}$) can be thus calculated with the following relations.

$$\mathrm{R_{cal}} = \mathrm{R_b} + \mathrm{R_s} \ (17)$$

$$\mathrm{R_{rep}} = \min\left\{\frac{(\mathrm{R_{cal}})_{\mathrm{mean}}}{\zeta_{\mathrm{mean}}}; \frac{(\mathrm{R_{cal}})_{\mathrm{min}}}{\zeta_{\mathrm{min}}}\right\} \ (18)$$

$$\mathrm{R_d} = \frac{\mathrm{R_{rep}}}{\gamma_{\mathrm{Rc}} * \gamma_{\mathrm{Rd}}} \ (19)$$

Where:

- $\mathrm{R_{cal}}$ is the calculation resistance as the sum of shaft resistance and base resistance
- $\mathrm{R_{rep}}$ is the representative resistance calculated as the sum of the shaft and base resistance
- $\mathrm{R_d}$ is the design resistance, which includes the added safety due to limited information
- ζ_{corr} is the correlation factor which is determined in Table 2
- γ_{Rc} is the partial factor accounting for statistical uncertainty in the resistance model for the chosen installation method, EN1997 recommends a value of 1.1
- γ_{Rd} is the partial factor accounting for the model (epistemic) uncertainty of the chosen calculation model, EN1997 recommends a value of 1.1

$(\mathrm{R_{cal}})_{\mathrm{min}}$ is the minimum resistance found between the investigated CPTs, while $(\mathrm{R_{cal}})_{\mathrm{mean}}$ is the mean resistance observed between the observations. EN1997 analyses every CPT isolated on its resistance and then determines the minimum and mean between the found values.

Partial factors are necessary to derive the design values for the pile (Eq.19). The partial factors recommended in EN1997 depend on the calculation and installation methods and therefore are independent of the soil properties. Details on the partial factors are given in Appendix 5. These partial factors are accounting for the model uncertainty (model factor – γ_{Rm}) and the uncertainties due to the installation and pile types (γ_{Rc}).

When designing pile foundations, one has a multitude of optimization options to derive a pile geometry which complies with the requirements set by EN1997. In this study, it was chosen to do an optimization of the side length of the cross-section of a pile foundation with a pre-defined depth. In practice, one could also choose to optimize the shaft length or shaft length/geometry to derive the most economic design. Approaches by Dierckx et al. (2020) proposed a probability-based assessment for the combined optimization approach and compared the results to numerical solutions. While in practice a material-focused optimization is desirable, economically a single optimization for the side length with predefined pile depth can be executed. This is shown by design methods by Bauer (2019). This has the added benefit of prefabricating uniform piles with limited length, which can reduce production costs. A design procedure based on the optimization of the side length of a foundation pile is therefore justified.

The design dimension is defined as the side length of the rectangular pile cross-section, such that the structure complies with the standards set in EN1997. The goal of the design is to determine the design dimension such that the resulting structure fulfils the requirements set in EN1997. This is mainly done with the Eurocode model pile methods described in EN1997 – Section 6.6. The resulting design dimensions are then used as input to the limit state function as described in Figure 2.

3.4 PROBABILISTIC QUANTIFICATION MODELS

The probabilistic quantification models estimate the resistance of the designed pile foundations dependent on the CPTs. To do that, a probability distribution is estimated for each layer for the shaft friction ($\mathrm{q_s}$), like Eq. 15. The process is illustrated in Figure 5. For the Koppejan resistance ($\mathrm{q_K}$) the distribution is estimated based on the observed CPTs. Since the Koppejan resistance is dependent on the dimensions of the piles, the process of updating the Koppejan resistance is also dependent on the chosen design dimension. Figure 5 shows (Plots 1 and 3) the quantification of the Koppejan resistance ($\mathrm{q_K}$) with a fixed dimension.

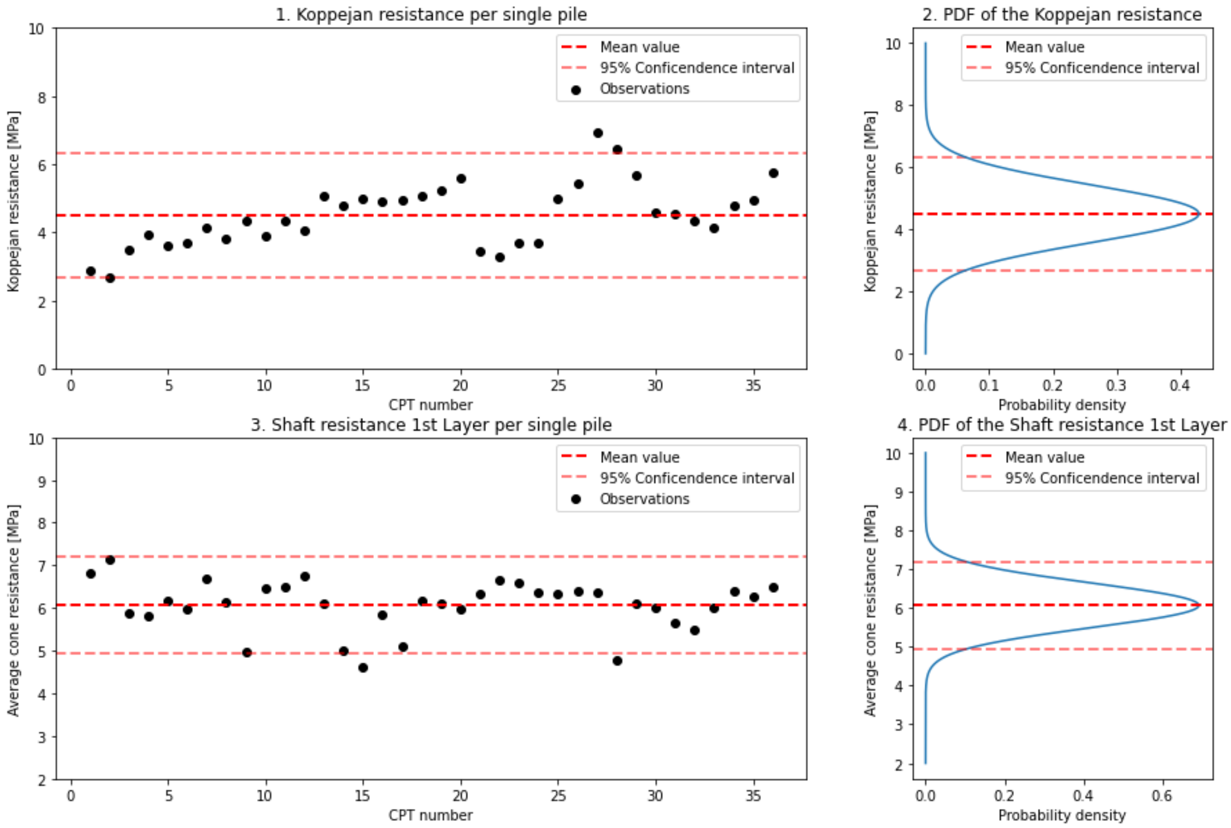

FIGURE 5 - PROBABILISTIC QUANTIFICATION OF THE RESISTANCES

For each CPT one observes 1 value of the Koppejan resistance and one value of average shaft resistance per layer as shown in Figure 5 (Plots 1 and 3). These observations are then translated to the probability density function (PDF) estimations (Plots 2 and 4) by the different quantification models. The statistical method for the estimation of the PDF differs per model while the observations are shared between all of them. Therefore, the quantification models differ in the statistical treatment of the observations, while the calculation methods are equal to the methods presented in section 3.2. The point estimate for the Shaft frictions (q_s) in the quantification models are only dependent on the average cone resistances in the layer of interest and are translated into the shaft resistance via Eq. 15.

The Koppejan resistance (q_K) is dependent on the structural dimensions of the pile, even before being translated to the Base resistance via Eq. 16. Therefore, the PDFs and observations in Figure 5 – Plot 1 need to be quantified for every iteration of the new CPT inputs, since that can influence the estimated Koppejan resistance per CPT and thus the PDF.

MODEL UNCERTAINTY IN THE PROBABILISTIC QUANTIFICATION MODELS

To integrate translation and model uncertainty which is not accounted for by the quantification methods into the probabilistic quantification models a model factor (m_R) is integrated into the models. The model factor can be influenced by the pile type, shape and installation method. based on the findings from Deltares (2020) the factor can be estimated such that the resistance showed a CoV of 10% compared to the field tests. This finding was found on the project side in Amsterdam (see Case Amsterdam) with field-testing of wooden piles. It is assumed that the method of van Mierlo & Koppejan (1952) is not strongly influenced by the pile material.

The total design resistance in the probabilistic quantification models is calculated with

$$R = \frac{R_b + R_s}{m_R} \quad (20)$$

Where:

- R is the design resistance in the probabilistic quantification models
- R_b is the base resistance in the probabilistic quantification models
- R_s is the shaft resistance in the probabilistic quantification models
- m_R is the model factor to account for model uncertainty in the quantification models

This model factor is equal for all three applied uncertainty quantification models.

Baseline Model [x]

The baseline model is used for the evaluation of the design dimensions based on the assumption that the pile base and the shaft resistance, can be fully described by a normal distribution if full information about the CPT field is available. This follows the principle that more measurements were done in the project area, leading to a better estimation of the parameters of the population (Johannesson, 2019). This approach is also supported by (CEN, 2019), where it is advised to integrate the maximum number of measurements if the measurements can be assumed to be in the same homogeneous field. Following this, the model is made that contains all CPT measurements of the project side if the overall Coefficient of Variation (CoV) of the calculated resistances is smaller than 25% (EN1997).

Shaft resistance

To verify that the assumption of a normally distributed cone resistance over a soil layer holds for the model(s), the observed values of the average cone friction within one layer of the soil profile are plotted and normal distribution is fitted upon the data, based on 36 CPTs. The results are presented in Figure 6.

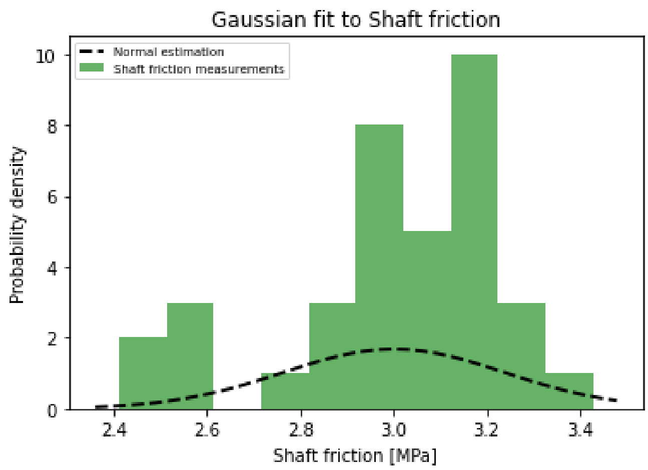

Figure 6 – Normal fit for the Shaft friction ($q_{s,}$)

The visual inspection of Figure 6 shows that the Gaussian distribution models the observations. This impression is supported by the Kolmogorov-Smirnov test for which the Null-hypothesis, that the data is not normally distributed, is rejected with a significance level of α = 0.05. This supports the visual observation that a gaussian fit can model the observations. With the average cone resistance known, the shaft friction (q_s) is then calculated with Equations 14 and 15, which are linear operations. From this follows that the shaft friction per layer and the total sum of all layers can be modelled by a normal distribution. This is consistent with assumptions made in (Ćosić, Šušić, Folić, & Bancila, 2016).

PILE BASE RESISTANCE

For a constant design dimension, the Koppejan resistance (q_K) can estimate with the van Mierlo & Koppejan (1952) if the CoV of the total resistance remains smaller than 25%. To verify if the assumption of a normally distributed Koppejan resistance is suitable to model the data, observations from 36 CPTs are plotted, and normal distribution is fitted to the results in Figure 7.

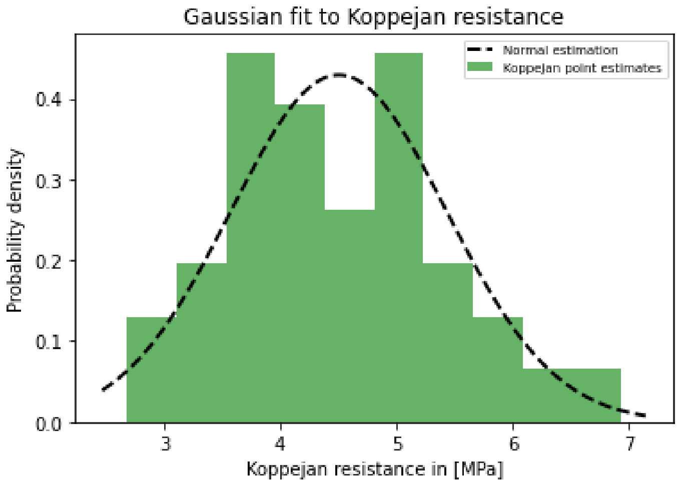

FIGURE 7 – NORMAL FIT TO KOPPEJAN RESISTANCE (q_K) FOR 1 DESIGN DIMENSION

Upon visual inspection, the Gaussian distributions seem to model the observations. Important here is that the continuous normal estimation allows for more extreme values in the tails of the probability density, thus extrapolation of observed data. This is important for the estimation of the limit state since it is expected that these extreme values lead to the failure of the structure.

The impression of normally distributed observations is supported by a Kolmogorov-Smirnov test for which the null hypothesis that the model does not fit the data cannot be rejected with a significance level of α = 0.02. From this, it is concluded that the Gaussian distribution can be a model for pile resistance. This is consistent with assumptions made in (Ćosić, Šušić, Folić, & Bancila, 2016).

TOTAL PILE RESISTANCE

The total design resistance will therefore be calculated with Equation 20. The results of the baseline model [X] serve as a benchmark to compare the performance of the probabilistic quantification models with the complete information for each case and therefore do not account for the limited information that is further investigated. That means that every iteration of the model contains the maximum amount of CPTs for the case. Changes in determining reliability levels for this model are only caused by changes in design dimensions because of the Eurocode design method, which is not based on complete information.

STUDENT-T PROBABILISTIC MODEL [A]

The Student-T model is created to evaluate the design of the design model with a frequentist approach. The mean of the design parameters within the CPT field is assumed to converge to a normal distribution. To account for the incompleteness of information in the Student-T model, the Student-T distribution is chosen to model the shaft friction (q_s) and Koppejan resistance (q_K). With the Student-T distribution, the model adapts to the limited information provided by the CPT.

The expected value for the Student-T distribution is directly calculated from the sample to mean with:

$$E(X) = \hat{\mu} = \frac{\sum_{i=0}^{N} x_i}{N} \ \upsilon > 2 \ (21)$$

Where:

- $E(X)$ is the expected value of the Student T distribution
- $\hat{\mu}$ is the sample mean
- x_i is a data observation
- N are the total number of observations
- υ is the degrees of freedom $(N-1)$

To account for limited information in the model the following correction factor is applied to the calculated variance of the observed data:

$$\mathrm{var}(X) = \hat{\sigma}^2 \frac{\upsilon}{\upsilon - 2} \ \text{for} \ \upsilon > 2 \ (22)$$

Where:

- $\mathrm{var}(X)$ is the variance of the Student T distribution
- $\hat{\sigma}$ is the sample standard deviation

From these equations, it can be concluded that the student T model is only valid for more than 4 independent observations, therefore the model results are only presented for N >= 4. This approach has been investigated to be a robust model by (Lin, Lee, & Hsieh, 2017) and was applied to a similar case by (Ronold, 2016).

BAYESIAN MODEL [B]

The third model that is used to derive point estimations for the design parameters is the Bayesian model. Here the model parameters of the distribution in question are not fixed as in the Student - T model. The uncertainty over the estimate of these parameters is also described by a probability distribution. This distribution can be updated using the Bayes theorem (Eq. 12) to arrive at updated posterior model distributions. If the prior probability distributions for the design parameters are chosen in a specific way, the product of the likelihood and the prior distribution can conjugate to a parametric distribution in the posterior. To keep the assumptions between the Baseline, Student-T and the Bayesian model consistent, the posterior model should describe the belief about the design parameter as a normal distribution. To achieve that the prior distributions for the prior belief of the precision/variability need to be gamma districted and the prior belief of the mean normally distributed. Further, a dependence of both the mean and the precision/variability needs to be implied such that both are conditioned on the data that is observed as shown in Figure 8 (Jordan, 2020).

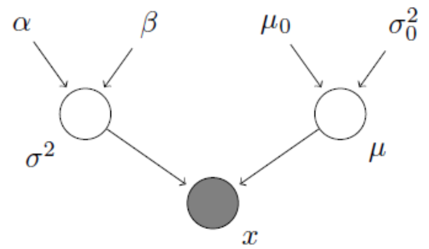

FIGURE 8 - DEPENDENCY GRAPH FOR THE BAYESIAN MODEL (JORDAN, 2020)

This approach to constructing the Bayesian data model has the practical advantage that the posterior updates for the data model can be expressed as close form equations:

$$\mu_{post}|\tau, x_1, x_2, \dots, x_n = N\left(\frac{n\tau}{n\tau + \vartheta\tau_\vartheta}\bar{x} + \frac{\vartheta\tau_0}{n\tau + \vartheta\tau_0}\mu_0 \ , n\tau + \vartheta\tau_\vartheta\right) \ (23)$$

$$\tau_{post}|\mu_\vartheta, x_1, x_2, \dots, x_n = Ga\left(\alpha_0 + \frac{n}{2} \ , \beta_0 + \frac{1}{2}\sum(x_i - \bar{x})^2 + \frac{n\vartheta}{2(n+\vartheta)}(x_i - \mu_\vartheta)^2\right) \ (24)$$

Where:

- μ_{post} is the mean of the posterior distribution of the estimated parameter
- $x_1, x_2, \dots, x_n$ are observations 1 to n
- n is the number of observations that are used to derive to $\bar{x}$
- $\bar{x}$ is the mean of the observed data (n observations)
- $\tau = \frac{1}{\sigma^2}$ is the precision/variability of the distributed data derived from n observations
- ϑ is the number of observations that are used to derive μ_0
- $\tau_\vartheta = \frac{1}{\sigma_0^2}$ is the precision/variability of the mean from the posterior with ϑ observations
- μ_0 is the mean estimate of the prior probability distribution for the mean
- μ_ϑ is the posterior estimate for the mean based on ϑ observations
- τ_{post} is the precision/variability derived from the posterior with n observations
- α_0 is the prior shape parameter of the gamma distribution
- β_0 is the prior location parameter of the gamma distribution

3.5 LOAD MODELS

This section explains the two load models which are used in the reliability analysis. These models are used as an input for the Eurocode design and the probabilistic quantification models, as explained in In Section 3.1. The design load consists of a static/permanent load (G) and a variable load (Q).

SEMI PROBABILISTIC LOAD MODEL

The semi-probabilistic load model is proposed (CEN, 2019). The total design load for this model is determined by:

$$F_d = G_d + Q_d \ (25)$$

For which:

- F_d is the total design load following (CEN, 2019)
- G_d is the permeant design load
- Q_d is the variable design load

The design values for the permanent and variable loads are determined with:

$$G_d = G_k * \gamma_g \ (26)$$

$$Q_d = Q_k * \gamma_Q \ (27)$$

For which:

- G_k is the characteristic value of the permanent load (expected permanent load)
- γ_G is the partial factor of the permanent load derived from EN1997- Table A.1.8 (in both cases 1)
- Q_k is the characteristic value of the variable load (98% -quantile of the Gumbel load distribution)
- γ_Q is the partial factor of the variable load derived from EN1997- Table A.1.8 (in both cases 1.3)

Given a value for the total design load the values for G_d and Q_d can be calculated following the procedure in Appendix 1 - Semi probabilistic load model. The partial factors recommended in Eurocode 1997, $\boldsymbol{\gamma_G}$ and $\boldsymbol{\gamma_Q}$, in combination with the characteristic values are meant to compensate for the Aleatoric and Epistemic uncertainty in the load occurrence for the pile foundations.

FULL PROBABILISTIC DESIGN LOAD

The second model used in the reliability assessment is a fully probabilistic approach proposed in EN1990 if a deterministic estimation of the design load is known. The distribution for the permanent and variable load can be estimated based on the values of G_k and Q_k from the semi-probabilistic load model.

The model is described as follows:

$$F = G + Q \ (28)$$

Where:

- F is the total load estimated by the probabilistic load model
- G is the permanent load distribution described by a normal distribution
- Q is the variable load distribution described by a Gumbel distribution

EN1990 represents the static load by a normal distribution with a CoV of 5%, with a mean value that is equal to the expected value of the load. The variable load is represented by a Gumbel distribution which is used to represent the expected value of a returning extreme value of a phenomenon (NIST/SEMATECH, 2012). The Gumbel distribution is calibrated such that the Return period of the characteristic value Q_k from the Eurocode is 50 years, thus that the probability of exceedance for $P(Q_k) <= 0.02$, this is assuming that the variable load for the piles is equivalent to climate action or other reoccurring annual maxima. The ratio of the relative contribution of the variable to static load (χ) was chosen to be 1/3. The study by Phoon & Tang (2015) showed the importance of different load combinations on the assessed reliability for strip foundations. When the results are investigated it can be assumed that differences in load combinations also influence the reliability outcomes for pile foundations if the relative influence of the load model uncertainties is high (α > -0.7). Therefore, sensitivity analysis of the load ratio (χ) could provide more insight into the interaction between reliability assessment and load uncertainties. Statements about the relative influence of the load model are highly dependent on this ratio. For more details on the calculation of the probabilistic load, model see Appendix 2

3.6 CALCULATION SETUPS

To evaluate the reliability levels of the achieved designs by EN1997, 2 different calculation setups are distinguished. Both setups follow the structure in Figure 9. The difference in these setups is the choice for the load model in the uncertainty characterization.

The Eurocode design requires a semi-probabilistic load model, which therefore is always applied for the calculation. The main difference is that in the uncertainty characterization, one setup works with the probabilistic load model, while the second setup just evaluates quantified resistance against the theoretically required resistances, thus the design load. Figure 9 shows the scheme presented in Figure 2 simplified and adapted for the setups.

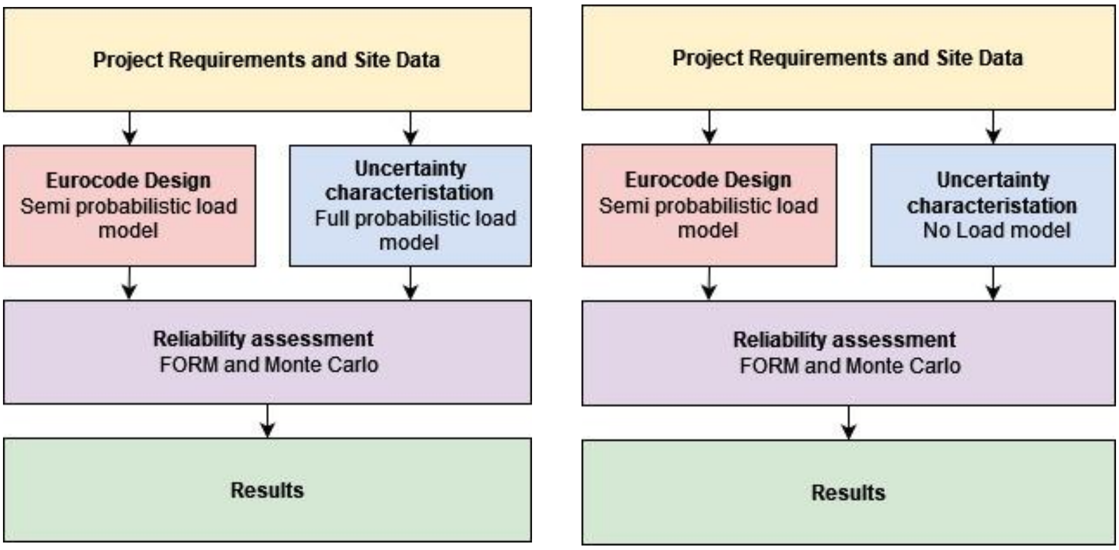

FIGURE 9 – SETUP WITH PROBABILISTIC LOAD MODEL (LEFT) AND WITHOUT PROBABILISTIC LOAD MODEL (RIGHT)

This difference between the two setups is mainly to analyze the resistance model without an added influence of load uncertainties. A practical benefit of a calculation setup which excludes the load model is that in practice engineers often are required to design a structure based on a given design value, without the additional information on the load properties.

4. CASE AMSTERDAM

This section presents the reliability assessment for the first case study, the Case Amsterdam. Frist the case data is introduced, and then the design problem and the design choices are presented, to establish the case and the assumptions taken for the reliability assessment. Thereafter the design results of the EN1997, the reliability assessment, a sensitivity analysis, and the calibration of the partial and correlation factors are presented. A second reliability assessment is presented, isolating the uncertainty of the resistance model. After those results, conclusive statements are formulated for this case study.

4.1 DATA LOCATION AND GRID POSITION – CASE AMSTERDAM

The project area for the pile foundation is located in Amsterdam, The Netherlands. This locates the area in a region which is characterized by a small holocoen sand layer with soft soils such as clay and peat underneath. The exact location of the project side is shown in Figure 10 (left).

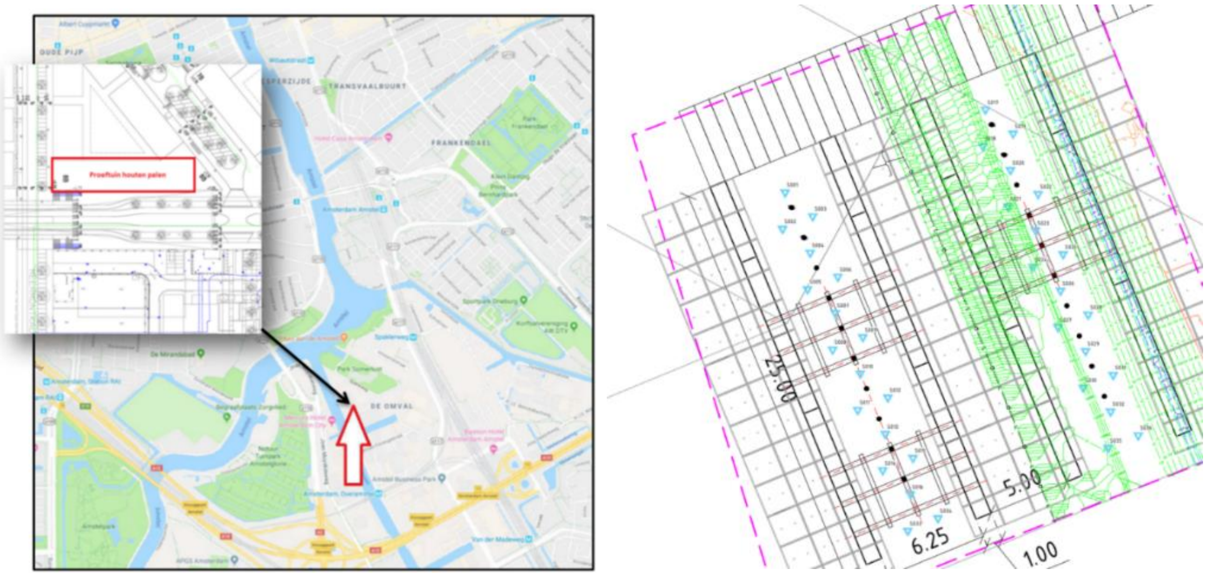

FIGURE 10 – GENERAL MEASUREMENT LOCATION (LEFT) AND CPT GRID (RIGHT) (DELTARES, 2020)

As Figure 10 shows are the project area located in the southeast of Amsterdam in a quarter called De Omval. The region is used as an industrial area and border to a channel connected to the river Amstel in the west.

Within the project area, 36 CPTs are positioned in the grid as shown in Figure 10 (right) below. The grid consists of 36 measurements up to a depth of -25m of the surface. The measurements are oriented such that the CPTs form triangles around the test piles.

4.2 SITE DATA ANALYSIS AND DESIGN CHOICES – CASE AMSTERDAM

The data used to both create and evaluate the design are based on the presented CPT field. The region of Amsterdam is characterized by a soil profile consisting of soft peat and clay layers interrupted by sand layers which correspond to sedimentation of sea sand between the ice ages, 116.00 to 11.700 years ago (Deltares, 2020). The CPT measurement together with the soil samples from Deltares (2020) resulted in the assumed profile which is presented in Figure 11 below.

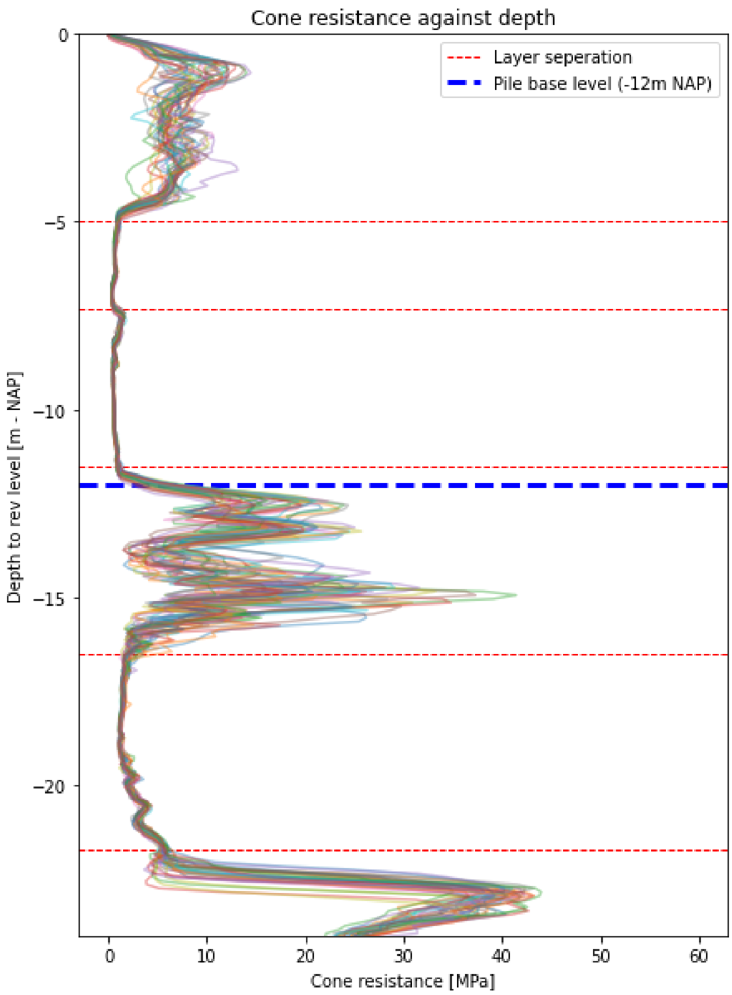

Soil layer	Starting Depth [-m NAP]
1st Layer -Sand	0
2nd Layer - Peat	5
3rd Layer - Clay	7.3
4th Layer - Sand	11.5
5th Layer -Clay	16.5
6th Layer - Sand	21.7

FIGURE 11 - CONE RESISTANCE FOR ALL CPTS (LEFT) AND SOIL PROFILE (RIGHT)

Since the 1st (holocoen) sand layer does not offer enough bearing strength to withstand loads of large structures, in Amsterdam pile foundations are used to increase the bearing capacity of foundations. These piles need to reach a layer with sufficient stability to cope with loads of the structures. In most cases, the foundation piles are installed up to a depth within the 4th layer which consists of sand (thus starting from -11.5m N.A.P). The design choice for further investigations was to set the foundation pile length to 12m from the surface, such that the pile's bases are positioned in the 4th Layer. The blue line in Figure 4 shows the design level for the pile base.

From the investigation of the available site data (Figure 11) design choices are made. The choices regarding the pile material, the installation method, and the pile geometry are presented in Table 3. These choices remain are consistent for both the Eurocode design model and the probabilistic quantification models.

TABLE 3 - PILE PROPERTY CHOICES FOR THE DESIGN AND ASSESSMENT MODELS

Pile property	Choice
Geometry (cross section)	Rectangular
Pile length (L)	-12 [+m NAP]
Material	Precast concrete
Design load (F_D)	0.55 [MPa]
Installation method	Full displacement

The choice for the pile material is precast concrete since the material is common for European construction of deep foundations (Dziadziuszko & Sobala, 2018). The value for the design load (F_d) is arbitrarily chosen so that the expected design dimensions are within the margins of practical applications. Further, the pile cross-section is designed to be rectangular and constant throughout the whole length of the pile. The types of piles which are analyzed are Full Displacement Piles (FDP) as presented in EN1997.

From the soil profile (Figure 11) we can extract the soil type present at all depths of interest. Together with Table C.2 from EN1997 the following pile class factors can be determined. The table is given in Appendix 5.

TABLE 4 - PILE CLASS FACTORS FOR CASE AMSTERDAM (EN1997 – TABLE C.2)

Parameter of interest	Pile class factor following Table
Shaft friction 1st Layer (Sand)	0.01
Shaft friction 2nd Layer (Peat)	0
Shaft friction 3rd Layer (Clay)	0.02
Shaft friction 4th Layer (Sand)	0.01
Base resistance (mainly 4th Layer, Sand)	0.7

The pile class factors in Table 4 are determined with EN1997 and are implemented into both the design and probabilistic quantification models. The probabilistic quantification compensates for the deterministic nature of the chosen length and the translation (pile class factors) with the model factor (Eq. 22). The model factor (m_R) integrates the added translation and model uncertainty, where it is implied that the expected values of these factors are in line with the values provided by EN1997.

4.3 VARIABLE SETUP – CASE AMSTERDAM

The following short section summarizes all the combinations of the model variables in the Eurocode design and the probabilistic quantification models, thus the choice for the load model.

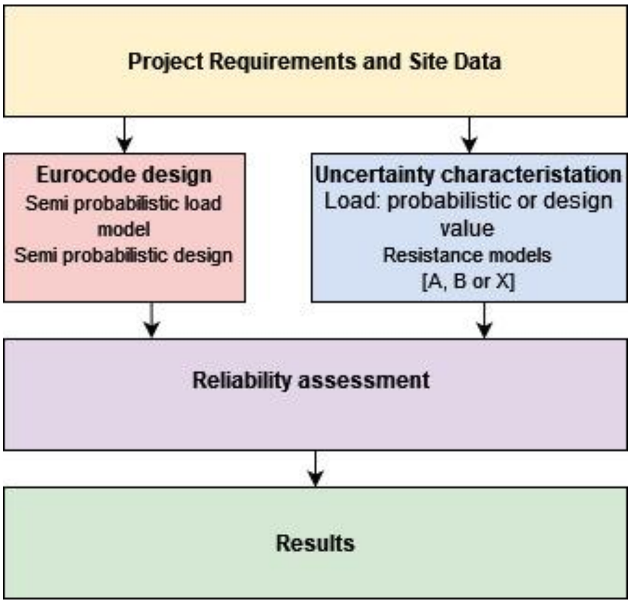

FIGURE 12 - VARIABLE INPUT LOCATION FOR THE ASSESSMENT

Figure 12 shows that in the Eurocode design, both the design method and the load model are always semi-probabilistic.

In the uncertainty characterization model, a choice between a fully probabilistic design load and a deterministic design load can be made, for which the variables are presented first in Table 5. Furthermore, the fully probabilistic resistance models were implemented. The different variable inputs, including the prior assumptions, distribution choices and Eurocode references, if applicable, are presented in Table 6.

LOAD MODELS

The table below gives a short overview of the used variables and values in the load models described in section 3.7. This choice of the variables will be consistent for both case studies presented in this report.

TABLE 5 - VARIABLE SETUP FOR THE LOAD MODELS

Variable	Distribution	Description
	Deterministic load	
Design load (F_d)	Deterministic	0.55[MPa]
	Semi probabilistic load model	
Permanent load ($\mathbf{G_k}$)	Deterministic	0.33 [MPa]
The partial factor for permanent load ($\boldsymbol{\gamma_G}$)	Deterministic	1 (EN1990 – Annex C.3)
Variable load ($\mathbf{Q_k}$)	Deterministic	0.166[MPa]
Partial factor variable load($\boldsymbol{\gamma_Q}$)	Deterministic	1.3 (EN1990 – Annex C.3)
	Probabilistic load model	
Mean permanent load (μ_G)	Normal	0.333[MPa]
Standard deviation permanent load (σ_G)	Normal	0.016 [MPa]
Mean permanent load (E(Q))	Gumbel	0.166 [MPa]1
Location parameter permanent load($\boldsymbol{\mu_G}$)	Gumbel	0.0938
Scale parameter variable load ($\boldsymbol{\beta_Q}$)	Gumbel	0.02193

The load models are uniform for all quantification models and independent of the CPTs data. This also implies that the expected load for the piles remains the same, independent of the spatial orientation of the pile in the field.

RESISTANCE MODELS

Table 6 provides an overview of the variables used in the different resistance models. First, the variables of the EN1997 design are presented, including a reference to specific sections if recommendations were used. For a detailed explanation of the quantification used in the models, see section 3.3

After that, the probabilistic quantification models are presented. Starting with the Baseline model [X]. Followed by the Student T model [A] and the Bayesian model [B]. For a detailed explanation of the calculation methods used see Section 3.4.

For more detailed information on the response of the models to the site data, the probability densities of the different resistances are presented and analyzed in Appendix 7.

TABLE 6 - VARIABLE SETUP FOR THE RESISTANCE MODELS

Variable	Distribution	Description
		Eurocode design resistance model variables (Semi probabilistic design)
Koppejan resistance(q_K)	Deterministic	Expected/Mean value from the sample, Dependent on design dimensions
Shaft resistance 1st Layer (q_{S1})	Deterministic	Expected/Mean value from the sample, Dependent on design dimensions
Shaft resistance 2nd Layer (q_{S2})	Deterministic	Expected/Mean value from the sample
Shaft resistance 3rd Layer (q_{S3})	Deterministic	Expected/Mean value from the sample
Shaft resistance 4th Layer (q_{S4})	Deterministic	Expected/Mean value from the sample
Partial model factor (γ_{Rd})	Deterministic	1.1 from Eurocode 1997 – Table 6.3
Partial resistance factor (γ_{Rc})	Deterministic	1.1 from Eurocode 1997 – Table 6.6
Correlation factor (ζ)	Deterministic	Dependent on data properties and number of tests, Given in Eurocode 1997 – Table 6.5 (Table 2)
		Baseline model resistance [X] quantification variables
Koppejan resistance(q_K)	Normal	$N(\widehat{\mu_K},\widehat{\sigma_K})$, Sample mean, sample standard deviation, always based on all 36 CPTs, Dependent on design dimensions
Shaft resistance 1st Layer (q_{S1})	Normal	$N(\widehat{\mu_K},\widehat{\sigma_K})$, Sample mean, sample standard deviation, always based on all 36 CPTs
Shaft resistance 2nd Layer (q_{S2})	Normal	$N(\hat{\mu},\hat{\sigma})$, Sample mean, sample standard deviation, always based on all 36 CPTs
Shaft resistance 3rd Layer (q_{S3})	Normal	$N(\hat{\mu},\hat{\sigma})$, Sample mean, sample standard deviation, always based on all 36 CPTs
Shaft resistance 4th Layer (q_{S4})	Normal	$N(\hat{\mu},\hat{\sigma})$, Sample mean, sample standard deviation, always based on all 36 CPTs
Model factor (m_R)	Normal	$N(1{,}0.1)$ No systemical bias, with expected 10% variations in total resistance by (Deltares, 2020)
		Student T resistance model [A] quantification variables
Koppejan resistance(q_K)	Student - T	$T(\widehat{\mu_k},\widehat{\sigma_{k\ T}})$, Sample mean, For degrees of freedom corrected sample standard deviation, Dependent on design dimensions
Shaft resistance 1st Layer (q_{S1})	Student - T	$T(\widehat{\mu_{S1}},\widehat{\sigma_{S1\ T}})$, Sample mean, For degrees of freedom corrected sample standard deviation, Dependent on design dimensions
Shaft resistance 2nd Layer (q_{S2})	Student - T	$T(\widehat{\mu_{S2}},\widehat{\sigma_{S2\ T}})$, Sample mean, For degrees of freedom corrected sample standard deviation
Shaft resistance 3rd Layer (q_{S3})	Student - T	$T(\widehat{\mu_{S3}},\widehat{\sigma_{S3\ T}})$, Sample mean, For degrees of freedom corrected sample standard deviation
Shaft resistance 4th Layer (q_{S4})	Student - T	$T(\widehat{\mu_{S4}},\widehat{\sigma_{S4\ T}})$, Sample mean, For degrees of freedom corrected sample standard deviation
Model factor (m_R)	Normal	$N(1{,}0.1)$ No systemical bias, with expected 10% variations in total resistance, from tests by (Deltares, 2020)
		Bayesian resistance model [B] quantification variables
Koppejan resistance mean (μ_K)	Normal	$N(\mu_0,\sigma_0)$, Prior mean $\mu_0 = 5\,[MPa]$, Prior standard deviation $\sigma_0 = 1[MPa]$
Koppejan resistance precision (τ_K)	Gamma	$G(\alpha_0,\beta_0)$, Prior shape factor $\alpha_0 = 1[-]$, Prior scale factor $\beta_0 = 1$
Shaft resistance means 1st Layer (μ_{S1})	Normal	$N(\mu_0,\sigma_0)$, Prior mean $\mu_0 = 5\,[MPa]$, Prior standard deviation $\sigma_0 = 1[MPa]$
Shaft resistance variability 1st Layer(τ_{S1})	Gamma	$G(\alpha_0,\beta_0)$, Prior shape factor $\alpha_0 = 1[-]$, Prior scale factor $\beta_0 = 1$
Shaft resistance means 2nd Layer (μ_{S2})	Normal	$N(\mu_0,\sigma_0)$, Prior mean $\mu_0 = 1\,[MPa]$, Prior standard deviation $\sigma_0 = 1[MPa]$
Shaft resistance variability 2nd Layer(τ_{S2})	Gamma	$G(\alpha_0,\beta_0)$, Prior shape factor $\alpha_0 = 1[-]$, Prior scale factor $\beta_0 = 0.01$
Shaft resistance mean 3rd Layer (μ_{S3})	Normal	$N(\mu_0,\sigma_0)$, Prior mean $\mu_0 = 1\,[MPa]$, Prior standard deviation $\sigma_0 = 1[MPa]$
Shaft resistance variability 3rd Layer(τ_{S3})	Gamma	$G(\alpha_0,\beta_0)$, Prior shape factor $\alpha_0 = 1[-]$, Prior scale factor $\beta_0 = 0.01$
Shaft resistance mean 4th Layer (μ_{S4})	Normal	$N(\mu_0,\sigma_0)$, Prior mean $\mu_0 = 3\,[MPa]$, Prior standard deviation $\sigma_0 = 1[MPa]$
Shaft resistance variability 4th Layer(τ_{S4})	Gamma	$G(\alpha_0,\beta_0)$, Prior shape factor $\alpha_0 = 1[-]$, Prior scale factor $\beta_0 = 0.01$
Model factor (m_R)	Normal	$N(1{,}0.1)$ No systemical bias, with expected 10% variations in total resistance (Deltares, 2020)

4.4 RESULTS EN1997 DESIGN – CASE AMSTERDAM

The EN1997 designs pile foundations such that the chosen design load (F_d), which may be derived from a semi-probabilistic load model is equal to the total design resistance (R_d). The limit state for the Eurocode designs is therefore defined as:

$$R_d - F_d \geq 0 \ (29)$$

Which underlines the deterministic nature of the semi-probabilistic design. The reliability assessment is done over different numbers of CPTs. This means that the CPTs are put one by one into the assessment model as described in section 4.2. First, a design is made based on only one CPT of the field. After the dimension for the design with one CPT is obtained, the next design is made based on 2 CPTs. This process is repeated till either the CoV of the resistance is bigger than 25% (Table 2) or all (36 in Case Amsterdam) CPTs are integrated into the design.

Figure 13 below shows the design dimension and the correlation factor against the number of CPTs [n].

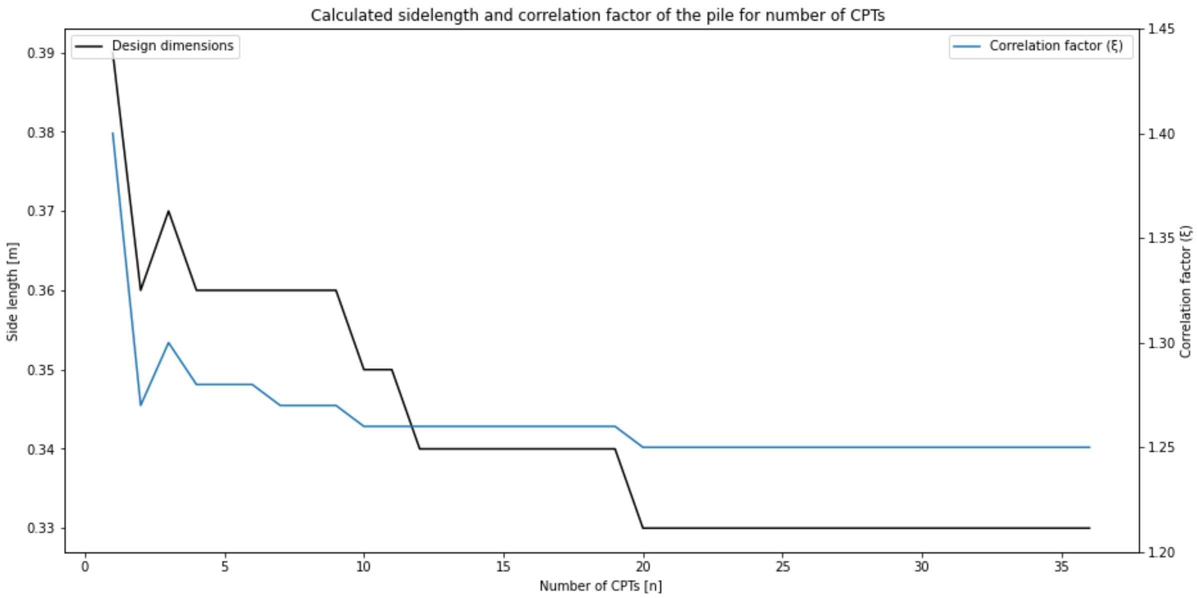

FIGURE 13 - RESULTS OF THE DESIGN MODEL

A clear decreasing trend of the design dimension (black line) is visible over the increasing number of CPTs. This trend is dependent on the corresponding correlation factor (blue line) which emphasizes the importance of the direct relationship between the correlation factor and the design dimensions (Eq. 18).

This correlation factor (ζ) transforms the calculation resistance to a characteristic value and is the first step of uncertainty treatment in the design process. Due to the homogeneity of the CPT field in Amsterdam, the EN1997 observed variability category from Table 2 (row) remains constant over the number of CPTs. Isolation of the quantity criterion is observed, thus the treatment of uncertainty due to limited observations in the EN1997 recipe. A decreasing trend in the correlation factor is observable, indicating the reduction of statical uncertainty with more observations.

An exception for this is the correlation factor corresponding to the design created with n = 3. This can be explained by the process in which the correlation factor is chosen in Table 2. If less than 3 CPTs are available, the design is always based on the minimum calculated resistance (R_{min} – Eq.18) found from set CPTs. If 3 or more observations are made the mean calculated resistance (R_{mean} –

Eq.18) is used to derive the design resistance and the correlation factor (ζ). This is combined with an increasing correlation factor. This explains the increase at n = 3 for the correlation factor, which also increases the design dimension.

4.5 RELIABILITY ASSESSMENT WITH PROBABILISTIC LOAD MODEL - CASE AMSTERDAM

In the following sections, 4.5, 4.6 and 4.7 the results of the assessment with a full probabilistic load model are presented and discussed for the Case Amsterdam. The limit state function in the reliability analysis can be described with:

$$\mathrm{Z} = \mathrm{R} - \mathrm{F} \ (30)$$

Following (CEN, 2019) the resulting reliability level (β) should be:

$$\mathrm{P}(\mathrm{R} < \mathrm{F}) = \Phi(\beta_{\mathrm{target}}) \ (31)$$

Where:

- $\mathrm{Z} \leq 0$ is a failure
- R is the resistance quantified by the probabilistic resistance models [A, B and X]
- F is the load quantified by the fully probabilistic load model
- Φ is the standard normal CDF
- β_{target} is specified by (CEN, 2019) with 3.8 for a lifespan of 50 years (Section 2.4)

The reliability analysis is done with a FORM or a Crude Monte Carlo simulation (MCs) method. The comparison between the results of both algorithms investigates if the simplifications, and linearization in the design point of the limit state function, of the FORM method, are a good approximation for the failure boundary.

If the results of both methods are comparable, this suggests that the limit state function for the designs for the Amsterdam CPT field is close to a linear in the standard normal space. This is expected since most of the variables influencing the limit state are normal like distributed and combined with linear operations. The results of the reliability analysis are presented in Figure 14.

To compare the outcome of the probabilistic models, the Bayesian model (red) and the Student T model(green), in performance the baseline model (blue) is also plotted in Figure 14. The solid line is the reliability index, and the probability of failure is determined with the FORM, the dashed line is assessed with the MCs. The MCs are done with 10 million samples per CPT input analysis.

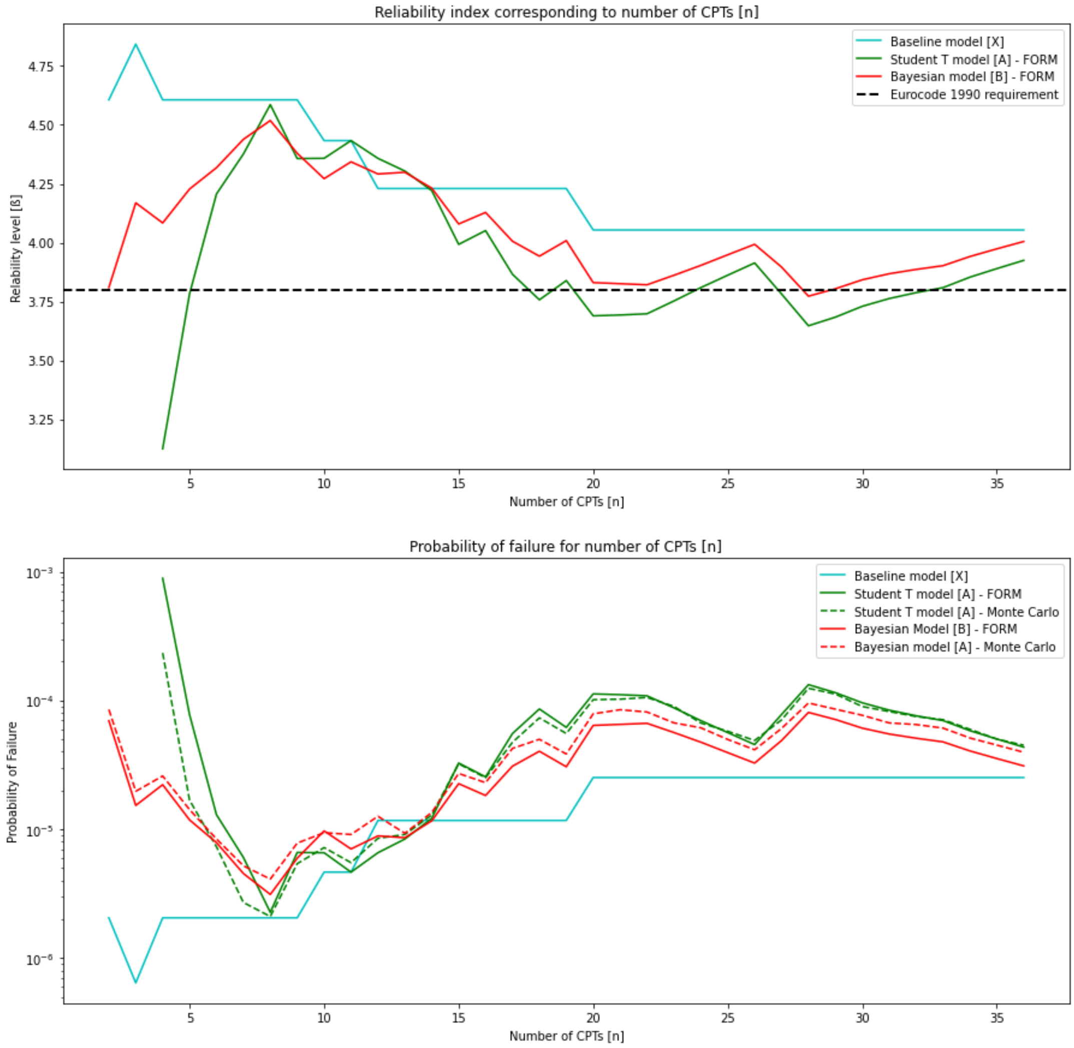

FIGURE 14 - RESULTS OF THE RELIABILITY ASSESSMENT WITH PROBABILISTIC LOAD MODEL

The first observation from Figure 14 are the similarities in the results between the different probabilistic models and the reliability methods used.

The FORM (solid line) for the models seem to react and assess the reliability within a small margin of error to the MCS method (dashed line). The difference in the methods decreases further if the number of CPTs that are used as inputs increases.

The maximum expected error in the probability of failure of the MCs lies around 15%, which was determined in Eq. 11. This value corresponds to the lowest probability that is observed (n=8) over the range of iterations. This further underlines the agreement between MCs and FORM for this case. This indicates that the limit state function could be close to the linear in standard normal space.

Another similarity can be observed in the agreement of the Student T [A] and the Bayesian model [B] at the upper range of the number of inputs for this Case, thus n > 10. With an increasing number of inputs, the difference between the models decreases further. This points towards a convergence of the parameter quantifications for both reliability methods and quantification models [A and B] with decreasing statistical uncertainty due to limited observations. Further is observable that the Baseline model [X] evaluates the design as more reliable in every iteration except for 10 < n < 14. The difference between the baseline model [X] and the other probabilistic quantification models [A and B] can be explained by local trends in the CPTs, see Appendix B - 6.

The second observation from Figure 14 is that for both tested models, Student T [A] and Bayesian [B], converge to the reliability target of β= 3.8 required by EN1990. For the range of CPT inputs, 5 > n > 15, the full probabilistic quantification models [A and B] evaluate the design dimensions from the EN1997 design as bigger than required by the EN1990 reliability target.

An exception is the Student T model, which assesses that the design dimension derived from the EN1997 recipe is less reliable for n =4, thus with higher statistical uncertainty due to limited observations. A similar result can be obtained for the Bayesian model [B] if less informative prior estimations of the resistances are implemented into the model.

From Eqs. 15 and 16, it is expected that the Koppejan resistance (q_K) and the Shaft Friction (q_s) in the first layer has influence largest influence on the calculated resistance. These variables, together with the design dimensions and the reliability index for the FORM are presented in Figure 15.

It should be noticed that the CoV of the EN1997 and the probabilistic quantification models are determined with a different approach than the probabilistic quantification models, thus they are plotted over a different scale (Plot 4).

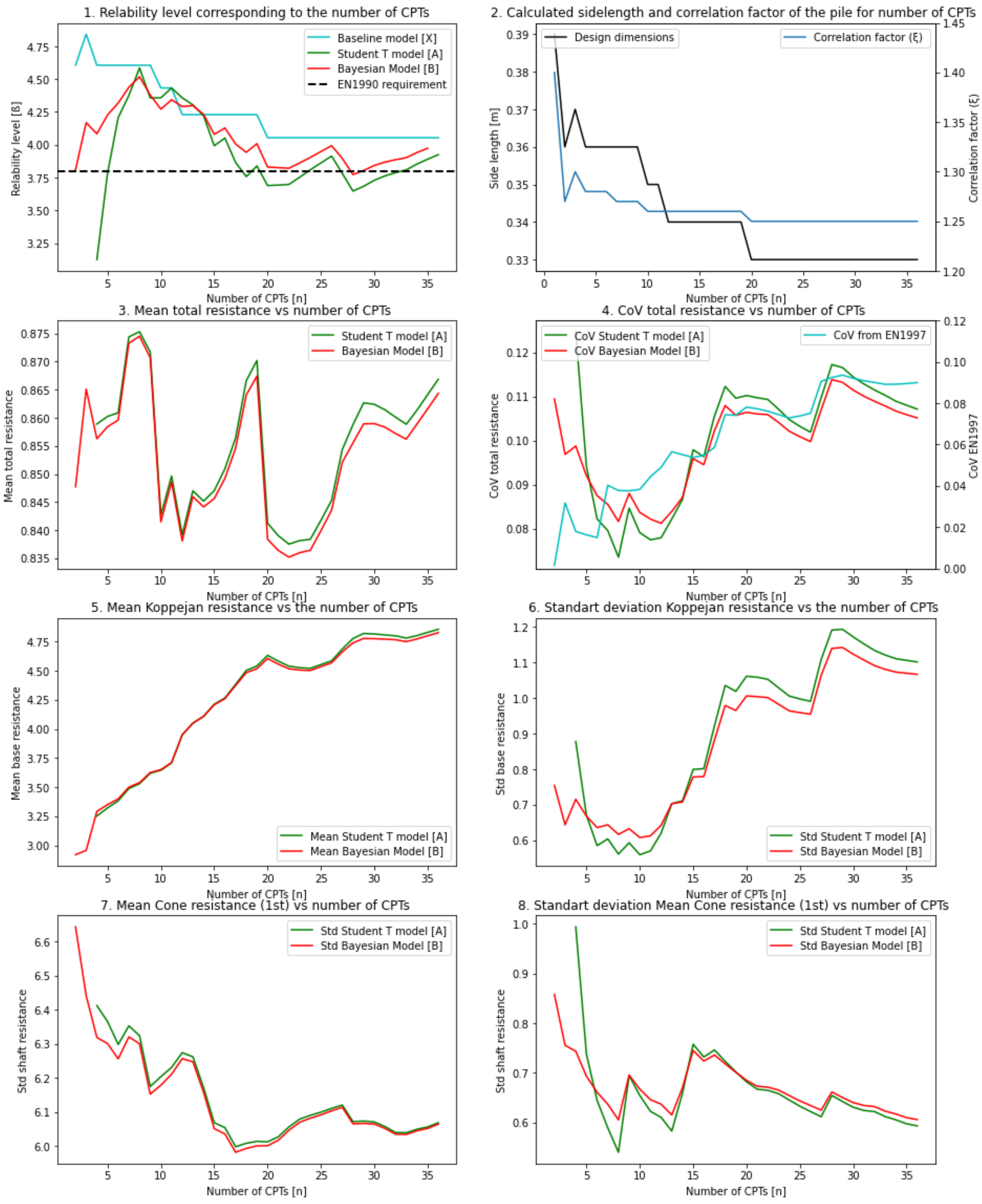

FIGURE 15 - RELIABILITY INDEX, DESIGN DIMENSIONS AND SIGNIFICANT RESISTANCE QUANTIFICATIONS

For the Case Amsterdam, both quantification models [A and B] showed a strong agreement with the derived design parameters over the range of CPT inputs (Plots 5 – 8), indicating a good convergence of the models, which is also observable in Appendix 7. This further indicates that the treatment of both the spatial variability and the uncertainty due to limited observations (CPTs) is comparable for both models in Case Amsterdam.

Furthermore, it can be observed that the general trends for all three models [A, B and X] in plots 46 and 8 over the whole CPT range resemble the behaviour of the failure probability (Plot 1) in Figure 14 and are therefore inverse proportional to the assessed reliability index. The strongest connection is observable between the total CoV of the quantification models [A and B] (Plot 4) and the uncertainty surrounding the Koppejan resistance (Plot 6). This suggests a strong influence of the Koppejan resistance (q_K) quantification of the assessed Reliability index (Plot 1). This can be explained by the relatively weak soft layers surrounding the shaft of the piles, see Figure 11. Due to the non-linear behaviour of the Koppejan method, the EN1997 designs are very sensitive to weak sections within the pile base layer (4th layer) where the Koppejan resistance is mainly determined.

Furthermore, is visible that the Koppejan resistance shows an increasing trend for increasing inputs [n]. This suggests a local trend in soil strength in the foundation layer of the site. This finding is supported by the observations of the Single CPTs in Appendix 6. This trend additionally leads to a decrease in the design dimensions independent of the correlation factor as visible for n = 12.

In the range of 5 > n > 16, the quantified uncertainty of the total resistance is lower than 12%, suggesting homogeneous soil conditions in the observed CPT field. Under these conditions, the designs from EN1997 are assessed to be more reliable than EN1990 would require and thus conservative.

Small differences in the quantification of the standard deviations in plots 6 and 8 are visible for n > 15. The underlying reason for these differences is the influence of the prior information provided to the Bayesian quantification [B], which is of the strongest effect if fewer observations are made.

4.6 SENSITIVITY ANALYSIS OF THE UNCERTAINTY OF THE CONTRIBUTION VARIABLES – CASE AMSTERDAM

To investigate the observed results in Figure 15 about the dominant role of the Koppejan resistance (q_K) a sensitivity analysis of all contributing variables in the models is done. This has a further advantage in that the relative influence of the resistance model and the load model can be investigated. This information makes statements about the importance of a probabilistic load model compared to the load model possible. The sensitivity analysis is done with the influence factors presented in section 2.2. The results are given in Figure 16 below.

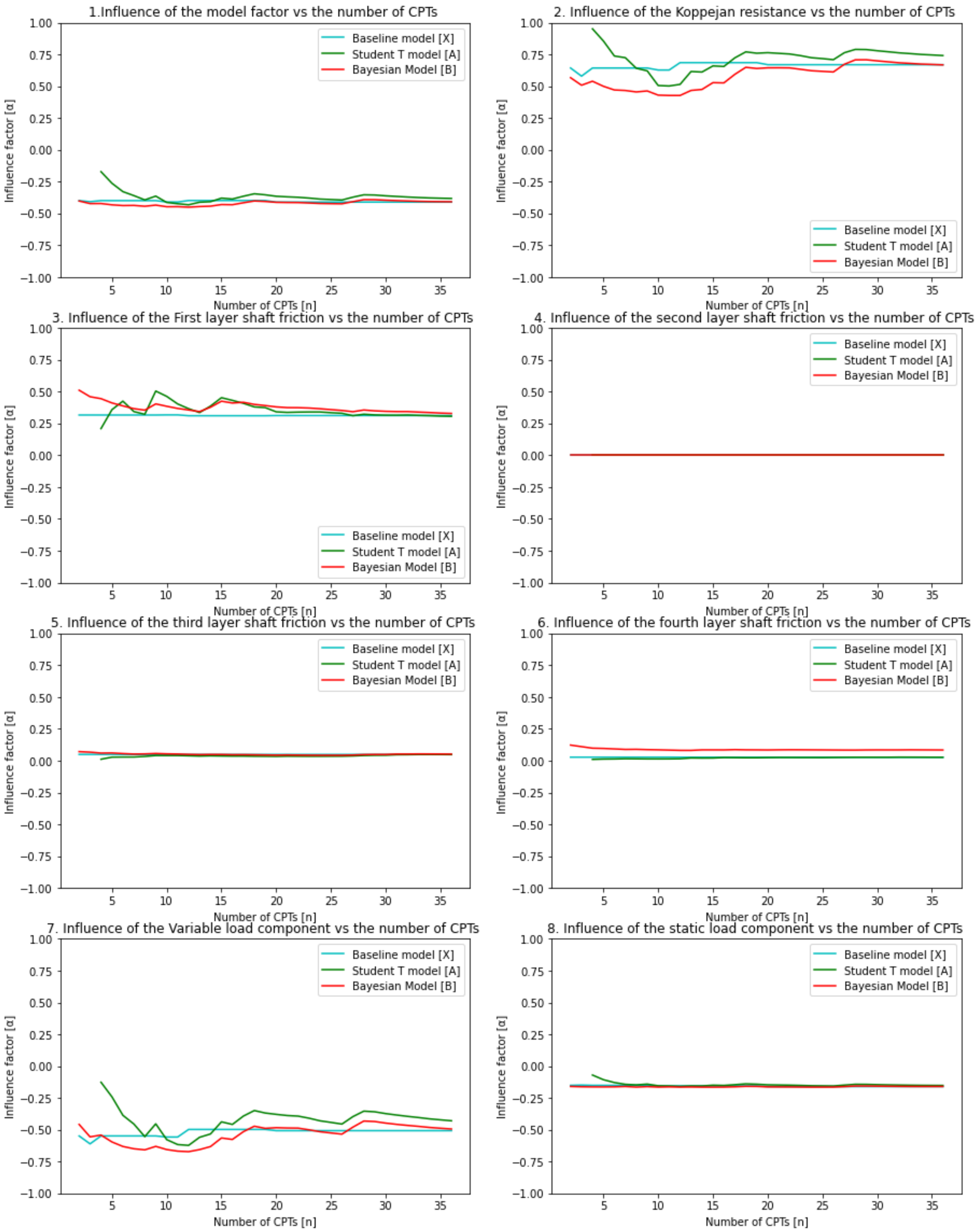

FIGURE 16 - DIFFERENT INFLUENCE FACTORS (Α) FOR ALL CONTRIBUTING VARIABLES

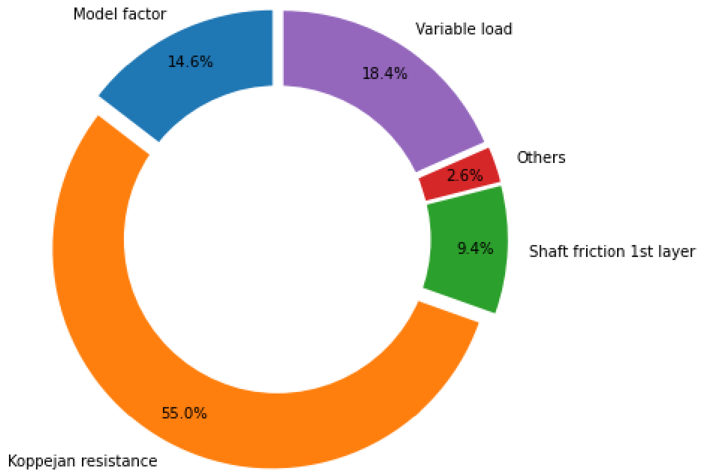

FIGURE 17 - THE SQUARED INFLUENCE FACTORS OF THE STUDENT T MODEL [A] FOR 36 INPUTS

The influence of different variables fluctuates over the range of CPT inputs and between the models, indicating a change in relative importance for different design dimensions and tests integrated.

The main observation from Figure 16 and Figure 17 is that the dominant influence on the assessed reliability is exercised by the uncertainty of the Koppejan resistance(Plot 2). This observation is consistent with the observations made in Figure 15. Furthermore, it can be observed that trends for all three models [A, B and X] over the whole CPT range resemble the behaviour of the failure probability in Figure 14 and are therefore anti-proportional to the assessed reliability index.

Another behaviour of the model is that the role of the shaft resistances for the soft soil layers (2^{nd} and 3^{rd}) are neglectable when compared to the influence of the Koppejan distribution and the shaft friction ($q_{s,1}$) of the first layer. The 4^{th} layer is also from a small influence since the pile shaft length of 0.m is relatively small compared to the first layer (1^{st}). The shaft frictions determined for the 2^{nd}, 3^{rd} and 4^{th} layers are summarized as “Others” in Figure 17 and the relative contribution is lower than 1%.

From this, it can be concluded that the influence of resistances, which are located in sand layers, and thus the layers with the highest observed average cone resistance are most influential on the bearing capacity of the piles and the assessed reliabilities (see Figure 11).

From the calculated influence factors from Figure 16, a separation between the resistance variables plots 1 to 6, and load variables, plots 7 and 8, can be made to determine the influence of the load and the resistance model on the assessment outcome. This is done with Eq. 11.

If no sensitivity analysis is done, EN1990 Annex C4.4 recommend the following values for the combined influence factors. An $\alpha = 0.8$ is recommended for the resistance model and the load with $\alpha = -0.7$ EN1990 (Section C4.4.2). These recommendations are further compared to the results of the sensitivity analysis in Figure 18.

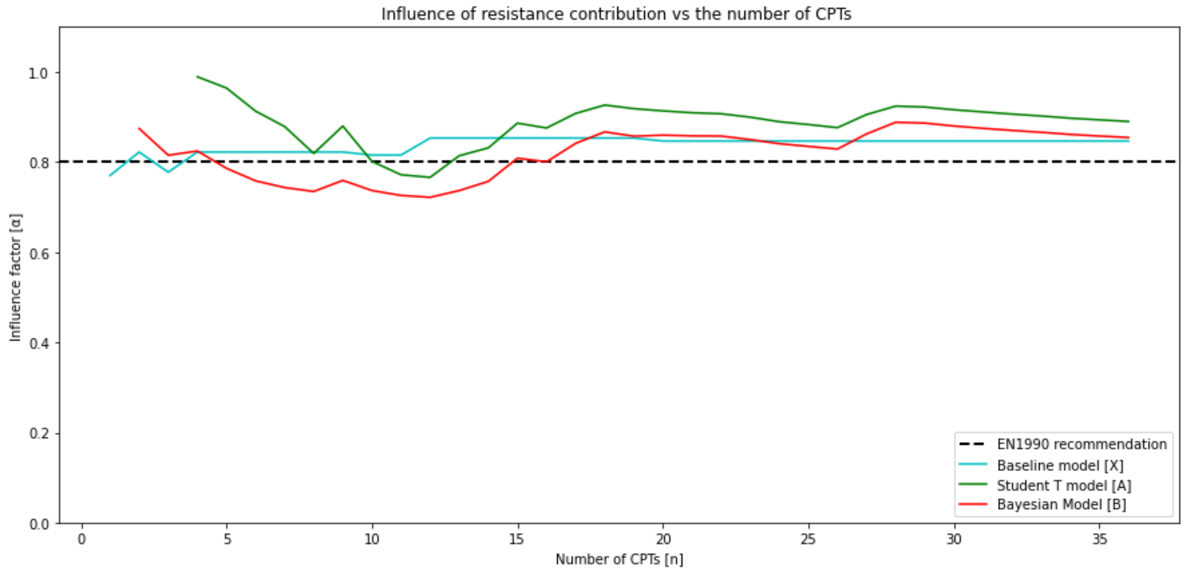

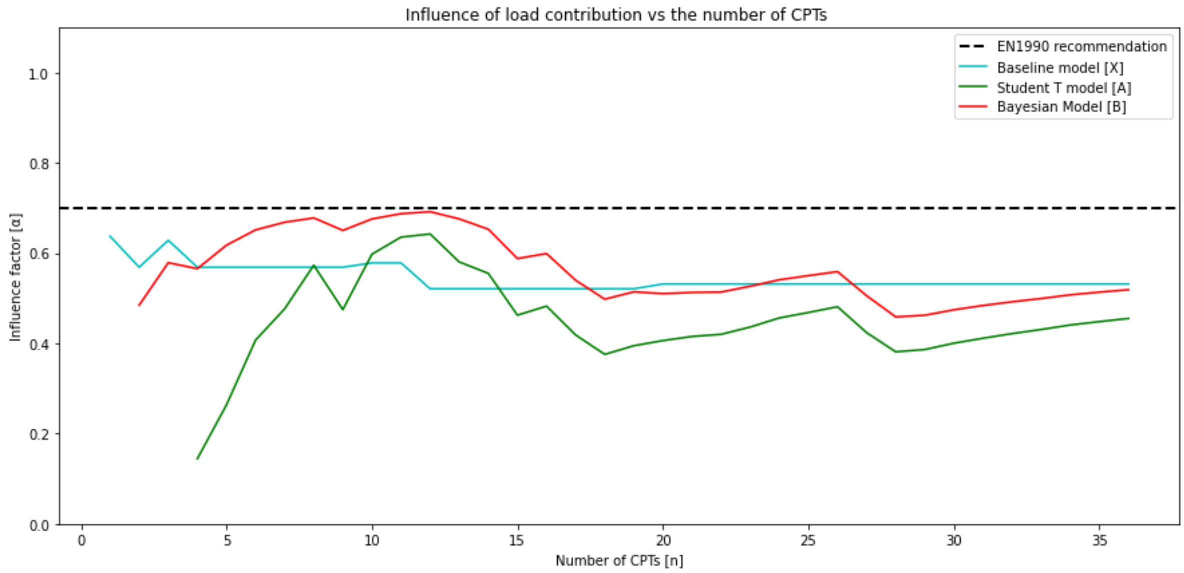

FIGURE 18 - RESULTS FOR THE INFLUENCE FACTORS FOR THE RESISTANCE AND THE LOAD MODEL

Since the sum of the squares of all influence factors is equal to 1 per definition an anti-proportional behaviour of the relative influence of the load and resistance model is observable.

The resistance model seems to be from dominant influence on the assessed reliabilities in Case Amsterdam. In contrast, the load model is mostly assessed to be less relevant for the reliability assessment than the EN1990 recommends. With decreasing uncertainty in the resistance model, in the range of $5 < n < 15$, it is from less influence than over the rest of Inputs whole which is expected since the amount of uncertainty surrounding the resistance is smaller. This again can be explained by the trends and increase in spatial variability presented in Appendix A-6.

4.7 PARTIAL AND CORRELATION FACTOR CALIBRATION FOR THE RESISTANCE MODEL – CASE AMSTERDAM

To further the treatment of uncertainty by EN1997 in the design process, calibrating the partial and correlation factors for the design recipe provides insight. The following section presented and discussed two different approaches to achieve this, first the analysis of the calibration of the partial factors, with fixed correlation factors and second the calibration of the correlation factors with fixed partial factors.

To calibrate both the correlation and the partial factors for the model pile method, the following assumptions are made. First, the total resistance quantified by the quantification model [A and B] is approximately normally distributed. Both the Student T [A] and the Bayesian model [B] are normally distributed and linearly combined. The normality of the model factor is given in the test by Deltares (2020). With this, the calibration of the partial factors following Eq. 6 is possible.

The Eurocode gives two separate partial factors for the resistance, which are determined by the uncertainty correction in the semi-probabilistic Eurocode design. The first partial factor ($\gamma_{Rc)}$ aims to cover the spatial variability and the uncertainty due to limited observations of the resistance. The second partial factor (γ_{Rd}) covers Epistemic model uncertainty. The results of the calibration of the resistance(γ_{Rc}), model (γ_{Rd}) and combined partial factor(γ_{M}) for the FORM method are presented below.

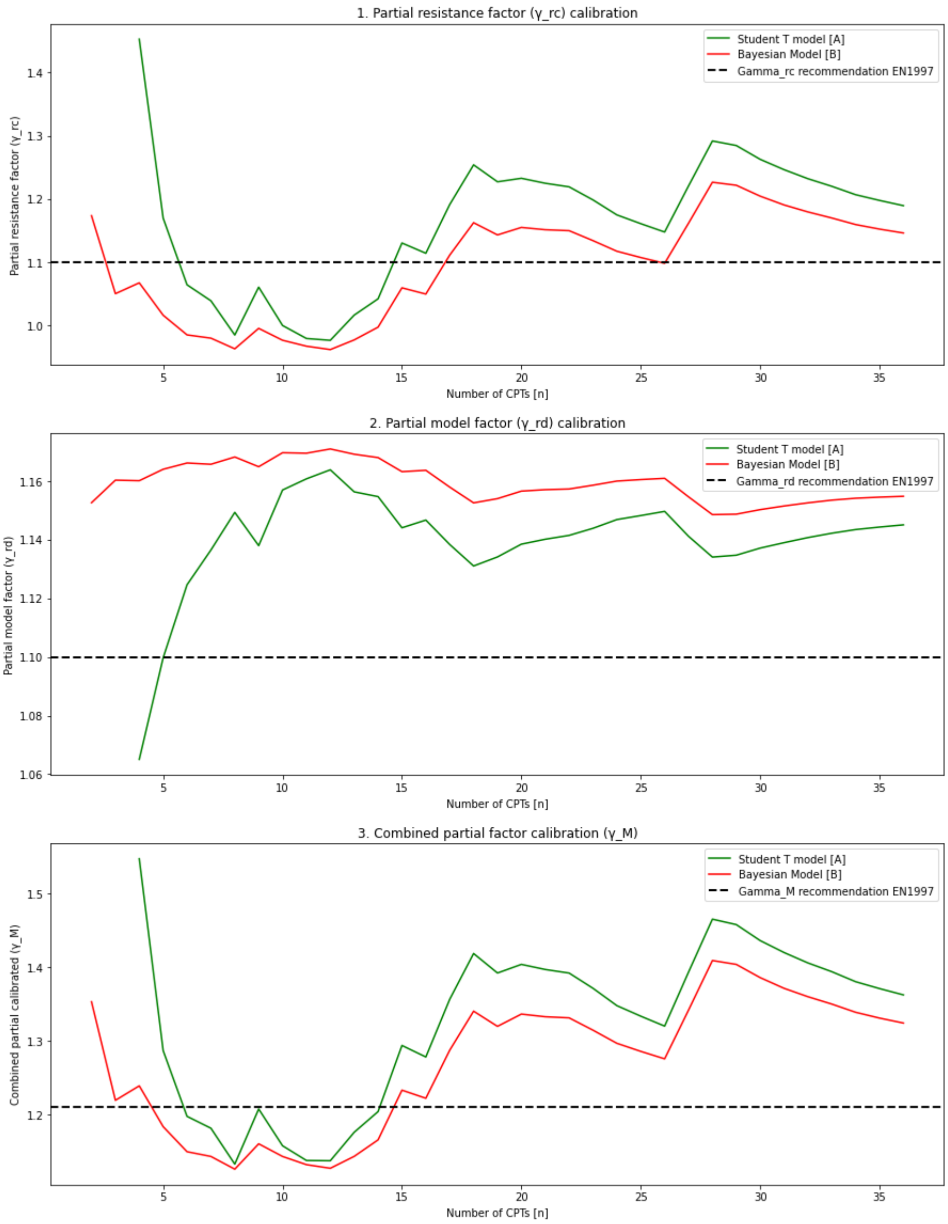

FIGURE 19 - CALIBRATED PARTIAL FACTORS FOR THE RESISTANCE

When Figure 19 is investigated the three main observations can be made. First, the calibration of the resistance partial factor (γ_{Rc}) shows a familiar pattern relating to the recommended value from the EN1997 than the assessed reliability index to the set target (Figure 14). In the lower range of inputs, the recommendation of 1.1 is estimated to be more conservative than would be necessary for the resulting design dimensions. This is in line with the findings in Figure 15 (Plot 1 and 4) if the uncertainty of the total resistance is quantified with small spatial variability, and thus the design resistance from EN1997 is bigger than required. From Eq. 6 it is known that the partial factor is the relation between the representative value and the design value. Therefore, a smaller γ_{Rc} is expected for the range of inputs where the reliability assessment evaluated the design dimension as a conservative choice. In the high range of CPTs, thus n < 16, the calibration showed that the uncertainty for the resistance model is lower than EN1997 recommends. The partial factors in EN1997 are lower than the optimal values to cover the uncertainty of the resistance model (Figure 18).

The second observation is that the calibrated values for the partial model factor (γ_{Rd}) are also higher than the EN1997 recommendation. This is in line with findings for the partial resistance factor, thus an underestimation of the influence of the resistance from EN1997.

The findings for both partial factors (γ_{Rc} and γ_{Rd}) are reflected in the combined total partial factor (γ_M). The calibration shows that most values for the combined partial factor are smaller than the optimal values from the probabilistic calibration.

The partial resistance factors being lower than optimal, however, does not result in insufficient reliability, as we have seen in the previous sections. The reason is that the (fixed) partial load factors seem to be higher than necessary or optimal and compensate the sub-optimal values on the resistance side. This hypothesis is supported by influence factors of the load being roughly around -0.5, which is lower than the recommended default value of -0.7, thus indicating that the load uncertainty is less influential in the problem at hand compared to structures in general.

Another way to approach the calibration of the EN1997 design is the calibration of the correlation factor (**ζ).** For the following results, the partial factors are set to be constant and equal to the recommended values from EN1997 as presented in Table 6. The results are presented in Figure 20.

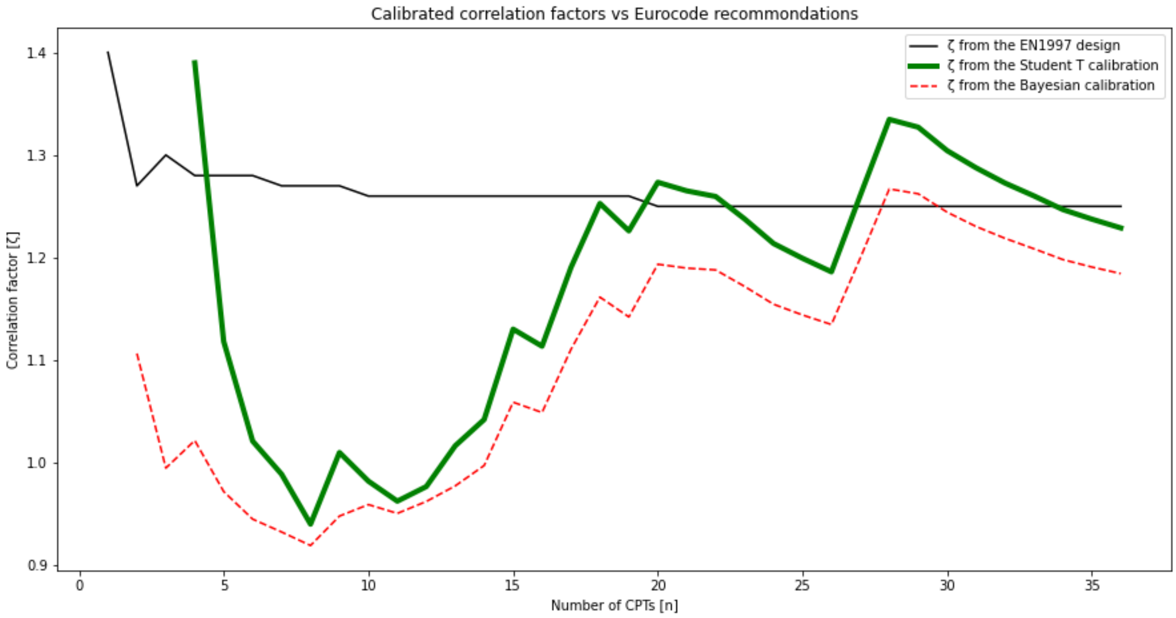

FIGURE 20 - CALIBRATION OF THE CORRELATION FACTOR

The reoccurring pattern in the calibration, meaning the conservative Eurocode design estimates for the lower range of n < 16 and good agreement with the Eurocode recommendation at the higher range, are also visible in the calibration of the combined partial factor (Figure 19 – Plot 3). It can be concluded for this case that the correlation factor (ζ) is conservative in the range where the CoV of the total resistance of the probabilistic quantification is smaller than 12%.

4.8 RESULTS FOR CALCULATION SETUP WITHOUT LOAD MODEL – CASE AMSTERDAM

A second reliability assessment is done without the addition of a probabilistic load model. This means that for the assessment the limit state is defined as the point where the design resistance is smaller than the expected design resistance, thus excluding the uncertainty of the load. EN1997 can design the structure based on a predefined deterministic load, the limit state function can be described as:

$$Z = R_{theoretical} - F_d \ (32)$$

Following EN1990 the resulting reliability level (β) should be:

$$P\left(R_{d,EU} < R_{theoretical}\right) = \Phi\left(-\alpha * \beta_{target}\right)(33)$$

Where:

- Φ is the standard normal CDF
- α has a recommended value of 0.8 but can be the object of a sensitivity analysis
- β_{target} is specified by (CEN, 2019) with 3.8 for a lifespan of 50 years

The results of the reliability assessment without the load model are presented below. From Equation 31, it is expected that the overall achieved reliability index is smaller than the index evaluated with the load model since the uncertainty of the load is neglected and a worst-case scenario of 50 years of reoccurring loads is created.

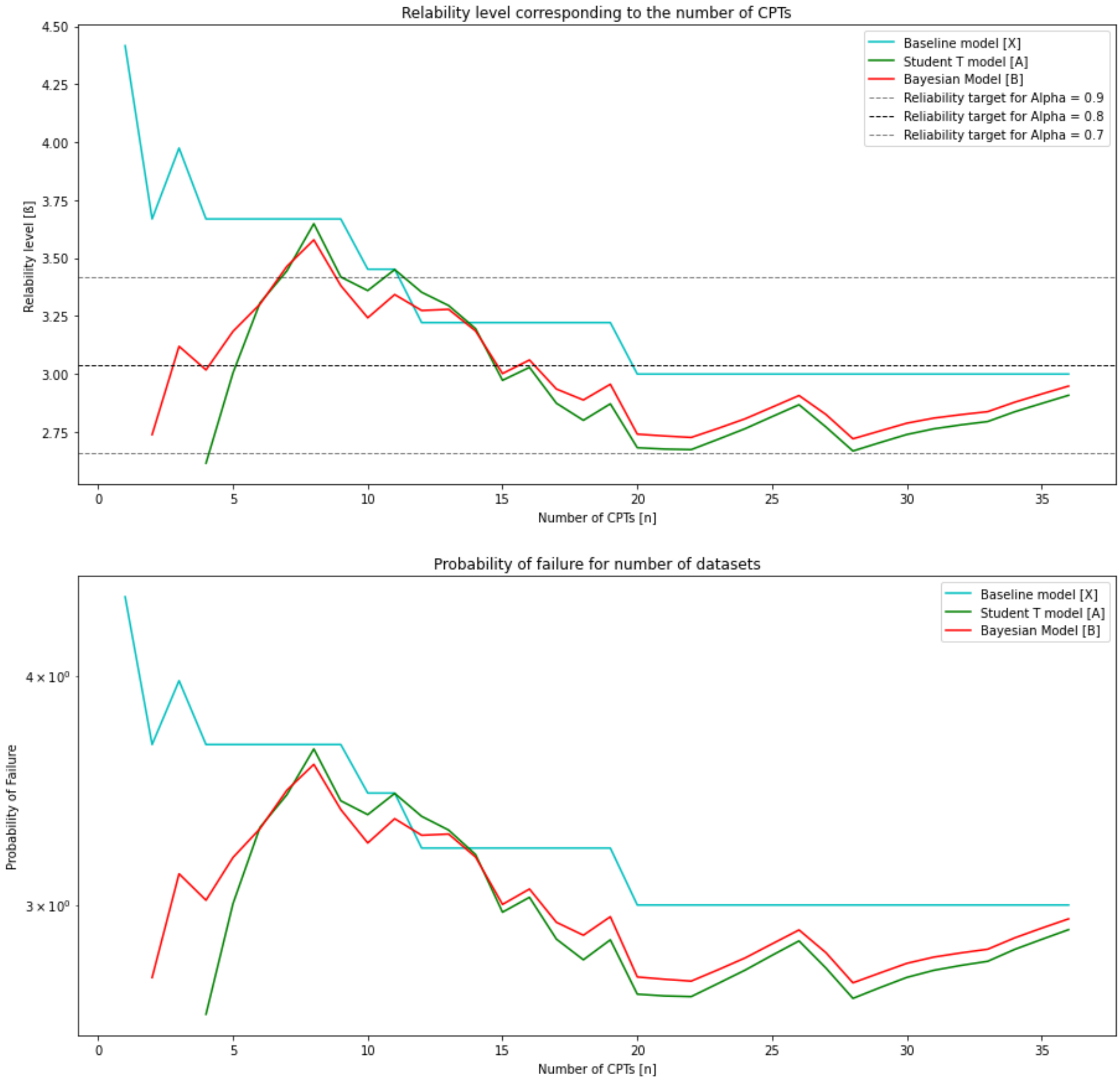

FIGURE 21 – RESULTS OF THE RELIABILITY ASSESSMENT WITHOUT PROBABILISTIC LOAD MODEL

EN1997 recommends an influencing factor of $\alpha_{resistance}$ = 0.8 for the resistance side if the relative influence of the load and resistance model is unknown. For Case Amsterdam, this recommendation seems to be on the low side if n > 16, where the reliability index from Figure 14 converged towards the set target from EN1990. Indicating a conservative value of the design load.

Figure 21 shows that the general reliability pattern regarding the number of CPT inputs is also observed in Figure 14. The main difference is that the recommendation of EN1990 for this calculation requires a higher reliability index as evaluated if the higher range of CPT inputs is investigated, n > 17. This indicates an underestimation of the spatial variability and the uncertainty due to limited observations for EN1997 designs, compared to EN1990 requirements. This impression is underlined if the relative importance of the resistance model is investigated in Figure 18, where the load is closely linked to the CoV of the total resistance and thus higher for the lower end of CPT inputs.

On the other hand, is the relative influence (Figure 18) of the load model lower than the EN1990 requirement of 0.8 for the lower range of the inputs, thus 5 < n < 15. This increases the impression that the designs achieved for very homogeneous resistances are even more conservative than the results from Figure 14 imply.

The relative influence of the model quantifications presented in Figure 15 remains the same if the load model is excluded. The conclusion of the dominant role of the Koppejan resistance is again visible, as presented in Appendix 8. The ratio of the influence of the variables in the resistance model is the same as observed in Figure 16, the main difference is that the exclusion of the load model leads to a total increase of the influence of all remaining variables since the squared sum of the factors remains 1.

4.9 CONCLUSIONS - CASE AMSTERDAM

After analyzing the results of the reliability assessment for the CPT field in Amsterdam the following statements can be made of the EN1997 designs with homogeneous soil conditions:

1. The uncertainty surrounding the Koppejan resistance (q_K) is of the largest influence on the assessed reliability as visible in Figure 15 (Plot 1 and 6) and Figure 16 (Plot 2). This leads to the conclusion that the strong (sand) layers in the soil profile have the biggest impact on the assessed reliability and achieved bearing capacity. This is further supported by the sensitivity analysis where the soft layers are from negligible influence (Figure 16).

2. Due to the discrete method for the treatment of the statistical uncertainty with the correlation factor (Table 2), two plateaus in both the correlation factor and the design dimensions are visible in Figure 13. On the plateaus, 9 < n < 20 and 19 < n 36 the correlation factor is constant. The underlying reason is the discrete logic of Table 2 for accounting for the number of observations. This is in contrast with the fully probabilistic quantification models [A and B] which integrate the statistical uncertainty continuous with Eq. 21 and the updating process in section 3.4. However, this stepwise accounting for the statical uncertainty had no significant impact on the assessed reliabilities in Figure 14 and Figure 21, thus indicating that the discrete method of accounting for statical uncertainty caused by the number of observations in the EN1997 design does not lead to significant sensitivity of the design dimensions and assessed reliabilities.

3. If the CoV of the calculated resistance, thus the spatial variability of the soil resistance, in the probabilistic quantification models [A and B] a lower than the defined variability category of 12% in Table 2, the resulting Eurocode design dimensions in this case study are evaluated to be more conservative, thus a bigger design dimensions, than required by the reliability target EN1990 (Figure 15 – Ploy 4). This suggests that an additional category for CoV < 12% for the resistance could optimize designs if the spatial variability can be expected to be homogeneous. This conclusion was underlined in the findings in Figure 20.

4. If limited data is available, thus n < 10, the Bayesian model [B] can lead to accurate assessments if the prior assumptions are chosen representative, thus compensating for the uncertainty due to limited observations (Figure 14). The Priors have a strong influence if limited data is provided, and therefore a good estimation of the layer strength is necessary to benefit from the updating model. If less informative priors are used the Bayesian model [B] is as conservative as the Student T model [A] for limited observations The Student T model, therefore, indicates a bias towards a less reliable design if the number of observations (CPTs) is low, in Case Amsterdam n < 7 (Figure 14 and Figure 21). This can be explained by the influence of Eq. 20 which in this case estimates the uncertainty for limited observations to be larger than the integration of the statistical uncertainty through the correlation factor from Table 2 in the EN1997 design suggest.

5. The influence of the model uncertainty (as estimated based on Deltares (2020)) is higher than the partial model factor in EN1997 (Figure 19 – Plot 2) suggests. The optimal partial load factor for the investigated cases, based on calibration using the design value method, is slightly higher than the value of 1.1 in EN 1997.

6. The combination of the two partial factors on the resistance side is lower than the recommended combined partial factor (γ_M). This is a direct consequence of the underestimation of the influence of the uncertainties in the resistance model. This is also supported by the findings in Figure 21, where the assessed reliability of the isolated resistance model is lower than the EN1990 recommendation. This is caused by the fixed partial factors assumed in the load model (Appendix A-1) and therefore a conservative design value of the load. Following Figure 19, the partial load factors could be reduced since the influence of the load components is relatively small, if calibrated for this particular problem in isolation.

7. The reliability target set in EN1990, thus a reliability index of 3.8, seems to be achieved by the EN1997 designs for the Amsterdam CPT field under the chosen fully probabilistic models. This means that designs based on the proposed model pile method in EN1997 fulfil the reliability requirements set in EN1990. With a low number of inputs, the designs are evaluated to be conservative, for Case Amsterdam. This can be explained by statement 3.

8. The findings for the isolation of the resistance model indicate that a reliability assessment without a probabilistic load model and optimized partial factors for the resistance can lead to similar results as an assessment with a probabilistic load model. This is evident in Figure 16 and Figure 17 where the uncertainty of the resistance is higher, and the influence of the load is lower than EN1990 recommends. Consequently, the designs based on the design value (Appendix A-1) were too large, thus leading to a less reliable assessment than Figure 14, which was determined with a probabilistic load model. Since the partial factors for the load model Appendix A-1 are fixed, a trial and error calibration of the resistance partial factors could be done, which corresponds to the assessed reliabilities in Figure 14.

The final conclusions from these statements will be drawn in Section 6.2. The statements serve as a summary of the observed relationships in the assessment for Case Amsterdam.

5. CASE ALMERE

The second case which is analyzed in this report is Case Almere. The side data given for this case are extracted from TNO (2022). The site data consists of 36 CPTs positioned near the city of Almere in the central north of the Netherlands, east of the capital Amsterdam. The soil profiles in Almere are known for their high spatial variability in the Netherlands and therefore offer a different insight into the EN1997 design process than the CPTs provided for the case study in Amsterdam.

5.1 DATA LOCATION AND GRID POSITION – CASE ALMERE

The project area investigated in Case Almere is in the centre of the city Almere, which is in the region of Flevoland. Figure 22 shows the general location of the CPT field in the context of the region Amsterdam on the left, and the grid orientation of the CPTs at the location on the right.

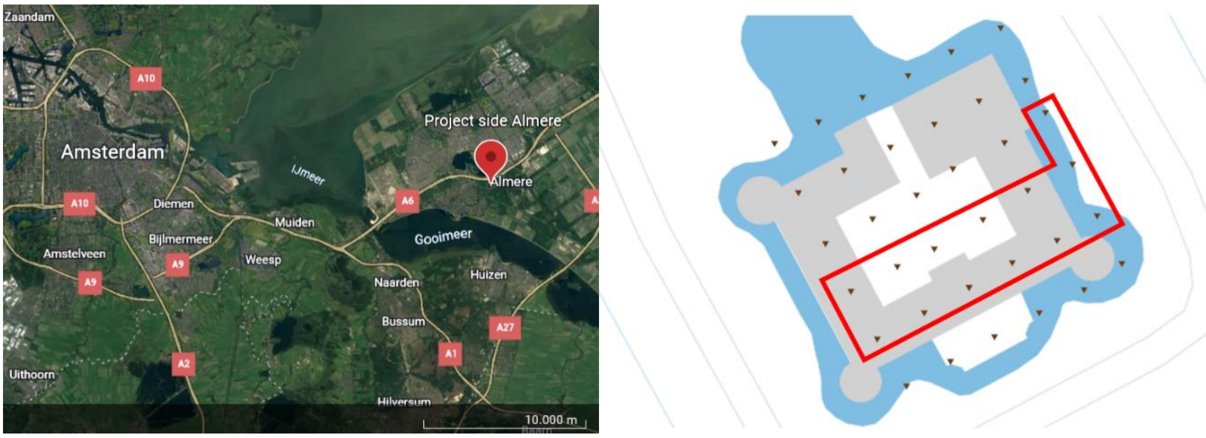

FIGURE 22 – PROJECT LOCATION (LEFT) FOR ALMERE (GOOGLE EARTH, 2022) AND CPT GRID (LEFT) (TNO, 2022)

The project area in Almere has a similar geological history as the location in Amsterdam. The soil profile is characterized by sedimentation processes in the Pleistocene and Holocene period. During this period due to changes in sea level, sedimentation of sands and other finer particles led to a soil profile which consists of soft soils, mainly clay, organic clays and peat layers, interrupted by sand layers. These sand layers are correlated with the evolution of the river Rhine and Maas in the area which lead to sand deposition.

Within the project area, 36 CPTs were positioned in the grid shown in Figure 22 below. The encircled CPTs within the red boundaries marked in Figure 22 are excluded in the following assessment. The CPTs in the red area show different characteristics than the rest of the CPT measurements, mainly a shallower sand layer, which leads to spatial variability of the determined resistance by the calculation methods of more than 25%. To obey the design rules of EN1997 from Table 2 these CPTs need to be therefore excluded and could be analysed as a different dataset. After the subdivision of the encircled area, 22 CPTs remain for the design of the foundation pile foundation, thus the CPTs outside of the red shape.

The grid consists of 36 measurements up to a depth of -25m of the surface. The CPTs cover the whole area of interest such that a pile design can be safely created for the area with an average distance of 16m between the measurements.

5.2 SITE DATA ANALYSIS AND DESIGN CHOICES – CASE ALMERE

In the case of the Almere, the provided data for the design consists of 21 CPTs as established in 5.1. The CPTs can be analyzed to derive a soil profile of the area. Additionally, to the provided CPTs, TNO (2022) provides a soil sample of the area. Further, a CPT classification of the soils is done with the Robertson classification method. After cross-referencing the classifications to the sample, the following soil profile is assumed.

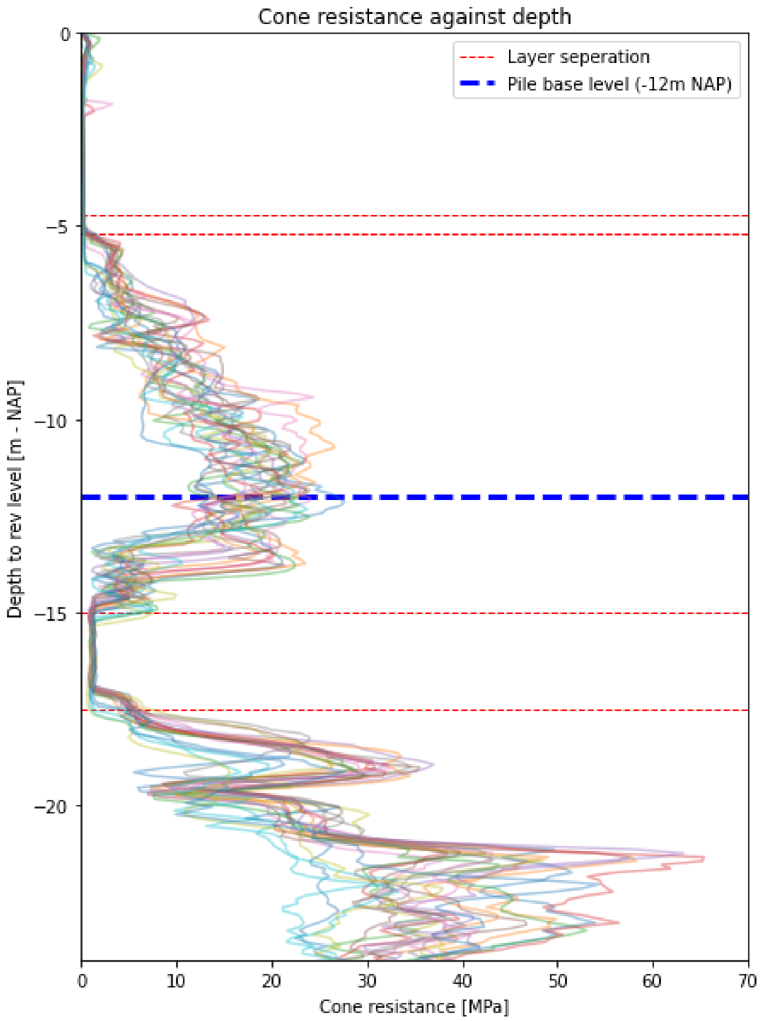

Soil layer	Starting Depth [-m NAP]
1st Layer – Clay	0
2nd Layer - Peat	4.7
3rd Layer – Sand	5.2
4th Layer - Clay	15
5th Layer - Sand	17.5

FIGURE 23 - CONE RESISTANCES OF ALL CPTS (LEFT) AND RESULTING SOIL PROFILE (RIGHT) FOR ALMERE

The soil profile in the project area can be characterized by 5 distinct layers. The first layer is a soft clay layer which is a result presents and drainage of the seawater in during the repopulation of the Almere area. Below that clay layer, a small peat layer is found only spanning a total depth of 0.5m. The peat layer is mainly ignored in the design due to Table 7.

The 3rd consists of fine sands. The properties of the sand layer were derived from the CPTs classification and the soil samples. This layer will serve as the foundation layer of the piles since it is expected that the necessary strength of the pile will be reached if the pile's bases are placed into the sand layer.

Further below the foundation layer, another clay layer is presented, however, the influence area of the Koppejan resistance (q_K) is not expected to reach this depth since there is a depth since the start of the layer is more than 4m deeper than the pile base.

The design choices for the material, pile shape, pile length, pile installation method and design load are consistent with the choices in Table 3, thus with Case Amsterdam. This means that a precast, square concrete pile with a shaft length of 12m is chosen for the field. In practice, it would be expected that the shaft length is chosen such that the pile base is positioned into a strong sand layer. A depth of 12m guarantees both more consistent results between the CPTs, thus less CoV and a position within the strong sand layer.

From the soil profile for the Almere (Figure 23), one can extract the soil type present at all depths of interest. Together with Table C.2 from EN1997 the following pile class factors can be determined. The table is given in Appendix 5.

TABLE 7 - PILE CLASS FACTORS FOR CASE ALMERE (EN1997 - C.2)

Parameter of interest	Pile class factor following Table
Shaft friction 1st Layer (Clay)	0.02
Shaft friction 2nd Layer (Peat)	0
Shaft friction 3rd Layer (Sand)	0.01
Base resistance	0.7

The pile class factors described in Table 7 are implemented both in the EN1997 design and the uncertainty characterization, and thus are consistent in all resistance models in the assessment.

The objective of the Eurocode design is to optimize the side length of a rectangular precast concrete cross-section such that the design fulfils the requirements set in EN1997. This means a material optimization of the lowest allowed side length of the foundation piles.

The calculation setup follows the same structure as for the case in Amsterdam. Thus, starting with an assessment with a load model and finishing with an assessment without a load model. A simplified scheme of the calculation setup can be found in Figure 9.

5.3 VARIABLE SETUP - CASE ALMERE

This section introduces the choices for the variables in the load and resistance models for Case Almere.

VARIABLE SETUP FOR THE LOAD MODEL

The design choices for both the Amsterdam and the Almere cases are consistent with Table 5, which leads to the same load models, which are derived from EN1990 (Section 6.2.2). This implies that the load model is the same as presented in section 4.3 of the report.

VARIABLE SETUP FOR THE RESISTANCE MODELS

The following table gives an overview of the variables used in the resistance models for the Almere field. First, the variables of the EN1997 design are presented, including a reference if recommended values are used. For a detailed explanation of the calculation methods used, see section 3.3.

After that, the variable setups of the probabilistic quantification models are presented. Starting with the baseline model [X]. Followed by the Student T model [A] and the Bayesian model [B].

For more information on the evolution and reaction of the model to the site data, the probability densities of the different resistances are presented and analyzed in Appendix C-10.

TABLE 8 - VARIABLE SETUP FOR THE RESISTANCE MODELS FOR CASE ALMERE

Variable	Distribution	Description
		Eurocode design resistance model variables (Semi probabilistic design)
Koppejan resistance(q_K)	Deterministic	Expected/Mean value from the sample, Dependent on design dimensions
Shaft resistance 1st Layer (q_{S1})	Deterministic	Expected/Mean value from the sample, Dependent on design dimensions
Shaft resistance 2nd Layer (q_{S2})	Deterministic	Expected/Mean value from the sample
Shaft resistance 3rd Layer (q_{S3})	Deterministic	Expected/Mean value from the sample
Shaft resistance 4th Layer (q_{S4})	Deterministic	Expected/Mean value from the sample
Partial model factor (γ_{Rd})	Deterministic	1.1 from Eurocode 1997 – Table 6.3
Partial resistance factor (γ_{Rc})	Deterministic	1.1 from Eurocode 1997 – Table 6.6
Correlation factor (ζ)	Deterministic	Dependent on data properties and number of tests, Given in Eurocode 1997 – Table 6.5 (Table 2)
		Baseline model resistance [X] quantification variables
Koppejan resistance(q_K)	Normal	$N(\widehat{\mu_K}, \widehat{\sigma_K})$, Sample mean, sample standard deviation, always based on all 36 CPTs, Dependent on design dimensions
Shaft resistance 1st Layer (q_{S1})	Normal	$N(\widehat{\mu_K}, \widehat{\sigma_K})$, Sample mean, sample standard deviation, always based on all 36 CPTs
Shaft resistance 2nd Layer (q_{S2})	Normal	$N(\hat{\mu}, \hat{\sigma})$, Sample mean, sample standard deviation, always based on all 36 CPTs
Shaft resistance 3rd Layer (q_{S3})	Normal	$N(\hat{\mu}, \hat{\sigma})$, Sample mean, sample standard deviation, always based on all 36 CPTs
Shaft resistance 4th Layer (q_{S4})	Normal	$N(\hat{\mu}, \hat{\sigma})$, Sample mean, sample standard deviation, always based on all 36 CPTs
Model factor (m_R)	Normal	$N(1,0.1)$ No systemical bias, with expected 10% variations in total resistance by (Deltares, 2020)
		Student T resistance model [A] quantification variables
Koppejan resistance(q_K)	Student - T	$T(\widehat{\mu_k}, \widehat{\sigma_k}_T)$, Sample mean, For degrees of freedom corrected sample standard deviation, Dependent on design dimensions
Shaft resistance 1st Layer (q_{S1})	Student - T	$T(\widehat{\mu_{S1}}, \widehat{\sigma_{S1}}_T)$, Sample mean, For degrees of freedom corrected sample standard deviation, Dependent on design dimensions
Shaft resistance 2nd Layer (q_{S2})	Student - T	$T(\widehat{\mu_{S2}}, \widehat{\sigma_{S2}}_T)$, Sample mean, For degrees of freedom corrected sample standard deviation
Shaft resistance 3rd Layer (q_{S3})	Student - T	$T(\widehat{\mu_{S3}}, \widehat{\sigma_{S3}}_T)$, Sample mean, For degrees of freedom corrected sample standard deviation
Shaft resistance 4th Layer (q_{S4})	Student - T	$T(\widehat{\mu_{S4}}, \widehat{\sigma_{S4}}_T)$, Sample mean, For degrees of freedom corrected sample standard deviation
Model factor (m_R)	Normal	$N(1,0.1)$ No systemical bias, with expected 10% variations in total resistance, from tests by (Deltares, 2020)
		Bayesian resistance model [B] quantification variables
Koppejan resistance mean (μ_K)	Normal	$N(\mu_0, \sigma_0)$, Prior mean $\mu_0 = 14\ [MPa]$, Prior standard deviation $\sigma_0 = 5[MPa]$
Koppejan resistance variability (τ_K)	Gamma	$G(\alpha_0, \beta_0)$, Prior shape factor $\alpha_0 = 2[-]$, Prior scale factor $\beta_0 = 11$
Shaft resistance means 1st Layer (μ_{S1})	Normal	$N(\mu_0, \sigma_0)$, Prior mean $\mu_0 = 0.5\ [MPa]$, Prior standard deviation $\sigma_0 = 1[MPa]$
Shaft resistance variability 1st Layer(τ_{S1})	Gamma	$G(\alpha_0, \beta_0)$, Prior shape factor $\alpha_0 = 1[-]$, Prior scale factor $\beta_0 = 0.01$
Shaft resistance means 2nd Layer (μ_{S2})	Normal	$N(\mu_0, \sigma_0)$, Prior mean $\mu_0 = 1\ [MPa]$, Prior standard deviation $\sigma_0 = 1[MPa]$
Shaft resistance variability 2nd Layer(τ_{S2})	Gamma	$G(\alpha_0, \beta_0)$, Prior shape factor $\alpha_0 = 1[-]$, Prior scale factor $\beta_0 = 0.005$
Shaft resistance mean 3rd Layer (μ_{S3})	Normal	$N(\mu_0, \sigma_0)$, Prior mean $\mu_0 = 10\ [MPa]$, Prior standard deviation $\sigma_0 = 5[MPa]$
Shaft resistance variability 3rd Layer(τ_{S3})	Gamma	$G(\alpha_0, \beta_0)$, Prior shape factor $\alpha_0 = 1[-]$, Prior scale factor $\beta_0 = 6$
Model factor (m_R)	Normal	$N(1,0.1)$ No systemical bias, with expected 10% variations in total resistance (Deltares, 2020)

5.4 RESULTS EN1997 DESIGNS – CASE ALMERE

First, the design results from EN1997 for the Case Almere are analyzed. The design dimensions are the results of the Model pile method (EN1997 – Section 6.6). The design choices from Table 3 are applied in the design process. These design dimensions are used as an input for all probabilistic quantification models and are independent of the chosen load model as depicted in Figure 2. The resulting design dimensions are investigated for a range of CPT inputs. Figure 24 shows these results.

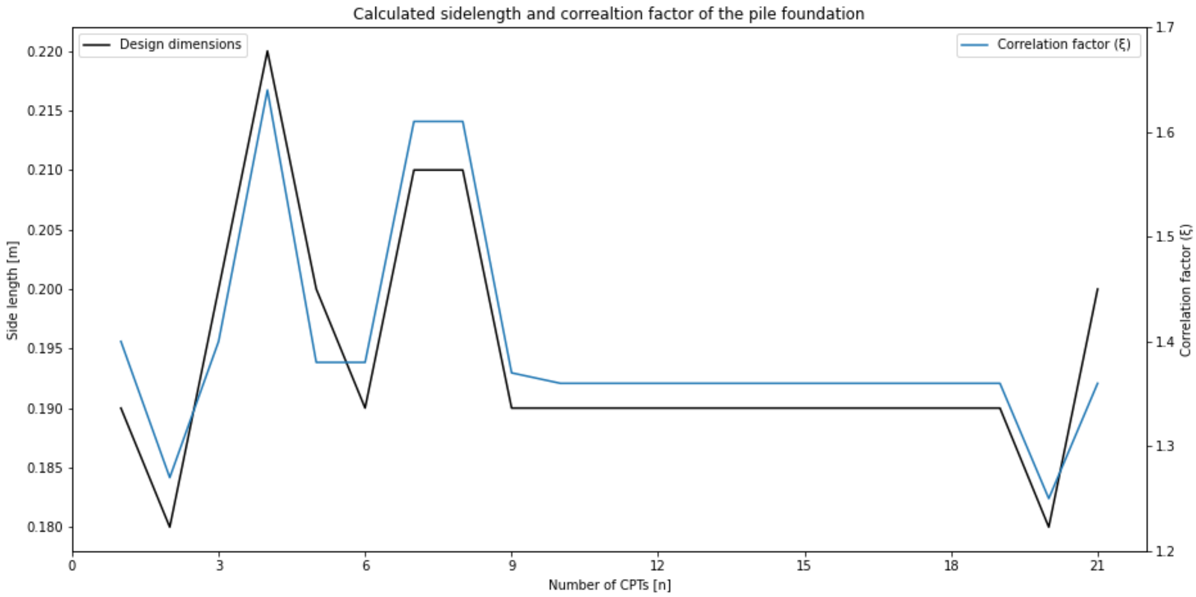

FIGURE 24 - EUROCODE DESIGN DIMENSIONS FOR ALMERE

The first observation for Figure 24 is that the fluctuations of both the design dimensions and the correlation factors (ζ) are less predictable than for a homogeneous CPT field (Case Amsterdam – Chapter 4). This indicates a higher sensitivity of the model to the CPT inputs if the overall CoV, thus spatial uncertainty, of the resistance of the CPT field is larger. The trends and values coming from the CPT measurements are presented in Appendix C-9.

For $3 < n < 10$, the relative variance of the calculated resistance seems to be higher compared to the rest of the input range, this leads to fluctuations in the correlation factor resulting in jumps in the spatial variability category (rows) in Table 2.

The design dimension also changes due to the change in total expected resistance. As visible for n = 5. The variance category determined by the Eurocode remains constant with n = 6, but a reduction in design dimension is observable. This suggests an increase in expected resistance, thus an increase for Koppejan resistance (q_K) and shaft frictions (q_s) in the soil profile. This can be explained by the increase in resistance in the Koppejan resistance and the shaft friction for n = 6 (Appendix C-9).

There is a decreasing trend in the quantified resistances for both the Koppejan resistance and the shaft friction, with the direction of the CPT inputs. This compensates for the decrease of the correlation factor at n = 9. The decreasing trend again impacts the design dimensions at n = 20. More details of the CPT input values and the trends are given in Appendix C-9.

Further is visible that the correlation factor has a strong influence on the chosen design dimensions, which emphasizes the importance of Table 2 in the EN1997 design.

5.5 RELIABILITY ASSESSMENT WITH PROBABILISTIC LOAD MODEL - CASE ALMERE

In this section, the results of the reliability assessment for the CPT field in Almere and the resulting design dimensions are presented. All three probabilistic quantification models [A, B and X] are used to evaluate the load situation and the resistance of the designed pile foundation.

For this evaluation two different reliability methods, the MCS and FORM, are used and compared. The limit state is consistent with the choices for Case Amsterdam and follows the principle from Eq. 30. Figure 25 shows the results of the reliability analysis.

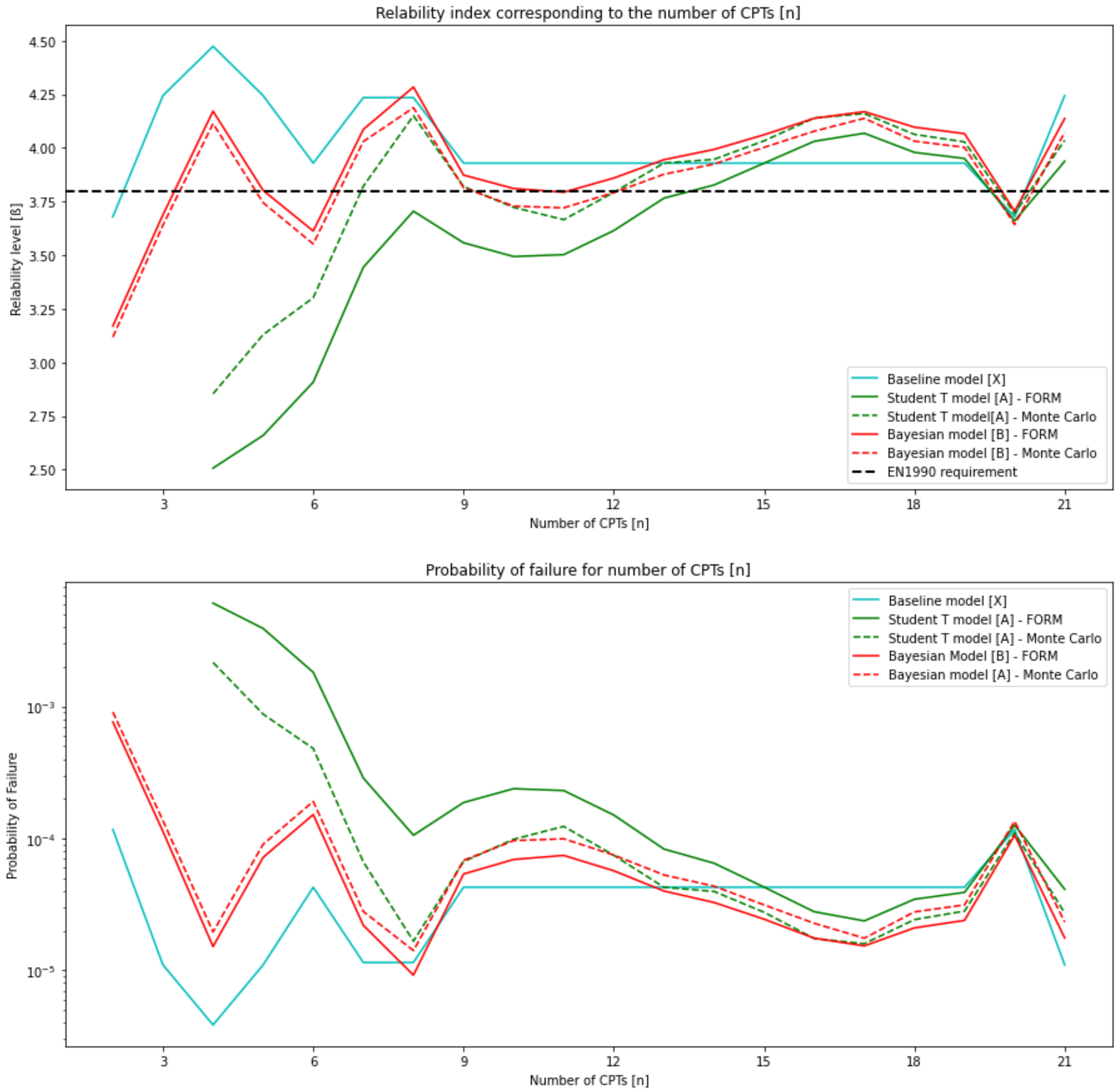

FIGURE 25 - RESULTS OF THE RELIABILITY ASSESSMENT FOR ALMERE

The first observation from Figure 25 is that the difference in assessed reliability between the quantification models [A and B] is larger than for Case Amsterdam (Chapter 4). For fewer CPT inputs, thus n > 14, the Student T model assesses the design pile as unsafe regarding the reliability target (β = 3.8) from EN1990. The Bayesian model [B] evaluates the design as unsafe for n = 2 observations. This difference decreases with more CPTs entering the design process, such that a convergence of both models, in the range of β = 3.8 ± 0.5, towards the EN1990 required reliability target is visible for n > 7.

The difference between the MCS and the FORM for Student T model [A] is larger for the lower range of inputs, while a convergence between the methods is observable for more inputs, suggesting an agreement of the reliability methods for the lower input range, n > 12. This suggests that a convergence of both the reliability methods and the different probabilistic quantification models towards the reliability target set in EN1990 is visible if the model pile method from EN1997 is followed.

To further investigate the influences of the different resistances resulting from the inputs and the design dimensions, the mean and standard deviations of total resistance, Koppejan resistance (q_K) and shaft friction ($q_{s,3}$) for the 3rd layer are presented in Figure 26.

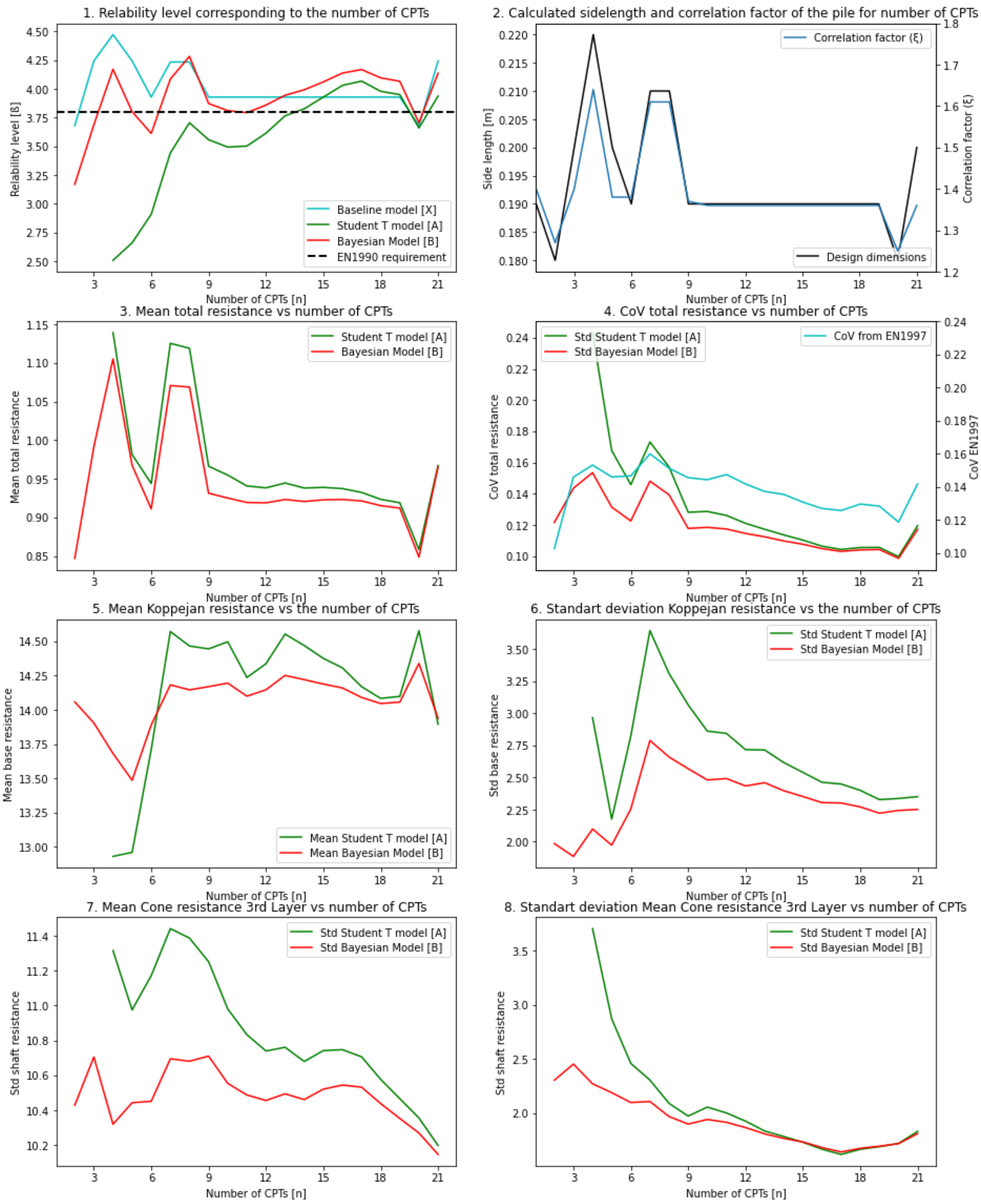

FIGURE 26 - RELIABILITY INDEX, MEAN AND STANDARD DEVIATIONS OF CONTRIBUTING VARIABLES

The total resistance (Plot 3) is calculated with Eq. 20. For plot 4 the CoV of EN1997 is determined as the calculated resistance in the field taken from Eq.13 between the CPTs, while the CoV of the probabilistic models is determined per layer for the shaft. This results in comparable but not identical results for the variability in the models. It was therefore chosen to plot them on different axis to highlight these differences.

From Figure 26 the following observations can be made. The variability of the total resistance is mainly following the trend of the variability in shaft friction ($\mathrm{q_{s,3}}$) of the 3rd layer (Plot8), which is steadily decreasing from a standard deviation of 3.5 MPa towards a value of 2 MPa, over the CPT range (n).

The Koppejan resistance ($\mathrm{q_K}$) also contributes such that the peak in plot 6 around n =7 is visible in the total variability of the resistance (Plot 4). Furthermore, is an anti-proportional relation between the total observed/estimated variance and the assessed reliability is visible (Plots 1 and 4). This suggests that the achieved reliability levels are dominated by the uncertainty in the models.

In plot 4 (blue line right scale) it is visible that there are two spikes in the CoV of the EN1997 resistance that exceeds the 15% threshold at n = 4 and n = [7,8]. These spikes both correspond to changes in assessed reliability (Plot1), design dimensions (Plot 2) and mean total resistance (Plot 3). This explains the slight increase in CoV from EN1997(Plot 4) where the blue line crosses the threshold of 15% which is changing the assigned correlation factor (ζ) in Table 2. Therefore, indicating a sensitivity due to the discrete nature of the EN1997 treatment of uncertainty.

5.6 SENSITIVITY ANALYSIS OF THE UNCERTAINTY OF THE CONTRIBUTION VARIABLES – CASE ALMERE

To investigate the influence of the quantified uncertainties on the assessment a sensitivity analysis of all contributing variables is done. The results are presented in Figure 27 below. It was chosen to exclude the influence of the 2nd layer due to the neglection of the layer's resistances for the designs.

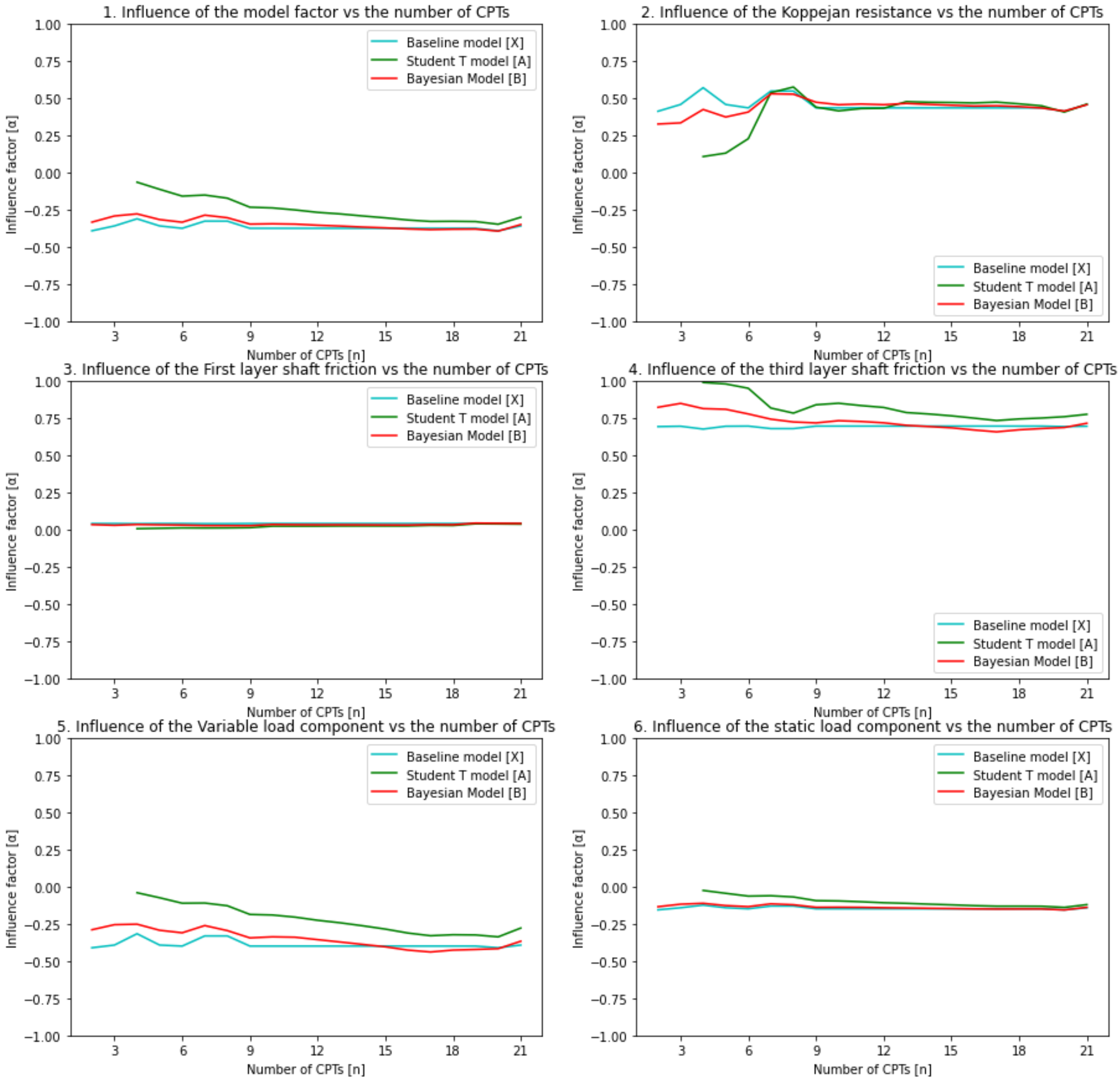

FIGURE 27 - INFLUENCE FACTORS OF THE CONTRIBUTING VARIABLES

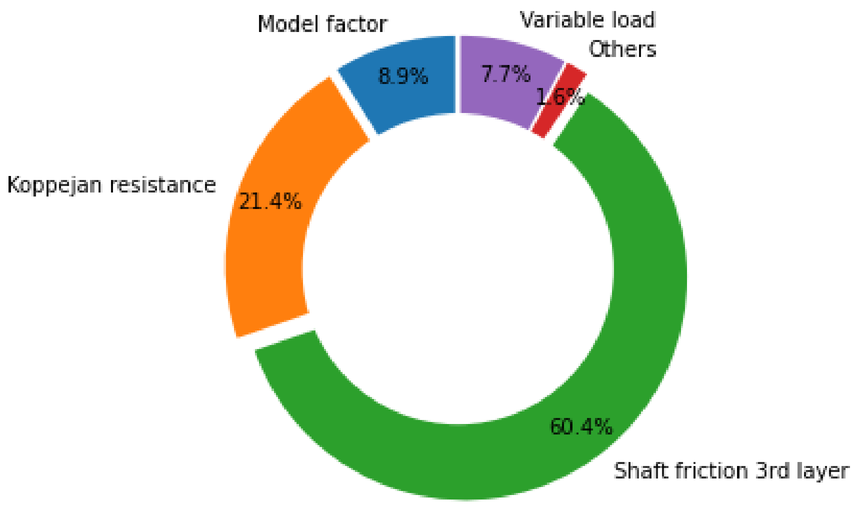

FIGURE 28 - THE SQUARED INFLUENCE FACTORS OF THE STUDENT T MODEL [A] FOR 21 INPUTS

In Figure 28, the static load and the shaft friction (q_s) of the 1st and 2nd layers have an Influence factor lower than 1% and are summarized in the chart as others. While investigating Figure 27 and Figure 28 the first noticeable observation is the high influence of both the Koppejan resistance (q_K) and the third layer shaft friction ($q_{s,3}$). For the last iteration, with 21 CPTs, the uncertainty of both resistances together contributes more than 80% towards the sensitivity of the assessed reliabilities and therefore are dominant in the analysis. Also, visible I the relatively high influence of the model factor can be explained due to the increased spatial variability in the found resistances. This finding is supported by all probabilistic quantification models [A, B and X].

Furthermore, is visible that the soft soil layers, the 1st and 2nd layer in the soil profile, are from negligible influence from the assessed reliability, which a combined contribution of less than 1% to the sensitivity. The same is visible for the static load component in the probabilistic load model Figure 27.

The Student T model evaluates the influence of the third layer shaft friction as more dominant than the Baseline [X] and the Bayesian model [B] suggest. This is visible at the lower ranges of CPT inputs, thus for n < 6. This is a direct consequence of the higher variance found for the Student T model in the 3rd layer shaft friction (Figure 26-Plot 8). Since the squared sum of the influence factors is 1, the influence of the Koppejan resistance (q_K) in this range is lower in model A than in both other models.

As for Case Amsterdam, the variables are divided into load and resistance model variables to investigate the relative influence of the uncertainties on both assessment sides.

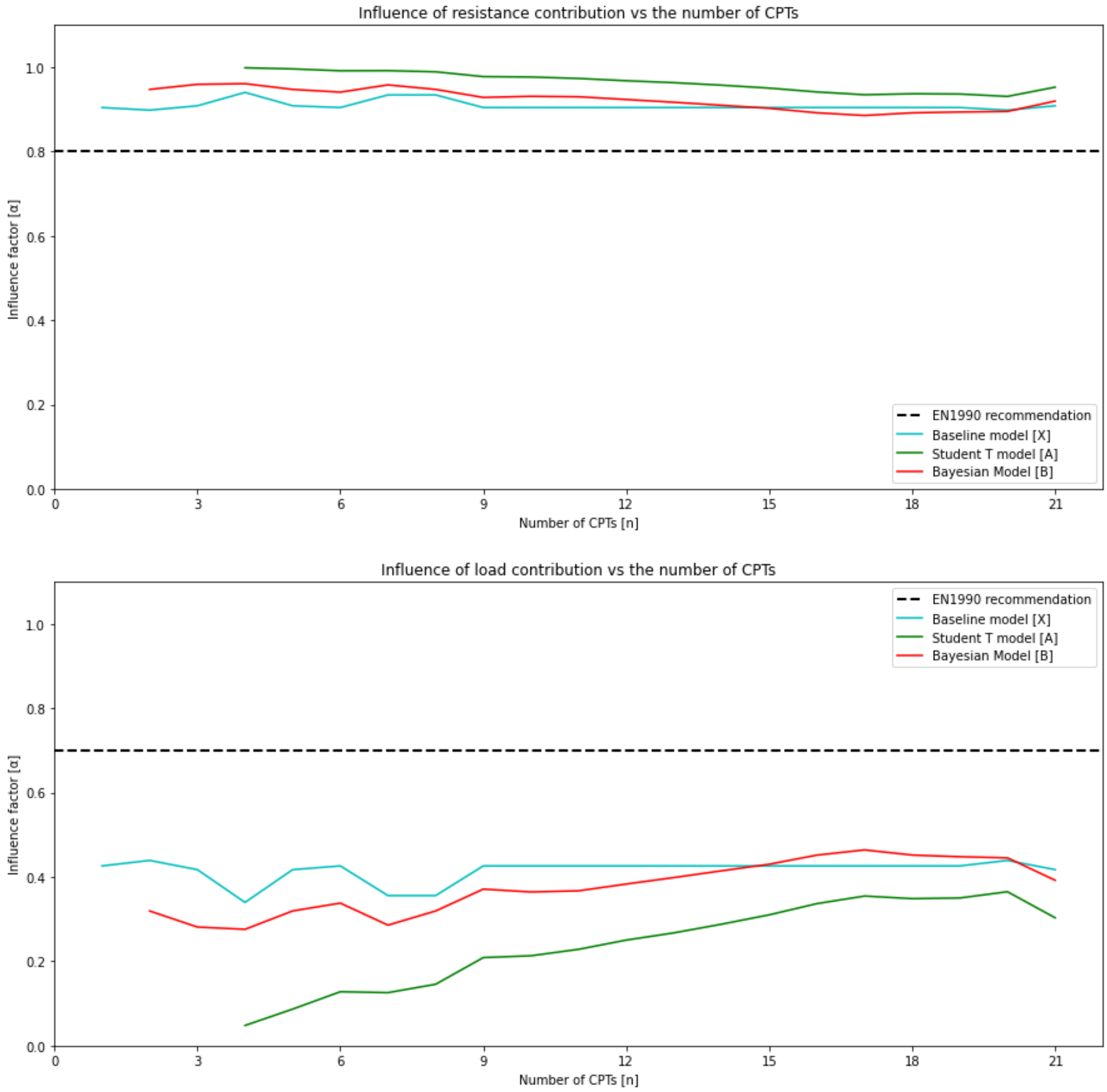

FIGURE 29 - RELATIVE INFLUENCE OF THE LOAD AND RESISTANCE MODEL

Figure 29 shows that for the Case Almere the resistance model dominates the reliability assessment, such that the influence value is consistently higher than the EN1990 recommendation of 0.8. This is already observed in Figure 28, where the two dominating variables, the Koppejan resistance (q_K) and the 3rd layer shaft friction ($q_{s,3}$) influence more than 80%. The load model contribution also includes the model factor which suggests that a value close to 0.9 is more suited in this case.

Consequently, the influence of the probabilistic load model is lower than for the homogeneous case, this leads to a relatively small contribution to the probabilistic uncertainty of the load model and suggests that this load quantification may not be necessary.

5.7 PARTIAL AND CORRELATION FACTOR CALIBRATION FOR THE RESISTANCE MODEL – CASE ALMERE

To analyze to which degree the fully probabilistic quantification models agree with the treatment of different types of uncertainties in the semi-probabilistic design, a calibration of the patrial factors is done. This calibration is based on the same assumptions as presented in Section 4.7, thus the normality of the resistance model and the model uncertainty. The influence factors taken from the

FORM analysis are used to calibrate the partial factors if the variable quantifications of models A and B are used.

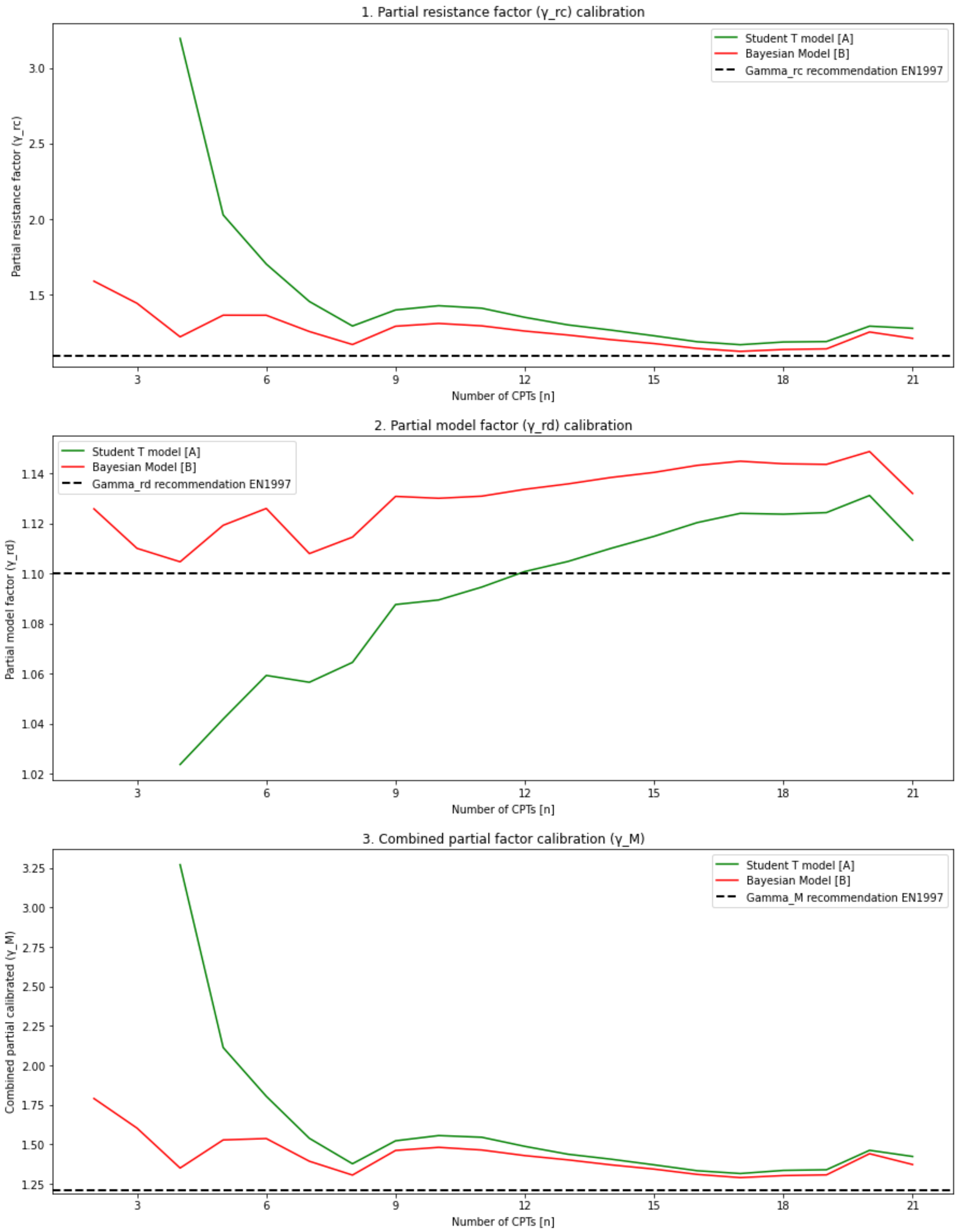

FIGURE 30 - CALIBRATION OF THE PARTIAL FACTORS

The calibration in Figure 30 (Plot 1) shows that the Eurocode recommendation for the partial resistance factor (γ_{RC}) of 1.1 is evaluated to be insufficient for the spatial variability and the uncertainty due to limited observations quantified by the probabilistic models [A and B]. The biggest difference between the recommendation is found for the Student T model [A] for the n < 8. This indicates that the Student T model [A] evaluates the uncertainty due to limited observations of the calculated resistance to be larger than the EN1997 suggests. This underestimation of the variability is visible in both models, A and B, and strongest if a small number of CPTs is integrated into the design (n < 8). This is expressed in a value for the combined partial factor of up to 3.5 in the Student T model [A], which is more than 300% of the recommendation of EN1997. This conservative estimate decreases rapidly till n > 8 and stabilizes to a value of 1.7 at n = 8. Thereafter a slower convergence toward the EN1997 recommendation is visible for increasing observations.

The partial model factor (γ_{RD}) recommendation of EN1997 is also lower than the optimal values based on the design value method, again suggesting an underestimation of the resistance model uncertainty. For n < 12, the Student T model assesses the partial model factor as too conservative. This can be explained by the dominating influence of the resistance uncertainty, which decreases the relative influence of the load model.

The underestimation of the spatial variability and the uncertainty due to limited observations in the resistance and the epistemic uncertainty lead toward an underestimation of the necessary combined partial factor. Since the partial factor calibration was based on Eq.6. This suggests that EN1997 underestimates the influence and uncertainty of the resistance in the model pile recipe, while overestimating the importance of the load model reflected in partial load factors which are over-conservative for the problem at hand.

The second way to calibrate the EN1997 recipe to the agreement with the probabilistic quantification is to adapt the correlation factor. This is done in Figure 31 below. This calibration is done independently of the calibration in Figure 30.

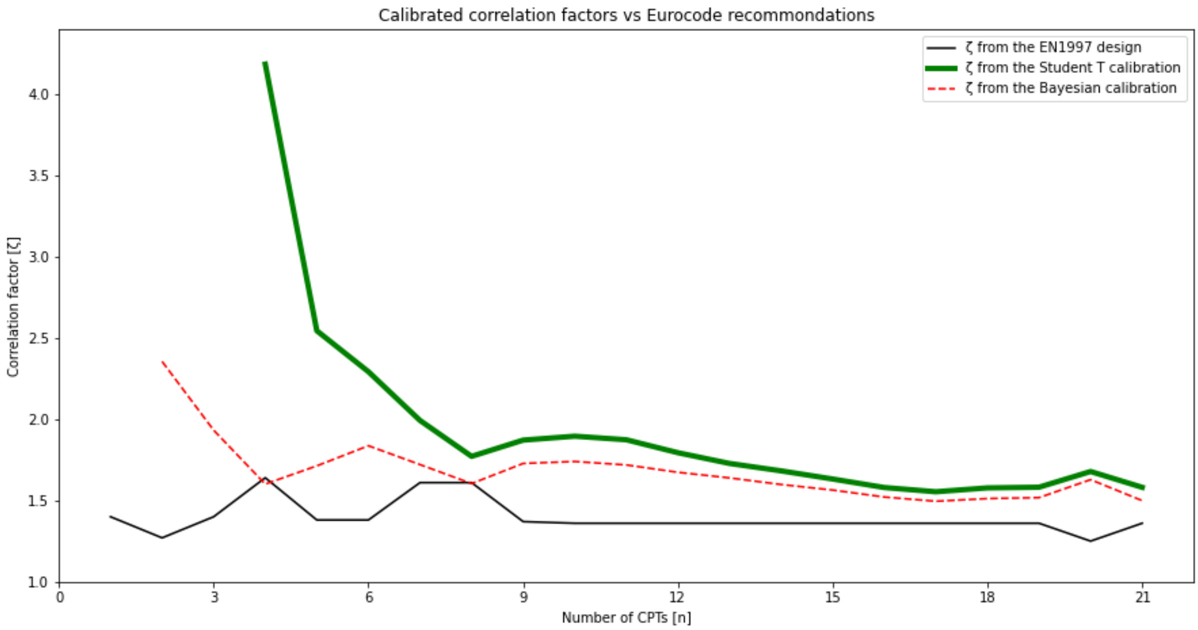

FIGURE 31 - CALIBRATION OF THE CORRELATION FACTOR

As Figure 31 shows, the calibration of the correlation factor (ζ) shows similar behaviour as the calibration of the partial resistance factor (γ_{RC}). The calibrated values of the probabilistic model are higher than the recommended values from Table 2, such that a probabilistic quantification is more conservative for the uncertainty correction for the correlation factor than EN1997 requires. This difference is the biggest if a low number of observations is integrated into the design, thus n < 6.

A difference in model behaviour is also visible if the probabilistic models [A and B] are compared to each other. The Bayesian [B] approach converges faster to a value that is close to the EN1997 design recommendations (n= 4), while the Student T model [A] is higher in absolute differences, up to 300%, in the correlation factor for limited information and needs a higher number of inputs to converge to a value close to the EN1997 design approach (n > 8). This indicates that the probabilistic model has a more conservative way of quantifying the uncertainty due to limited observations, thus through Eq. 21.

5.8 RESULTS FOR CALCULATION SETUP WITHOUT LOAD MODEL – CASE ALMERE

As for Case Amsterdam, a second assessment of the designed foundation piles is done. This assessment again investigates the whole range of CPT inputs. The difference to Section 5.5 is that the load model now is deterministic and assumes the design load. The assessment follows the same principles and simplification as the assessment in Case Amsterdam (section 4.8), therefore the limit state is equivalent to Eq. 31. The results from the FORM reliability method are presented in Figure 32.

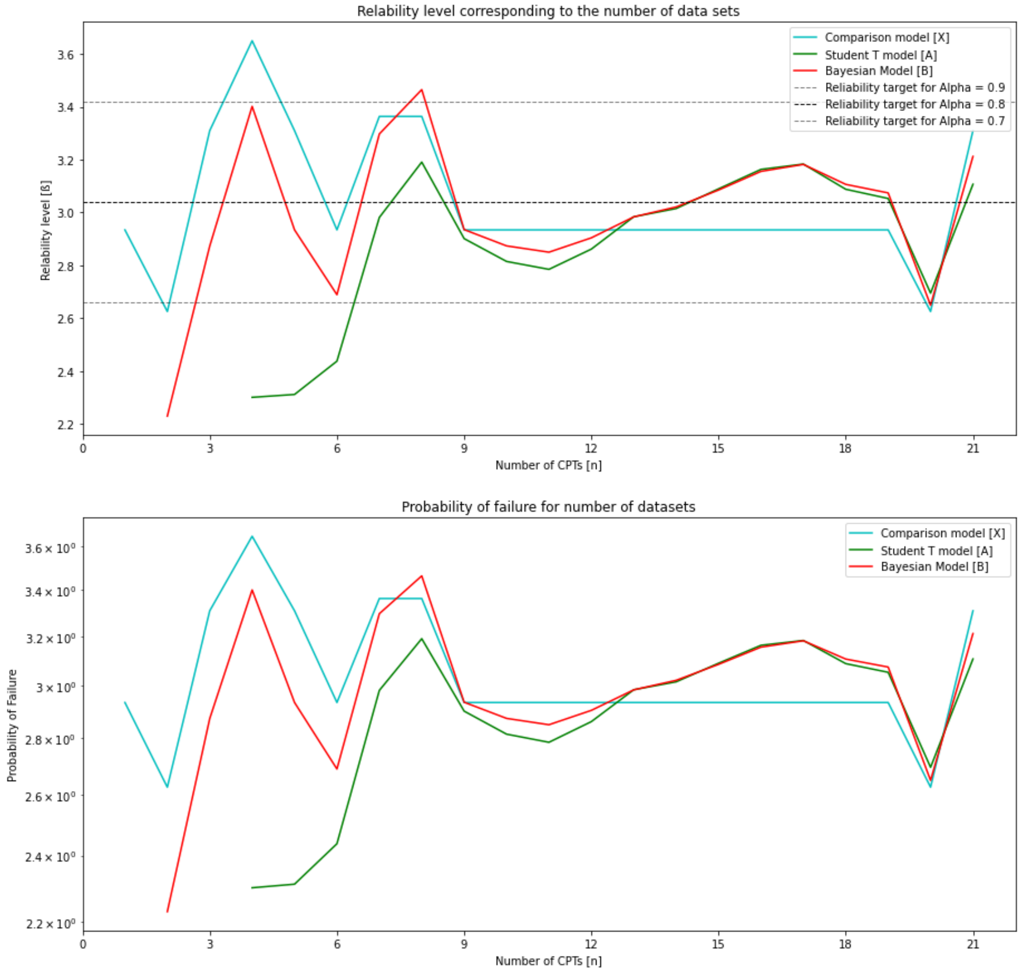

FIGURE 32 – RELIABILITY ASSESSMENT RESULTS WITHOUT THE LOAD MODEL

Figure 32 shows the results of the reliability assessment without the influence of additional uncertainty from the load model. The general shape of the assessed reliability follows the same trajectory as Figure 25. The recommended alpha value of α = 0.8 is taken from EN1990. This is already less conservative than the results from Figure 29 suggest. As visible from the reliability index is the isolated resistance reliability lower than the advised value for calibration for $8 < n < 14$. If this graph is seen in the context of Figure 29 it can be further concluded that the expected influence of the resistance model is higher than EN1997 expects. Therefore, the isolated analysis of the resistance model reveals that the EN1997 recommendations are lower than what EN1990 would require for the resistance. Again, indicating that the uncertainty on the resistance side is underestimated by the partial factors in EN1990 and EN1997 for pile foundations (while compensated by the partial load factors).

5.9 CONCLUSIONS - CASE ALMERE

From the observations made and results presented for Case Almere, the following conclusive statements are formulated made:

9. The most influential resistances regarding the assessed reliabilities are both found in the 3rd sand layer in the soil profile. In this case, the influences of the two variables resulting from this layer, shaft friction ($q_{s,3}$) and Koppejan resistance (q_K) are from dominant influence (α > 80%) on the assessed reliability, while soft layers are negligible (α < 1%) for the reliability analysis (Figure 26 and Figure 27)

10. Due to the larger spatial variability of the CPT field, the influence of the probabilistic load model (Figure 29) is lower than EN1990 suggests. Further, the influence of the isolated resistance uncertainty (Figure 32) is bigger than the EN1990 recommendation, thus dominating the sensitivity of the reliability assessment. This further underlines the conclusions from Figure 29. This suggests that in Case Almere a good quantification of the resistance model is more important than an elaborate probabilistic load model.

11. This underestimation of the uncertainty in the load model is underlined by the calibration of the partial factors for the resistance model (Figure 30). The assessment of the partial factor recommendation for both the spatial variability and the model uncertainty suggests higher values than EN1997 recommends. This indicates an insufficient coverage of the uncertainties in the resistance model by the EN1997 designs due to an underestimation of the influence of the uncertainties. However, this is compensated by an overestimation of the uncertainties in the load model, which assumes that an α_{Load}= -0.7 can be assumed. This further underlines that the resistance model is the dominating factor for pile foundation designs. This finding is also supported by Figure 32. For the isolated resistance model with the proposed design value, the assessed reliabilities are lower than $\alpha*\beta = 0.8*3.8 = 3.04$, thus the influence of the uncertainties is underestimated, otherwise, the reliabilities found resemble Figure 25.

12. The Student T model [A] shows that EN1997 designs have a bias towards underestimating the spatial variability and the uncertainty for a fewer number of inputs, n < 8 (Figure 25). Thus, the ranges with the highest uncertainty due to limited observations are evaluated to be less reliable than EN1990 suggests. Similar behaviour can be seen for the Bayesian model [B] if less informative Priors are used to design. This shows that informative priors for model B have the strongest influence for fewer numbers of CPT inputs, and therefore can help to derive to design that is in line with the reliability target in EN1990 faster. However, an opposite effect can occur if the priors are chosen in a non-representative way. If non-informative priors are used in the model, the same behaviour as for the Student T model is observable. The same interaction is also visible in the calibration of the partial resistance (Figure 30) and the correlation factor (Figure 31), thus suggesting an underestimation of uncertainty due to limited observations and spatial variability in lower ranges of inputs.

13. The design dimensions showed a high sensitivity of changes in CoV of the resistance for the total Eurocode resistance (Figure 26 – Plots 1, 2 and 4). This indicates that the discrete nature of the variability categories from Table 2, leads to significant changes in the advised correlation factor. This makes designing a foundation pile with the EN1997 recipe using

Table 2 difficult if the natural variability is close to the boundary of a natural variability category, thus between the rows of Table 2.

14. For larger numbers of CPT inputs ($n<8$), thus with decreasing statistical uncertainty the reliability assessment for both probabilistic quantification models [A and B] converges towards a value that is close to the EN1990 recommendations for a reliability target $\beta = 3.8 \pm 0.5$. (Figure 25). The isolation of the resistance model revealed that the recommendations for the partial factor and the correlation factors do not sufficiently cover the uncertainty due in the resistance model, therefore a design based on a deterministic load leads to an unsafe assessment of the structure since the proposed method to determine set load is conservative, leading to higher expected loads than necessary since the influence of the load model is overestimated.

6 COMPARISON OF THE CASES, CONCLUSIONS AND RECOMMENDATIONS

This section of the report summarizes and reflects the findings from both case studies to thereafter derive final statements for the research question. The conclusions are containing the answers to the research question formulated in Section 1.3. At last practical implications of the research findings and recommendations for further research are formulated.

6.1 COMPARISON OF THE CASES

The results and the conclusive statement of both case studies revealed similarities and differences. These findings are discussed and summarized in this section.

When comparing the results and conclusions from the two case studies, the first difference is in the agreement between the quantification models. In Case Amsterdam (Chapter 4), both quantification models [A and B] and reliability methods [FORM and MCS] agreed upon the assessed reliability of the design with a margin of $\beta \pm 0.1$ to each other. This difference is larger between the models and algorithms in Case Almere. The Student T and the Bayesian models assess reliability indexes with a difference up to $\beta \pm 1$ to each other. This difference is larger for a low number of observations and decreases further with an increasing number of observations. The difference can be explained by the stronger influence of the priors if fewer observations are made, see Statements 4 and 8. This effect was also found in studies by Cao & Wang (2013) and by Contreras et al. (2020).

While the reliability assessed in the lower range of observation is more reliable in Case Amsterdam, for Case Almere designs in the same range are less reliable than required by EN1990. This marks a significant difference between the case studies, which is linked to the spatial variability of the CPT field. In Case Amsterdam the soil conditions are very homogeneous such that the observed spatial variability (CoV) is smaller than 12%, which is close to the CoV observed by both probabilistic quantification models [A and B]. This leads to conservative designs since the correlation factors are larger than En1990 would require (Figure 20). In Case Almere the spatial variability observed with few observations is close to 15% for the EN1997 method but closer to 20% for the probabilistic models. That model pile method underestimates the amount of spatial variability of provided resistance, thus leading to a less reliable design than EN1990 requires.

The model uncertainty which was based on a test by Deltares (2020) for the case in Amsterdam, is relatively low when compared to other studies by ISSMGE (2021). This can be explained by the homogeneous soil properties found at the project location in Amsterdam and the non-bias nature of the model pile method also found in studies by Lehane et al (2007). However, the studies carried out by Lehane et al. (2007) and the ISSMGE (2021) do not include the model pile method investigated in this study but focus on other CPT or SPT-based methods. Therefore, a reliable model factor is hard to acquire without a test at the location of interest as was provided by Deltares (2020). Consequently, the same model factor is assumed for the Case Almere. In both cases, the cover of the model uncertainty in the EN1997 recipe is assessed to be larger than the model factor in the probabilistic quantification models [A and B] suggest.

Also in both cases, a convergence of the treatment of the combined uncertainties towards the recommended values from En1997 was observable, indicating that the total coverage of uncertainty in both cases is close to what EN1997 would require.

6.2 CONCLUSIONS

This section discusses the conclusions from the case studies in Amsterdam and Almere regarding the research questions posed in Section 1.3. This is done by first answering the sub-questions and then concluding with a final statement about the main question.

1 *How does the EN1997 model pile design recipe account for spatial variability and uncertainty due to limited information in the parameter estimation and how does this compare to fully probabilistic methods?*

The uncertainty in parameter estimation with the model pile method from En1997 is taken care of through the correlation factor ζ (Table 2) and the partial resistance factor (γ_{RC}). The correlation factor accounts for both the spatial variability and the uncertainty due to limited observations. This approach was compared with the uncertainty quantification models [Student T and Bayesian model] using the full probabilistic method for uncertainty quantification. <u>The reliability-based calibration of the correlation factor and the partial factor indicates that there is a good agreement with the reliability targets in EN 1990</u>. However, the results have revealed several issues.

First, if the spatial variability in the CPT field is smaller than 12%, the lowest category in Table 2, the resulting designs can be over-conservative. Second, <u>the discrete nature of the correlation factor makes the design results sensitive to minor changes in the observations if the categories for the encountered spatial variability change</u> (rows in Table 2). The sensitivity to the number of observations (CPTs) is minor compared to the spatial variability.

Additionally, designs based on a correlation factor seem to be biased towards underestimating the statistical uncertainty for a low number of CPTs. However, the performance of the treatment of the uncertainty seems to work if sufficient observations (more than 10) are made. This behaviour is observed both in Case Amsterdam for n < 6 (Figure 19 – Plot 1) and Case Almere for n > 9 (Figure 30 – Plot 1).

2 *How does the EN1997 model pile design recipe cover the model uncertainty in the design process and how does this compare to fully probabilistic methods?*

The model uncertainty is covered by EN1997 designs via the partial model factor. <u>The results suggest that the partial model factor in EN 1997 is lower than the optimal value calibrated by the design value method. The lower than optimal partial load factor seems to be compensated, however, by the higher than necessary partial load factors for the problems at hand</u>.

3 *What is the difference between the reliability target in EN1990 and the reliability assessed by the probabilistic quantification models?*

From Figure 14 and Figure 25 it is visible that there is an agreement between the general defined reliability targets from Eurocode 0 and the design outcomes of the model pile method from Eurocode 7. With a high number of CPT inputs, both probabilistic uncertainty quantifications seem to assess the design close to a value of the reliability target of β=3.8 (Eurocode 0).

However, due to the findings for the first sub-question, some differences between the reliability benchmark and the assessed reliabilities are observable, mainly if limited information is available (less than 10). <u>In conclusion, the assessed reliability indices (β) are within the range of 0.5 to the fully probabilistic target of 3.8 defined in Eurocode 0, if enough observations are available.</u>

What reliability levels are achieved by the pile design methods in draft EN 1997, and how do these compare to the reliability targets in EN 1990?

In conclusion, using the model pile method in draft EN 1997 results in foundation designs which essentially conform with the reliability targets in (draft) EN 1990. The combination of correlation factors and partial factors seems to cover the uncertainties arising from spatial variability, model uncertainty and uncertainty due to limited observations well in a general sense, at least for reasonably large numbers of CPTs (i.e., more than 10). For smaller numbers of CPTs, the design method can be over-conservative or under-conservative, depending mainly on the degree of spatial variability encountered in the observations (CPTs).

There seems to be potential for optimizing the partial factors by decreasing the factors regarding the loads and increasing the resistances factors. This is supported by the results of both case studies for which the influence of the resistance model was higher than EN1997 recommends, while the influence of the load model was lower.

These findings further imply the following. The reliability targets from EN1990 can be used to assess and design pile foundations which conform to the design approach of EN1997. It also seems feasible and practical to restrict the reliability analysis and design to the resistance side by considering the probability of exceeding the design value of the load, using standardized influence coefficients. This would remove the need for sophisticated stochastic/probabilistic load modelling, for which information is often lacking in practice.

All conclusions are made based on the two investigated cases and need to be reflected under the limitation of the information available.

6.3 PRACTICAL IMPLEMENTATION AND RECOMMENDATIONS

From the results and conclusion of the reliability assessment and the uncertainty analysis 4 practical recommendations for the performance of the model pile method in Eurocode 7can be made:

1. If representative and informative priors about the site characterization can be made, both case studies showed that the Bayesian quantification model [B] approach can be a powerful tool to assess the reliability and potentially design pile foundations with limited site investigation. While the informative priors used in the quantification model B in both cases are derived from CPT data close to the project side, acquiring a good estimation of the priors can be difficult in practice if limited data is available. In these cases, expert (local) knowledge can be used to quantify a good approximation to compensate for the lack of observations (Cao, Wang, & Lia, 2016).

2. It seems practical to restrict the reliability analysis to the resistance side by considering the probability of exceeding the design value of the load, using standardized influence coefficients, since the uncertainties in the resistance are from dominating influence on the achieved reliability levels. This would remove the need for sophisticated stochastic load modelling, for which often information is lacking in practice. This recommendation is bound to the assumption that the expected load is not dominated by variable load components, thus a similar ratio of 1/3 variable to 2/3 static load is feasible for the project. If the variable load component is large(r), designs and assessments are more conservative, thus more material intense than EN1990 would require.

3. How the spatial variability categories in Table 2 should be implemented in the design, can be made more transparent to prevent the sensitivity of the design to small changes in observed spatial variability (CoV). From the results of this thesis, it is visible that a hard boundary will lead to designs which are making the design process chaotic and unpredictable. Two solutions can be proposed. First, a continuous formulation of the calculation for the correlation factor could be formulated and included in Eurocode 7. This would make the choice for the correlation factor more transparent and would prevent sensitivity in designs. Second, the way the categories should be interpreted should be explained explicitly in EN1997. For example, an explanation of how to deal with a CoV of 17.5%, which is between 15 and 20% category, would support decision-making in the design and could mitigate unnecessary sensitivity. This approach would make the design still easy to apply in practice, by excluding an additional calculation, while improving the transparency of the design process.

4. Eurocode 7 should include more information about the treatment of model uncertainty in the design process of pile foundation. This can make the evaluation and verification of probabilistic models easier. This could include information about the assumed distribution for the model uncertainty/partial model factors as well as parametric information for the applied design method. Additionally, a decomposition of the different components in the model uncertainty could be integrated, thus a list of uncertainties which are included in the partial model factor.

5. The assessment framework of this thesis can be used as a basis for other design recipes and geotechnical structures. The workflow of the assessment is generalizable, thus offering a guideline on how to assess semi-probabilistic structures in terms of achieved reliability levels. The same is possible for the design of structures, for which the work and information flow of the reliability assessment can be reversed such that designs are created based on the probabilistic quantification models, which comply with a set reliability level. This provides a full probabilistic design approach which is also complying with the design philosophy in EN1997.

6.4 FURTHER RESEARCH RECOMMENDATIONS

This section provides a short recommendation to generalize and verify the results and conclusion of the assessment:

- To investigate if the proposed assessment framework from this study can be expanded towards different design methods, pile shapes and materials. This can help to further verify the findings from this study and insight if are specific to the chosen design or are generalizable can be obtained. This is especially interesting for the installation method since different partial resistance factors (γ_{RC}) are recommended for these methods. Further interesting is how far the convergence towards the reliability targets from EN1990 is a repeatable finding for different methods.

- Further studies could investigate the design recipes which are based on on-site dynamic pile testing from EN1997. This would deepen the understanding of the workings and therefore recommendations formulated in Table 2 since this design recipe also uses the correlation factor (ζ) for the treatment of spatial variability and uncertainties due to limited observations. The results would offer additional support to the recommendations given over the correlation factor (ζ) if similar results are obtained.

- An uncertainty quantification based on a random field approach as presented by Eijnden & Hicks (2011) can be compared to the point estimations for spatial variability obtained from the uncertainty quantification models. This can provide further insight into the comparability and robustness of the treatment of spatial variability in EN1997 and the uncertainty quantifications models. A random field approach could achieve higher accuracy with less site investigation and further could question the spatially independent approach of designing pile foundations in EN1997.

- An additional calibration attempt based on the found results for both cases could be done, which includes the possibility to calibrate the partial load factors. This could further support the conclusion about the relative influence of the resistance and load model and the statements about optimization of the partial factors.

REFERENCES

Baars, S. V., Rica, S., Nijs, G. D., Nijs, G. D., & Riemens, H. (2018). Dutch field tests validating the bearing capacity of fundex piles. *Cone Penetration Testing 2018 - Proceedings of the 4th International Symposium on Cone Penetration Testing, CPT 2018* (pp. 101-107). Delft: CRC Press/Balkema.

Baecher, G. B. (2017). Bayesian Thinking in Geotechnics. *ASCE: Geo-Risk 2017* (pp. 1-18). Denver, Colorado: American Society of Civil Engineers.

Bauer. (2019). *Full Displacement Piles - Method Statement.* Schrobenhause: BAUER Maschinen GmbH.

Brinkmann, R. (2021, October). *Probabilistic toolkit- User Manual.* Delft: Deltares. Opgehaald van Probabilistic Toolkit: https://www.deltares.nl/en/software/probabilistic-toolkit-ptk/

Cao, Z., & Wang, Y. (2013). Bayesian Approach for Probabilistic Site Characterization Using Cone Penetration Tests. *Journal of Geotechnical and Geoenvironmental Engineering / Volume 139 Issue 2*, 267–276.

Cao, Z., Wang, Y., & Lia, D. (2016). Quantification of prior knowledge in geotechnical site characterization. *Engineering Geology*, 107-116.

CEN. (2019). *Eurocode - Basis of structural and geotechnical design - EN1990.* CEN.

CEN. (2019). *Eurocode 7: Geotechnical Design (EN 1997).*

Ching, J., & Schweckendiek, T. (2021). *State-of-the-art review of inherent variability and uncertainty in geotechnical properties and models.* Opgehaald van ISSMGE Technical Committee 304: http://140.112.12.21/issmge/2021/SOA_Review_on_geotechnical_property_variablity_and_model_uncertainty.pdf

Contreras, L., Serati, M., & Williams, D. (2020). Bayesian approach for the assessment of sufficiency of geotechnical data. *Slope stability 2020* (pp. 609-624). Perth: Australian Centre for Geomechanics.

Ćosić, M., Šušić, N., Folić, R., & Bancila, R. (2016). Probabilistic Analysis of Bearing Capacity of Piles with Variable Parameters of CPT Test and Calculation According to the EN 1997-1. *Civil Engineering – Science and Practice* (pp. 1335-1342). Žabljak, Monteegro: GNP.

Das, B. M., & Sobhan, . (2016). Geotechnical engineering - A Historical Perspective. In . S. Braja M. Das, *Principles of Geotechnical Engineering* (pp. 1 - 12). ICCG.

Deltares. (2020). *Advies geotechnische draagkracht houten palen Amsterdam.* Delft/Amsterdam: Deltares.

Dierckx, K., Blom, J., & Ghalandari, M. (2020, May). *Benchmarking of single pile foundations, comparing Eurocode 7 with software programs*. Opgehaald van Data.fine.cz: https://data.fine.cz/handbooks-chapter-pdf/benchmarking-single-pile-foundations-comparing-eurocode7-software-programs.pdf

Dziadziuszko, P., & Sobala, D. (2018). Precast Concrete Piles in Europe – AARSLEFF's Experience. *Proceedings of China-Europe Conference on Geotechnical Engineering* (pp. 919-922). Vienna: Springer, Cham.

Frangopol, D. M. (2008). Probability concepts in engineering: emphasis on applications to civil and environmental engineering. *Structure and Infrastructure Engineering*, 413-414.

Google Earth. (2022, April). *https://earth.google.com*. Opgehaald van https://earth.google.com/web/search/Kasteel+Almere,+Oude+Waterlandseweg,+Almere,+Niederlande/@52.30876,5.19221652,-3.50395327a,192659.31417d,35y,0h,0t,0r/data=CigiJgokCS6jLPWICkpAEeeicZDaCUpAGajQB2QtPxFAIexrIvG_LBFA

Johannesson, E. (2019). Classical versus Bayesian Statistics. *Philosophy of Science Volume 87*, 302-318.

Joint Research Center. (2022, March). *https://eurocodes.jrc.ec.europa.eu*. Opgehaald van Abount the Eurocode: https://eurocodes.jrc.ec.europa.eu/showpage.php?id=1

Jordan, M. I. (2020, March). *https://math.mit.edu.* Opgehaald van https://math.mit.edu/~dav/05.dir/class15-slides-all.pdf

Koehler, E., Brown, E., & Haneuse, S. J.-P. (2009). On the Assessment of Monte Carlo Error in Simulation-Based Statistical Analyses. *The American Statistician - Volume 63*, 155-162.

Köhler, J., Sørensen, J. D., & Baravalle, M. (2019). Calibration of existing semi-probabilistic design codes. *13th International Conference on Applications of Statistics and Probability in Civil Engineering (ICASP13).* Seoul, South Korea.

Lehane, B. M., Schneider, J., & Xu, X. (2005). The UWA-05 method for prediction of axial capacity of driven piles in sand. *1st Int. Symp. on Frontiers in Offshore Geotechnics* (pp. 19–21). Denver, Colorado, United States: Univ. of Western Australia.

Lin, T. I., Lee, J. C., & Hsieh, W. J. (2017). Robust mixture modelling using the skew t distribution. *Stat Comput*, 81-92.

Marekk, P., & Kvedaras, A. K. (2012). From Partial Factor Design to Fully Probabilistic Reliability Assessment of Structures. *Journal of Geotechnical Engineering and management*, 252-259.

Muller, G., & Albertini, G. (2015, may). *A probabilistic approach to design civil engineering structures.* Opgehaald van www.epfl.ch: https://www.epfl.ch/labs/lsms/wp-content/uploads/2018/10/A_probabilistic_approach_to_design_civil_engineering_structures.pdf

NEN. (2019). *NEN-EN 1997-1+C1+A1/NB -Nationale bijlage bij NEN-EN 1997-1.* NEN.

NIST/SEMATECH. (2012, May). *Handbook of Statistical Methods*. Opgehaald van e-Handbook of Statistical Method: https://www.itl.nist.gov/div898/handbook/

Otake, Y., & Honjo, Y. (2013). A simplified reliability analysis of spatial variability employing local average of geotechnical parameters. *Safety, Reliability, Risk and Life-Cycle Performance of Structures and Infrastructures - Proceedings of the 11th International Conference on Structural Safety and Reliability, ICOSSAR 2013*, (pp. 1995-2002). New York, NY.

Pham Quang, T., Vrijling, J., van Gelder, P., & Thu, T. (2010, May). *Reliability-tools in geotechnical design, an approach for river dike analysis.* Opgehaald van repository.tudelft.nl: https://repository.tudelft.nl/islandora/object/uuid%3Afa3618fb-02b4-460a-bd7c-21aedcd611cc

Phoon, K., & Tang, C. (2015). Model Uncertainty for the Capacity of Strip Footings under Negative and General Combined Loading. *12th International Conference on Applications of Statistics and Probability in Civil Engineering.* Vancover, Canada: University of British Columbia Library .

Queiroz, I. M. (2016). Comparison Between Deterministic and Probabilistic Stability Analysis, Featuring a Consequent Risk Assessment. *VII Brazilian Symposium on Rock Mechanics.* Belo Horizonte, Minas Gerais, Brazil: CBMR/ABMS and ISRM,.

Rheinfurth, M., & Howell, L. (1998). *Probability and Statistics in Aerospace Engineering.* Marshall Space Flight Center, Alabama: NASA.

Ronold, K. O. (2016). Characteristic soil strength for axial pile capacity and its estimation with confidence for offshore applications. *Structural Safety 63*, 81-89.

TAW. (1997). *Leidraad Waterkerende Kunstwerken en Bijzondere Constructies.* Technische Adviescommissie voor de Waterkeringen.

Taylor, D. W. (1948). *Fundamentals of soil mechanics.* New York: John Wiley & Sons.

Terzaghi, K. (1925). *Erdbaumechanik auf Bodenphysikalisher Grundlage.* Vienna: Deuticke.

TNO. (2022, March). *https://www.dinoloket.nl*. Opgehaald van https://www.dinoloket.nl

TNO. (2022, May). *TNO.nl*. Opgehaald van https://www.tno.nl/en/focus-areas/buildings-infrastructure-maritime/roadmaps/safe-and-sustainable-living-environment/building-innovation/foundation-problems/

van den Eijnden, A. P., & Hicks, M. (2011). Conditional simulation for characterising the spatial variability of sand state. *Computational Geomechanics Comgeo II*, 288-296.

van Mierlo, J., & Koppejan, A. (1952). Lengte en draagvermogen van heipalen. *Bouw*, 1-11.

Watson, S. R. (1994). The meaning of probability in probabilistic safety analysis. *Reliability Engineering and System Safety*, 261-269.

APPENDIX

APPENDIX A - GENERAL

APPENDIX 1 - SEMI PROBABILISTIC LOAD MODEL

Following (CEN, 2019) the ratio of permanent to variable load can be estimated with:

$$\chi = \frac{Q_{char}}{G_{char} + Q_{char}} \approx \frac{1}{3}$$

Where:

- χ is the ratio of permanent to a variable load (This value can be subject to a sensitivity analysis for the specific case)

If the assumption of (CEN, 2019) holds the characteristic values for the permanent and variable load with a known design load can be estimated with:

$$G_k = \frac{F_d}{\gamma_G + \frac{\chi}{1-\chi}\gamma_Q}$$

$$Q_k = G_k \frac{\chi}{1-\chi}$$

The resulting characteristic values and the final design load can be found with numerical solving. The partial factors are given in (CEN, 2019) as shown in the table below.

TABLE 9 - PARTIAL FACTORS FOR THE LOAD MODEL FROM (CEN, 2019)

Action or effect				Partial factors γ_F and γ_E for Design Cases 1 to 4				
Type	Group	Symbol	Resulting effect	Structural resistance	Static equilibrium and uplift		Geotechnical design	
Design case				DC1[a]	DC2(a)[b]	DC2(b)[b]	DC3[c]	DC4[d]
Formula				(8.4)	(8.4)		(8.4)	(8.5)
Permanent action (G_k)	All[f]	γ_G	unfavourable /destabilizing	$1{,}35K_F$	$1{,}35K_F$	1,0	1,0	G_k is not factored
	Water	$\gamma_{G,w}$		$1{,}2K_F$	$1{,}2K_F$	1,0	1,0	
	All[f]	$\gamma_{G,stb}$	stabilizing[g]	not used	1,15 [e]	1,0	not used	
	Water[l]	$\gamma_{G,w,stb}$			1,0 [e]	1,0		
	All	$\gamma_{G,fav}$	favourable[h]	1,0	1,0	1,0	1,0	
Prestress (P_k)		γ_P [k]						
Variable action (Q_k)	All[f]	γ_Q	unfavourable	$1{,}5K_F$	$1{,}5K_F$	$1{,}5K_F$	1,3	$\gamma_{Q,1}/\gamma_{G,1}$ [j]
	Water[l]	$\gamma_{Q,w}$		$1{,}35K_F$	$1{,}35K_F$	$1{,}35K_F$	1,15	1,0
	All	$\gamma_{Q,fav}$	favourable	0				
Effects of actions (E)		γ_E	unfavourable	effects are not factored				$1{,}35K_F$
		$\gamma_{E,fav}$	favourable					1,0

[a] Design Case 1 (DC1) is used both for structural and geotechnical design.

[b] Design Case 2 (DC2) is used for the combined verification of strength and static equilibrium, when the structure is sensitive to variations in permanent action arising from a single-source. Values of γ_F are taken from columns (a) or (b), whichever gives the less favourable outcome.

[c] Design Case 3 (DC3) is typically used for the design of slopes and embankments, spread foundations, and gravity retaining structures. See EN 1997 for details.

[d] Design Case 4 (DC4) is typically used for the design of transversally loaded piles and embedded retaining walls and (in some countries) gravity retaining structures. See EN 1997 for details.

[e] The values of $\gamma_{G,stb}$ = 1.15 and 1.0 are based on $\gamma_{G,inf}$ = 1,35 ρ and 1,2 ρ with ρ = 0.85.

[f] Applied to all actions except water pressures.

[g] Applied to the stabilizing part of an action originating from a single source.

[h] Applied to actions whose entire effect is favourable and independent of the unfavourable action.

[j] $\gamma_{Q,1}$ = corresponding value of γ_Q from DC1 and $\gamma_{G,1}$ = corresponding value of γ_G from DC1.

[k] See other relevant Eurocodes for the definition of γ_P where γ_P is materially dependent.

[l] For water actions induced by waves and currents, see Annex A.6.

APPENDIX 2 - FULLY PROBABILISTIC LOAD MODEL

From the given information about the distributions, the following equations can be derived

$$P(G > G_k) = 0.5 \rightarrow \mu_G = G_k = 0.333$$

$$CoV = 0.05 \rightarrow \sigma_G = 0.05 * \mu_G = 0.01666$$

With this, the permanent load distribution is fully defined. The distribution is shown in Figure 33 below.

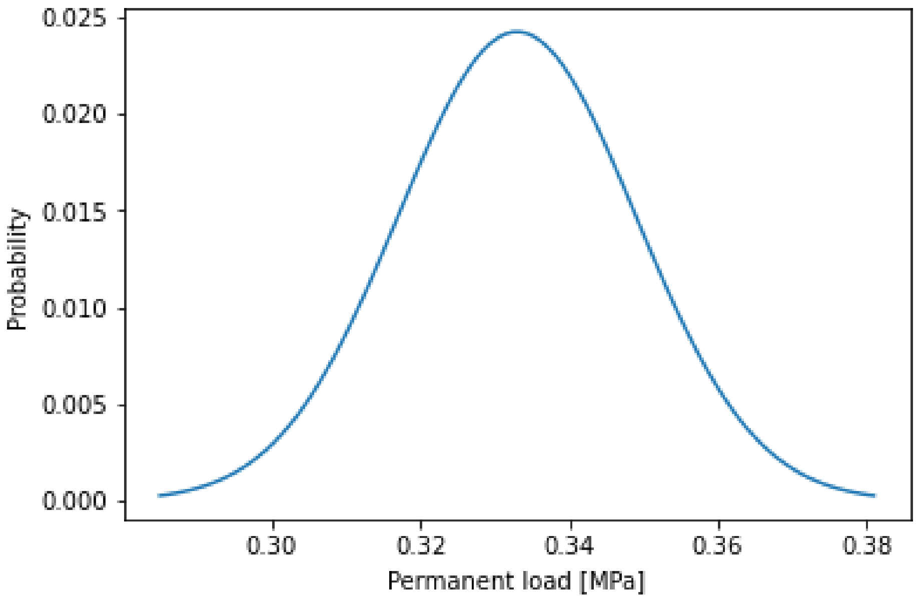

FIGURE 33 - PERMANENT LOAD DISTRIBUTION

The variable load distribution was required to fulfil the following requirements.

$$P(Q < Q_k) = 0.98$$

$$CoV = 0.3$$

Thus:

$$P(Q < Q_k) = e^{-e^{\frac{Q_k - \mu_q}{\beta}}} = 0.98$$

$$CoV_q = \frac{\beta\pi}{\sqrt{6} * (\mu_q + 0.5772\beta)} = 0.3$$

With these two equations given, one can numerically solve for the mode (μ) and the location parameter (β). This leads to the following results:

$$\mu_q = 0.08109$$

$$\beta_q = 0.02193$$

$$Mean_q = \mu_q + 0.5772\beta = 0.093755$$

With these parameters, the distribution of the variable loads is well defined. The distribution is shown in the figure below.

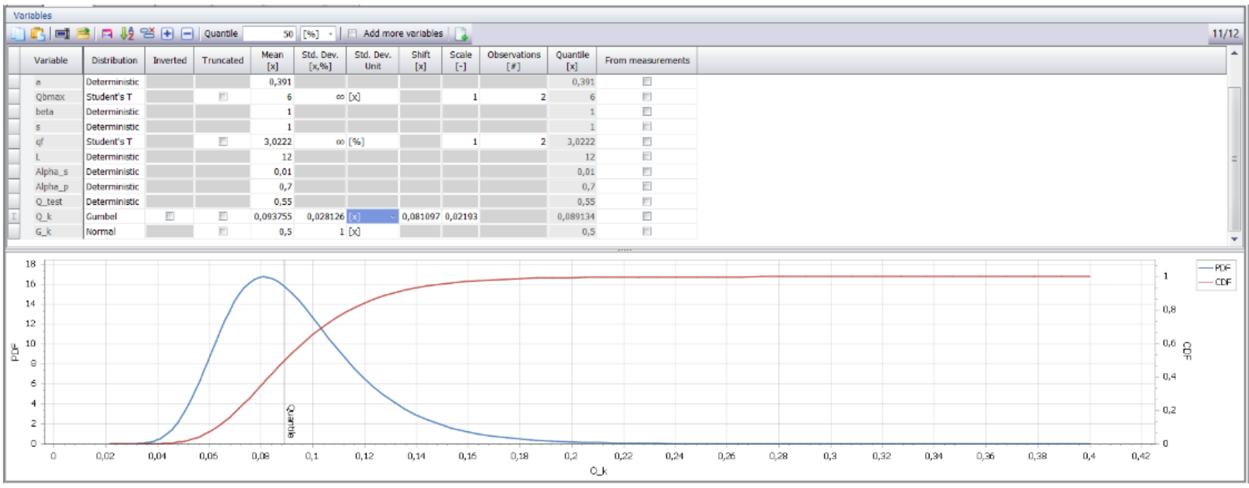

FIGURE 34 - LOAD MODEL DISTRIBUTION FROM PTK

Appendix 3 - Shaft friction in EN1997

The Pile Shaft Resistance is determined by the average measured cone resistance for the geotechnical unit. The geotechnical unit is further dependent on the homo/heterogeneity of the soil profile, the number of measurements and the precision of the measurement devices. In CPTs the cone resistance is measured directly over the length of the pile shaft. The corresponding equation to calculate the pile shaft resistance from section 6.6 In Eurocode 1997 is given below.

$$\mathrm{R_s} = \sum_{\mathrm{i}=1}^{\mathrm{n}} \mathrm{A_{s,i}} * \mathrm{q_{s,i}} \quad (\text{EN1997} - \text{Section 6.6})$$

For which:

- $\mathrm{A_{s,i}}$ is the area of the shaft in the i-th geotechnical unit
- $\mathrm{q_{s,i}}$ is the shaft friction of the i-th geotechnical unit
- n is the number of geotechnical units contributing to the shaft friction

While the cross-sectional area is only dependent on the geometry of the pile in question, the shaft friction of the geotechnical unit is calculated following an equation based on the chosen method and the national context. The case investigated in this study is in the Netherlands, therefore the Dutch National Annex (NEN, 2019) is referred to in the following section. From (NEN, 2019) the equation below:

$$\mathrm{q_{s,i}} = \alpha_{\mathrm{s}} * \mathrm{q_{c,i}}$$

For which:

- α_{s} is the transformation factor for the measured cone resistance to the calculation resistance
- $\mathrm{q_{c,i}}$ is the measured cone resistance in the CPT over the geotechnical unit i

The transformation factor is dependent on the pile material and the installation method, while the value for $q_{c,i}$ is taken directly from the CPT measurement. The Eurocode guidance for choosing the translation factors is shown in Appendix 5.

Appendix 4 - Pile base resistance Koppejan method

To determine the pile base resistance of the foundation piles from CPT data, the Koppejan (4D/8D) model is used (CEN, 2019). The equation determines the point bearing capacity with the minimum averages over three influence zones. The length of the zones is dependent on the equivalent diameter given in (NEN, 2019)

$$\mathrm{D_{eq}} = 1.13 * \mathrm{a} * \sqrt{\frac{\mathrm{b}}{\mathrm{a}}}$$

Where:

- $\mathrm{D_{eq}}$ is the equivalent diameter
- a is the shorter side of the pile cross-section
- b is the longer side of the cross-section

The cone resistance of a CPT measurement is a measure for the three zones and combined according to the equation below:

$$q_b = A_b * \frac{1}{2} * \alpha_p * \left(\frac{q_{c,I,gem} + q_{c,II,gem}}{2} + q_{c,III,gem}\right)$$

For which:

- A is the area of the pile foot [m^2]
- $q_{b,max}$ is the point bearing capacity following the model of Koppejan
- α_p is a correction factor for the point resistance in the foundation layer [-]
- β is a correction factor based on the pile foot form
- s is a correction factor for the form of the pile footing cross-section
- $q_{c,I,gem}$ is the minimum average measure of cone resistance in zone I, thus from the pile foot to 0.7 to 4 D_{eq}. The depth of zone 1 should be chosen such that $q_{b,max}$ is minimal
- $q_{c,II,gem}$ is the minimum average between the end of Zone I and the pile foot. The values of the cone resistance in Zone II are determined such that the cone resistance cannot be bigger than the value measured above
- $q_{c,III,gem}$ is the minimum average between the pile foot and a distance of 8 D_{eq} above that. The values of the cone resistance in Zone III are determined such that the cone resistance cannot be bigger than the value measured above.

From this follows that the Koppejan resistance is a non-linear function of the soil properties below and above the pile base, like the Mohr circles for soil stability.

ALGORITHMIC EXPLANATION OF THE KOPPEJAN METHOD:

The following steps are necessary to determine the Koppejan bearing capacity of the base resistance

1. Generate a vector consisting of the mean cone resistances for all possible values of q1. For all possible ranges of Zone 1 (0.7-4 D_{eq} below pile base):
    a. Generate a vector (a) of all cone resistances between the pile base and the end of zone 1 per geotechnical unit.
    b. Calculate the mean of the vector (a) to generate a possible value of q1
    c. Safe the generated mean as a possible value of q1 in vector (b)
    d. Increase the length of Zone 1 by a geotechnical unit (range 1 = range a+1).
2. Generate the corresponding values of q2 in a vector (c) for range = length of a.
    a. Find the end on zone 1 corresponding to the value that should be calculated in c
    b. From the endpoint of the corresponding zone c iterate upwards to the next geotechnical unit to create a vector d with values n
        i. If geotechnical d(n+1) > d(n) -> d(n+1) = d(n)
        ii. If d(n+1) < d(n) -> d(n+1) = d(n+1)
    c. Calculate the mean value of d and safe as an entry in vector c
3. Generate the corresponding values of q3 in a vector (e) for range = length of a.
    a. Find the last value of vector d (cone resistance at the pile base) corresponding to the value in vector a
    b. Generate vector f for which f(1) = end value of d
    c. From the endpoint of the corresponding zone 2 iterates upwards to the next geotechnical unit to create a vector f with values n
        i. If geotechnical f(n+1) > f(n) -> f(n+1) = f(n)
        ii. If f(n+1) < f(n) -> f(n+1) = f(n+1)

   d. Calculate the mean value of f and safe as an entry in vector e as possible values of q3
4. Find the minimum value of q1+q2+q3 by adding the corresponding values in vectors a +c +e to each other. This results in vector g
5. The minimum value of vector g is the design value for the pile resistance

APPENDIX 5 - PILE CLASS AND PARTIAL FACTOR RECOMMENDATIONS FROM EN1997

This table shows the deterministic values for the translation factors following EN1997. The table is cut in such a way that only the important information for the case is shown. For all choices of translation, factors consult EN1997.

TABLE 10 – PILE CLASS FACTORS FOR THE MODEL PILE METHOD FOR SANDS (CEN, 2019)

Table C.2 – Typical values of cs and cb for sands

Pile type	c_b	c_s
Driven precast concrete pile or closed ended steel pipe pile	0.70	0.010[a]
Cast in place piles made by driving a steel tube with a closed end, with the steel tube being reclaimed during concreting	0.70	0.014[a]
Driven open ended steel tube or H-pile	0.70	0.006[a]
Cast-in-place with temporary casing on top of a screw pile-tip, with the casing being removed and the screw tip remaining in the ground	0.63	0.009[a]
Continuous flight auger pile	0.56	0.006[a]
Bored pile	0.35	0.006[a]

[a] Values given for fine to coarse sands. For very coarse sands, reduce the values by 25 % and for gravels by 50 %

TABLE 11 - PILE CLASS FACTORS FOR SOFT SOILS (CEN, 2019)

Table C.3 – Typical values of cs for piles in clays, silts, and peats

Soil type	Cone resistance q_c (MPa)	c_s
Clay	≥ 2.5	0.03
	2.0-2.5	$0.02\ (q_c - 1.0)$[a]
	< 2.0	0.02
Silt	---	$\min(f_r, 0.025)$[b]
Peat	---	0

[a] q_c entered in MPa

[b] f_r = measured (uncorrected) friction ratio

TABLE 12 - PARTIAL FACTOR OF RESISTANCE VERIFICATION (CEN, 2019)

Table 6.6 (NDP) Partial factors for the verification of ultimate resistance of single piles for fundamental (persistent and transient) design situations and accidental situations

Verification of	Partial factor on	Symbol	Material factor approach (MFA) – both combinations (a)	Material factor approach (MFA) – both combinations (b)	Resistance factor approach (RFA): Pile class	model pile: Base	model pile: Shaft	ground model: Base	ground model: Shaft
Axial compressive resistance	Actions and effects-of-actions[1]	γ_F and γ_E	Not Used		All	DC1			
	Drag force due to settling ground	$\gamma_{F,drag}$				1.35			
	Ground properties[2]	γ_M				Not factored			
	Base and shaft resistance in compression	γ_{Rb} | γ_{Rs}			Full displacement	1.2 (1.0)[d]	1.0 (1.0)[d]	1.2 (1.0)[d]	1.05 (1.0)[d]
					Partial displacement	1.2 (1.0)[d]	1.0 (1.0)[d]	1.3 (1.0)[d]	1.05 (1.0)[d]
					Replacement	1.2 (1.0)[d]	1.0 (1.0)[d]	1.4 (1.0)[d]	1.15 (1.0)[d]
					Unclassified	1.35 (1.0)[d]	1.25 (1.0)[d]	1.5 (1.0)[d]	1.25 (1.0)[d]
	Total resistance in compression	γ_{Rc}			Full displacement	1.1 (1.0) [d]		1.1 (1.0) [d]	
					Partial displacement			1.2 (1.0) [d]	
					Replacement			1.3 (1.0) [d]	
					Unclassified	1.3 (1.0) [d]		1.4 (1.0) [d]	
Axial tensile resistance	Actions and effects-of-actions[a]	γ_F and γ_E	Not Used		All	DC1			
	Ground properties[b]	γ_M				Not factored			
	Shaft resistance in tension	γ_{Rst}			Full displacement	1.15 (1.0) [d]		1.2 (1.0) [d]	
					Partial displacement			1.2 (1.0) [d]	
					Replacement			1.3(1.0) [d]	
					Unclassified	1.4 (1.0) [d]		1.5 (1.0) [d]	
Transverse resistance	Actions and effects-of-actions[a,c]	γ_F, and γ_E	DC4 (EFA[e]	DC3	Not used				
	Ground properties[b]	γ_M	M1	M2	Not Factored				
	Transverse resistance	γ_{Rtr}	Not factored		Not used				

[a] Values of the partial factors for Design Cases (DCs) 1, 3, and 4 are given in EN 1990 Annex A. For transverse resistance, DC1 may be used as alternative to DC4.

[b] Values of the partial factors for Sets M1 and M2 are given in EN 1997-1, Table 4.7

[c] Including drag force due to moving ground.

[d] Values in brackets are given for accidental design situations.

[e] See EN 1997-1, 8.2

TABLE 13 - TABLE MODEL FACTOR FOR LOAD TYPE AND MODEL METHOD (CEN, 2019)

Table 6.3 (NDP) – Model factor γRd for verification of axial pile resistance by calculation

Verification by		Model factor γ_{Rd}	
Ground Model Method	Ultimate Control Tests as specified in Table 6.2 (NDP)	1.2	
	Extensive comparable[a,b] experience without site-specific Control Tests	1.3	
	Serviceability Control Tests as specified in Table 6.2 (NDP)	1.4	
	No pile load tests and limited comparable experience[a,c]	1.6	
	Pile on competent rock using properties determined from field and laboratory tests	1.1	
		Compressive resistance	**Tensile resistance**
Model Pile Method	Pressuremeter test[d]	1.15	1.4
	Cone penetration test[d]	1.1	1.1
	Profiles of ground properties based on field or laboratory tests[d,e]	1.2	1.2

[a] Comparable experience' assumes documented records (or database) of static pile load test results conducted on similar piles, in similar ground conditions, under similar loading conditions from a certain number of sites n,

[b] Extensive comparable experience' assumes $n \geq 10$

[c] Limited comparable experience' assumes $n < 10$

[d] Value can be multiplied by 0.9 when accompanied by Ultimate Control Tests as specified in Table 6.4 (NDP)

[e] Ground strength properties determined at maximum vertical spacings of 1.5 m

APPENDIX B – CASE AMSTERDAM

APPENDIX 6 – VALUES FOR THE KOPPEJAN RESISTANCE AND THE ESTIMATED SHAFT FRICTION FOR A FIXED DESIGN DIMENSION (CASE AMSTERDAM)

To create the following plots, it is chosen that the design dimensions are consistent with a side length of 0.35m. The plot shows potential trends in the CPT field and makes a comparison of the influence of different conclusions easier. The order of the CPTs is consistent with the rest of the analysis for case 1. The trendlines (red) are linear fits to the data trends for visualization.

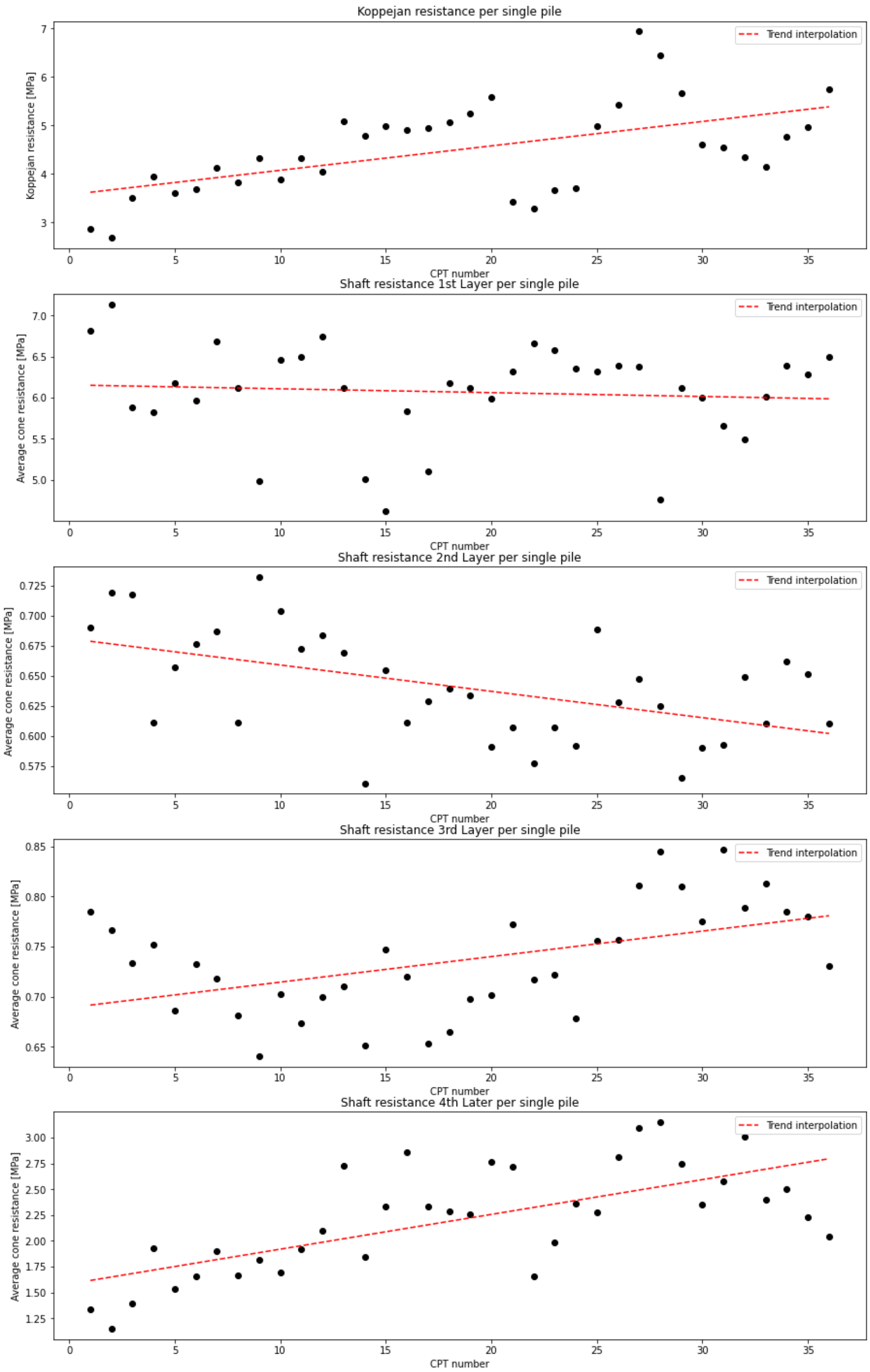

FIGURE 35 - CPT RAW DATA WITH TRENDS – CASE AMSTERDAM

APPENDIX 7 – PARAMETER QUANTIFICATION IN THE DIFFERENT MODELS – CASE AMSTERDAM

This section focuses on the design parameter quantification of the probabilistic uncertainty quantification (2). The quantification models are presented and compared to each other and the population estimation.

All applied models work with changing values for the quantification of the shaft resistance and the base resistance dependent on the number of CPTs and the chosen design dimension, which are integrated into the design and evaluation. The quantification of the resistances does not vary between the different calculation setups, thus the results for the quantification are presented for both setups together before focusing on the results of the specific setups.

The results of the quantification of the Koppejan resistance are presented in Figure 36 below.

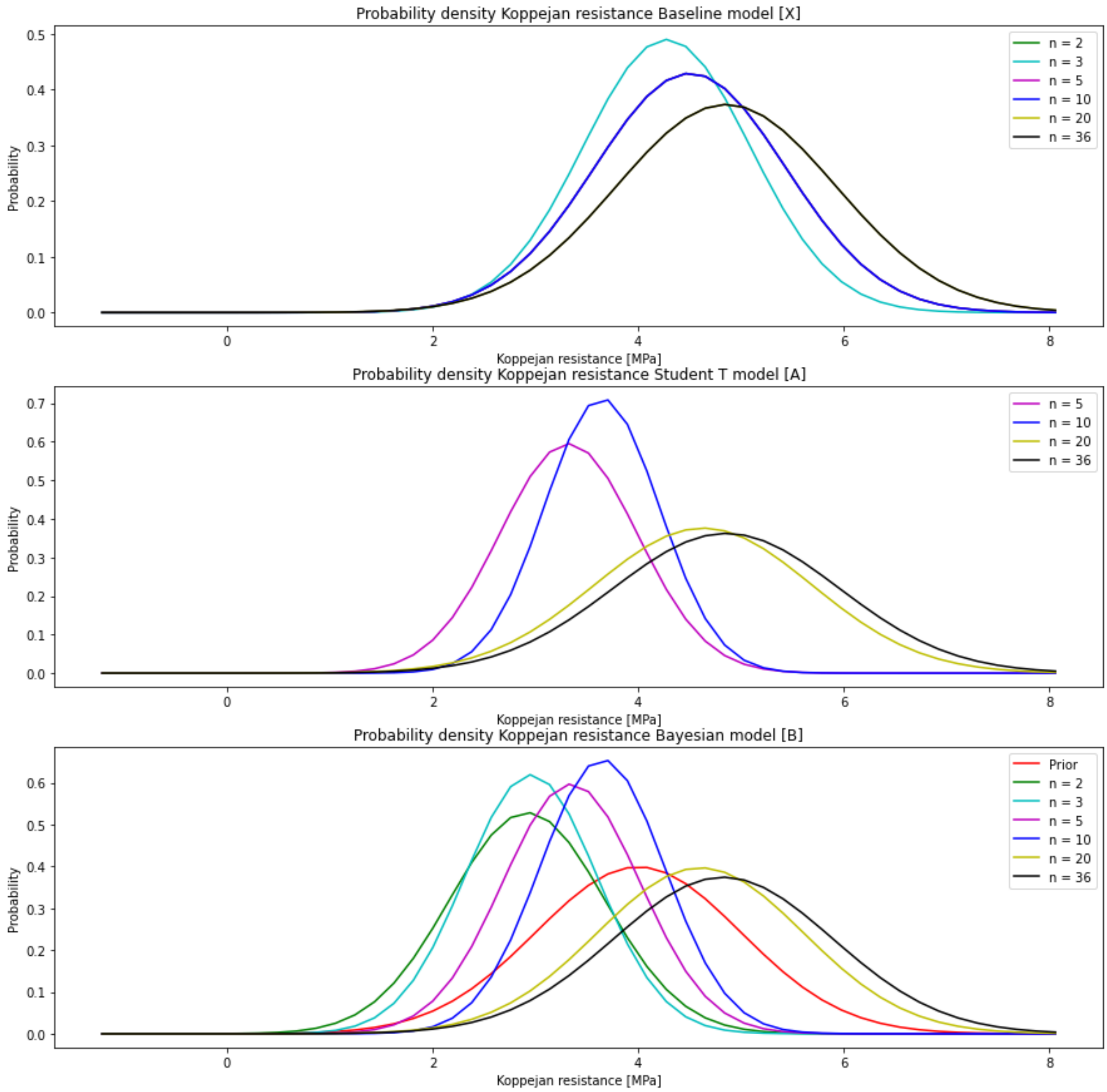

FIGURE 36 - QUANTIFICATION OF THE KOPPEJAN RESISTANCE IN DIFFERENT MODELS

Since the Koppejan resistance is both dependent on Design dimensions and the amount of CPT provided, a variation in two al three quantifications can be observed.

From the data is visible that the Koppejan resistance increases in the baseline model[X] with increasing CPT input. This may have two explanations. First due to the nonlinear behaviour of the Koppejan method is the result sensitive to changing design dimensions. This can result in a higher Koppejan resistance(q_k) for the quantification.

If one focuses on the population estimation, one can observe that the Koppejan resistance increases with an increasing number of CPTs. This indicated that with bigger design dimensions the Koppejan resistance is smaller than with smaller dimensions. This can be explained by the non-linearity of the Koppejan method (van Mierlo & Koppejan, 1952) which is highly influenced by the presents of weaker layers and in the CPT measurements. Therefore, if the pile dimension increases, the depth to investigate for weak layers increases, consequently decreasing the Koppejan resistance qK). This decrease then needs to be compensated by a larger side length of the pile.

If the values for the Student-t model [A] are investigated, it is visible that the spread of the distribution for the Koppejan resistance is higher for fewer CPT datasets. This can be explained by the nature of the T-distribution for which the spread of the value is heavily dependent on the number of observations (CPTs) following equation 13.

For the mean, a similar trend as for the baseline model can be observed which leads to the conclusion that the model is influenced in the same way as the population estimation, thus by the non-linearity of the Koppejan resistance qK).

Additionally, to the nonlinear effect, a trend in increasing expected values for the Koppejan resistance is observable which indicated that a trend for increasing strength is present following in the order of the CPT inputs. This trend is also visible in linear interpolation in Appendix 6.

An observation of the Bayesian model [B] shows the same indication of a trend in Koppejan resistance ($\mathrm{q_K}$) for increasing strength. Interesting is that the prior is chosen to be close to the population estimated, but the model diverges from this distribution for N < 10 and starts to show similar behaviour as the Student-t model [A], which again indicates a local trend of strength increase in direction of the CPT input order as indicated by Appendix 6.

The result for the quantification of the shaft friction ($\mathrm{q_{s,1}}$) for the 1st layer is presented below. It can be estimated that the shaft friction in this layer is the dominant factor for the shaft friction, since the average cone resistance, is one order of magnitude higher than for layers 2 and 3. The layer could be influential, but the shaft length in the layer is too short to make a significant impact on the total resistance. This is further investigated with the analysis of the influence factor.

Since the shaft friction is independent of design dimensions, and only depends on the mean cone resistance in the layer, a variation in design dimension does not change the result of the quantification, therefore in the population estimation, the shaft resistance is constant.

It was chosen to plot the value of the population estimates for the layers into the results for the Student-t model [A] and the Bayesian model [B] to enable the performance of the quantification models visually.

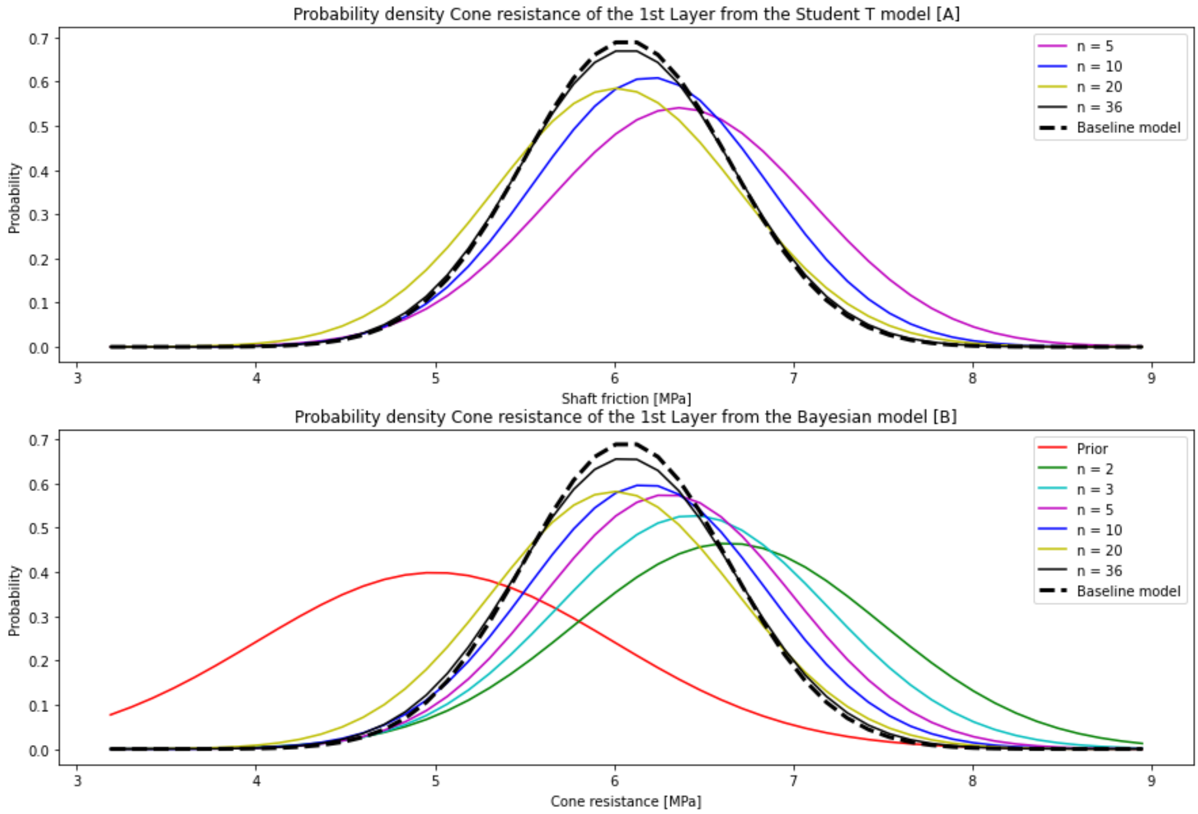

FIGURE 37 - QUANTIFICATION OF THE SHAFT FRICTION FOR THE 1ST LAYER IN DIFFERENT MODELS

For the shaft friction ($q_{s,1}$) of the first layer, an opposing trend in the expected shaft friction for the first layer is observable, where the average cone resistance in the first layer decreases with an increasing number of CPTs, indicating a negative trend of average cone resistance following the order of the CPT inputs. This impression is supported by Appendix 6 where a small decreasing trend for the shaft friction in the first layer is visible.

As for the Koppejan resistance qK), the Student T model [A], has a wider spread in the parameter estimation, compared with the Bayesian model for N< 10. This can be explained by the influence of Eq. 21. The model seems to converge towards the population estimation, which is logical given that the t-factor approaches 1 for increasing N.

The Bayesian model [B] shows similar behaviour to the Student T model [A], with the difference being the influence of the prior on the shaft friction estimation. The prior for the average cone resistance is lower than the baseline model[X], which consequently reduces the estimation of the expected values. This effect is more evident for N< 5 since the information from the prior has still a significant impact on the quantification. With more data available this effect becomes less significant.

For both models is visible that the mean converges to 10% within the baseline model after more than 10 inputs. This emphasises the homogeneity of the CPTs results for Case Amsterdam.

The rest of the shaft friction (q_s) has nearly no impact on the reliability assessment. The evolution of the resistance distribution is presented below. Generally, the same pattern as for the first layer applies, the model seems to follow the trends observed in Appendix 6

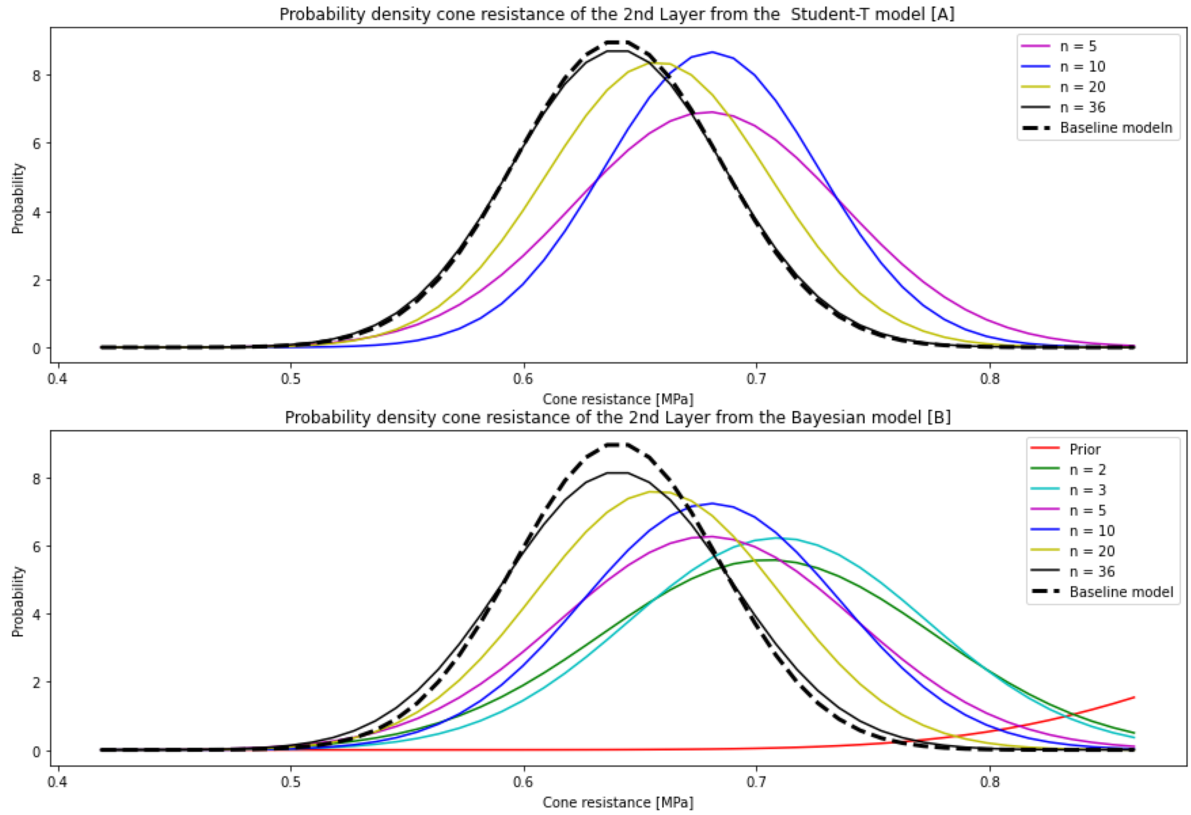

FIGURE 23 - SHAFT FRICTION QUANTIFICATION FOR THE 2ND LAYER

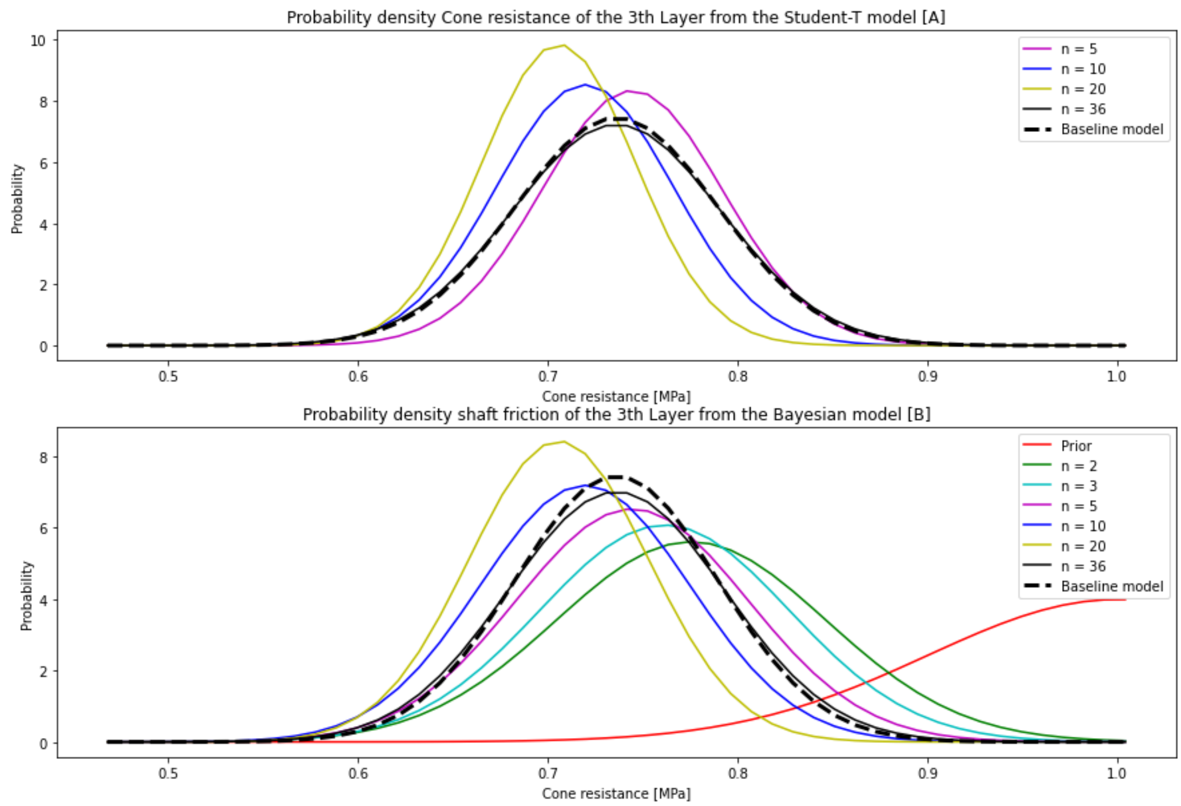

FIGURE 24 - SHAFT FRICTION QUANTIFICATION FOR THE 3RD LAYER

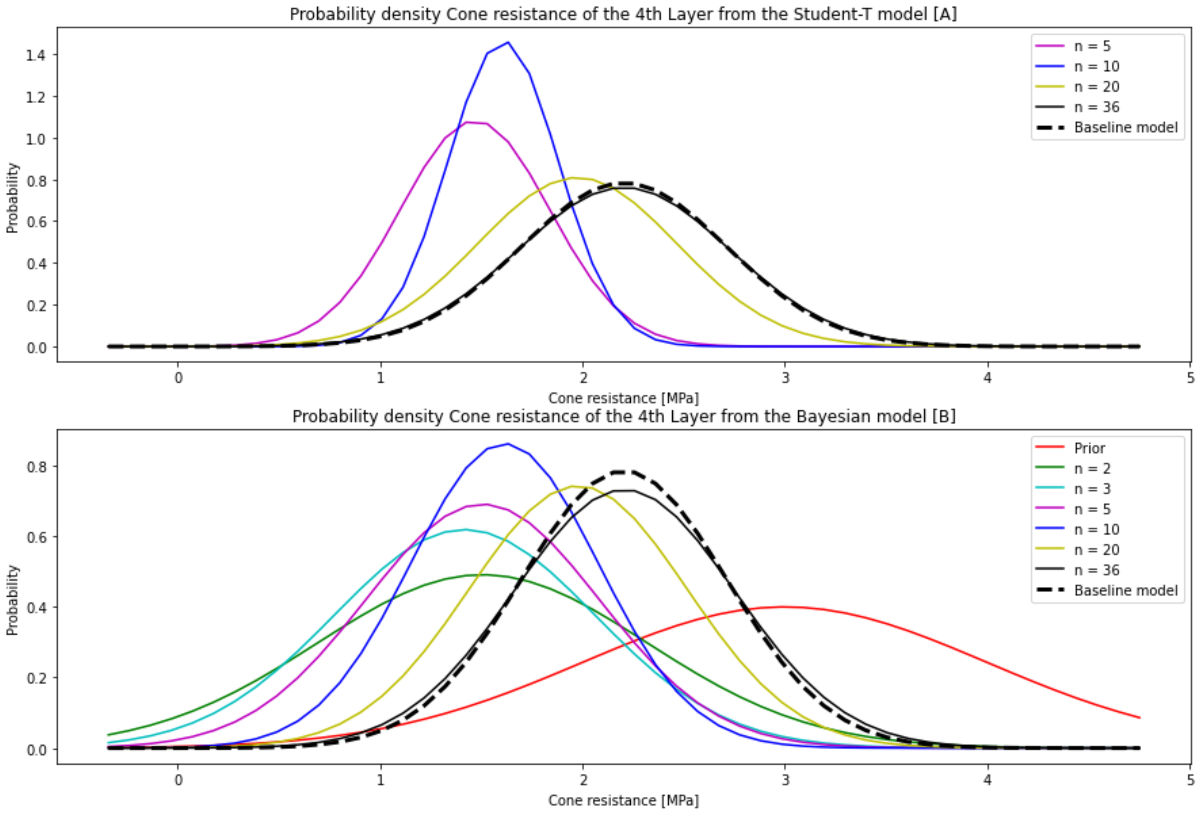

FIGURE 25 - SHAFT FRICTION QUANTIFICATION FOR THE 4TH LAYER

APPENDIX 8 – SENSITIVITY ANALYSIS FOR THE ISOLATED RESISTANCE MODEL (CASE AMSTERDAM)

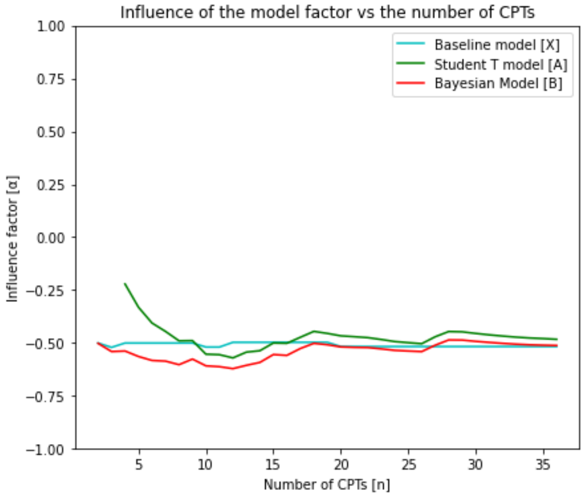

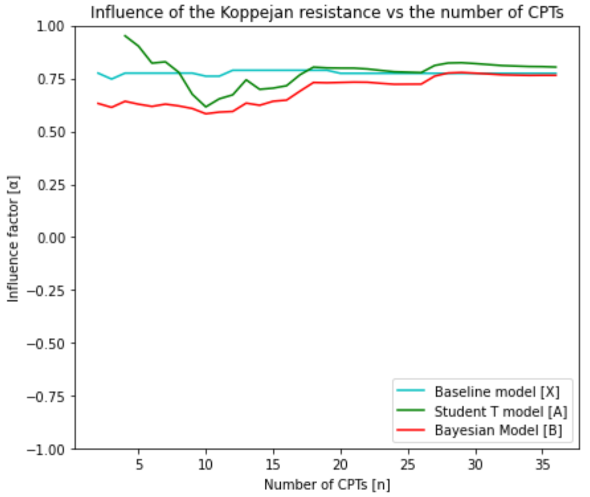

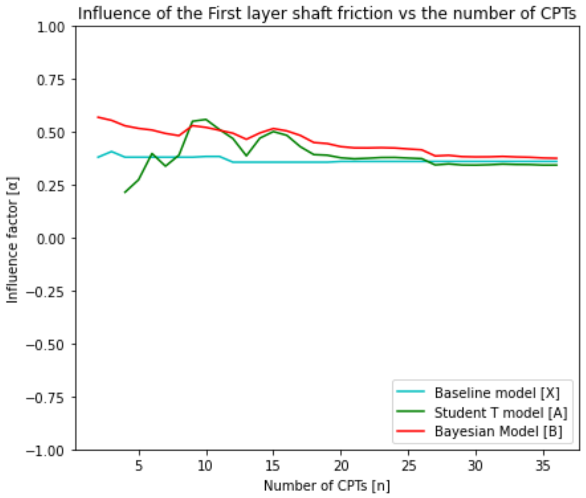

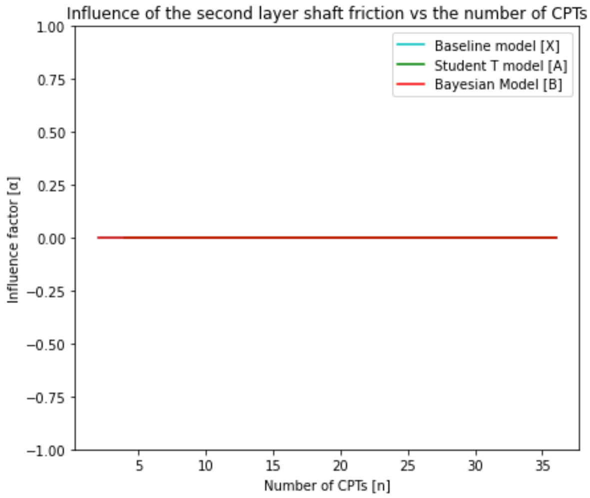

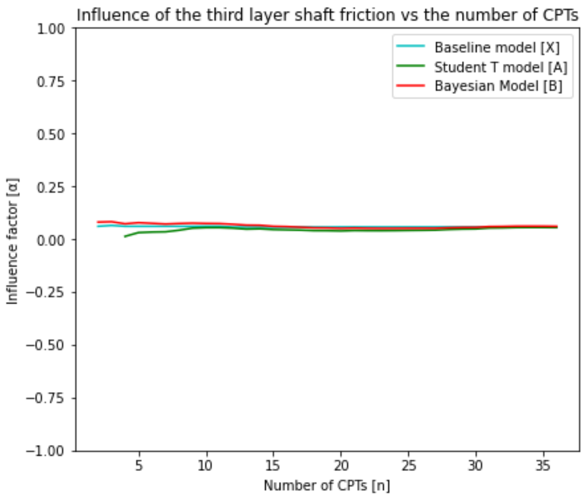

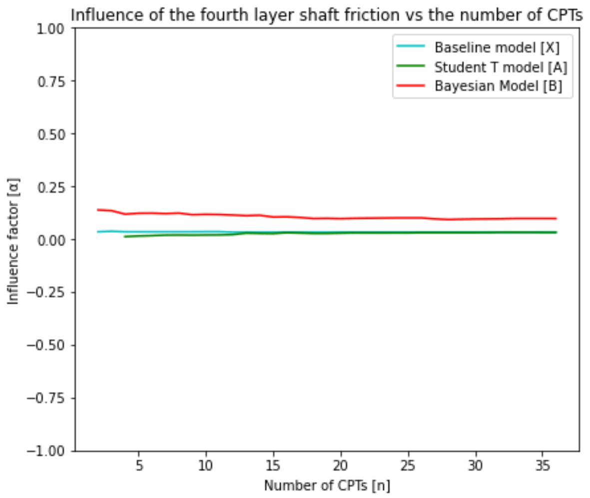

APPENDIX C – CASE ALMERE

APPENDIX 9 – VALUES FOR THE KOPPEJAN RESISTANCE AND THE ESTIMATED SHAFT FRICTION FOR A FIXED DESIGN DIMENSION (CASE ALMERE)

To create the following plots, it is chosen that the design dimensions are consistent with a side length of 0.25m. The plot shows potential trends in the CPT field and makes a comparison of the influence of different conclusions easier. The trendlines (red) are linear fits to the data trends for visualisation.

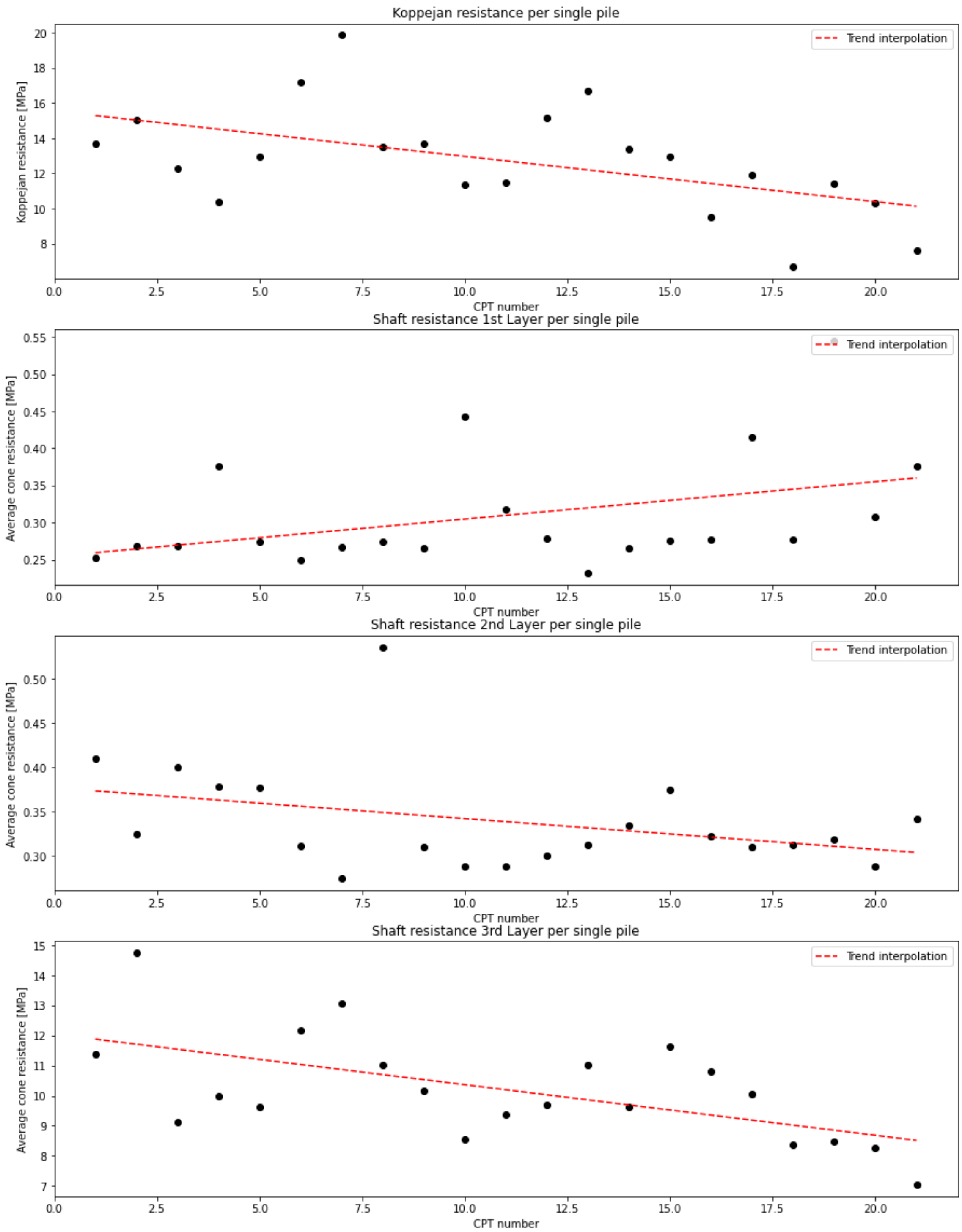

FIGURE 38 - CPT RAW DATA WITH TRENDS (ALMERE)

APPENDIX 10 – PARAMETER ESTIMATION OF THE QUANTIFICATION MODELS OVER THE CPT FIELD IN ALMERE

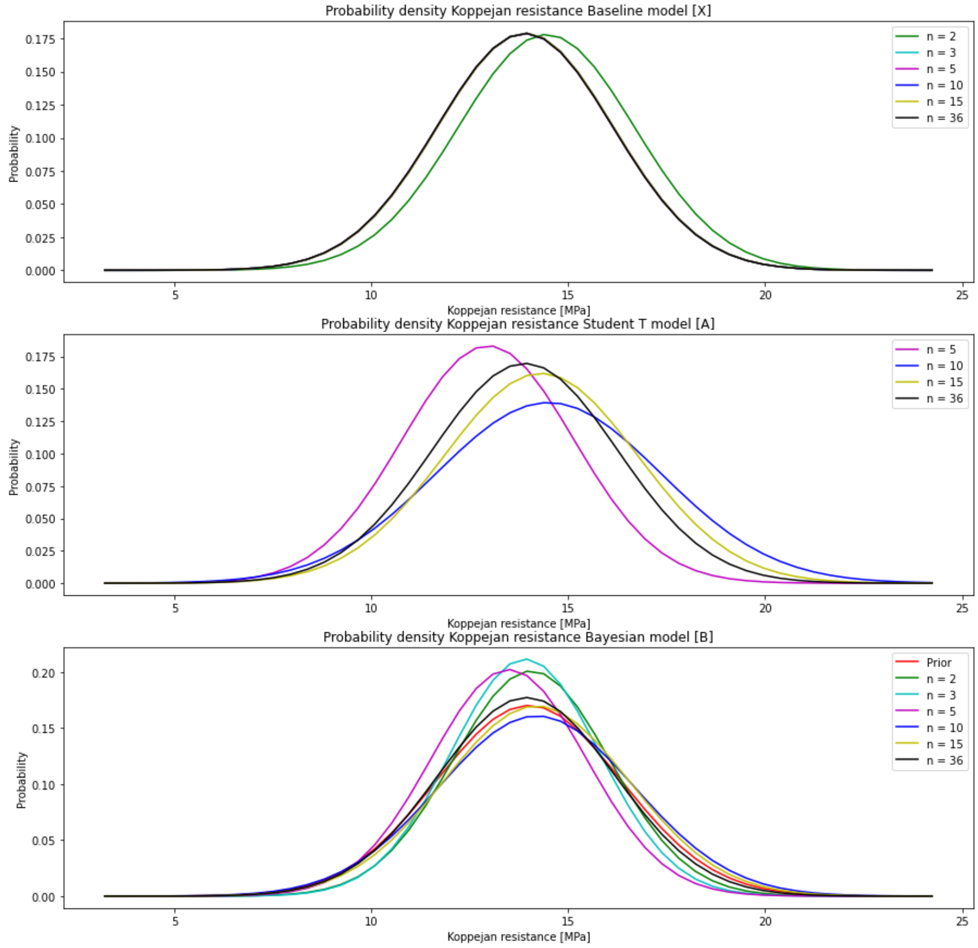

FIGURE 39 - KOPPEJAN QUANTIFICATION FOR CASE ALMERE

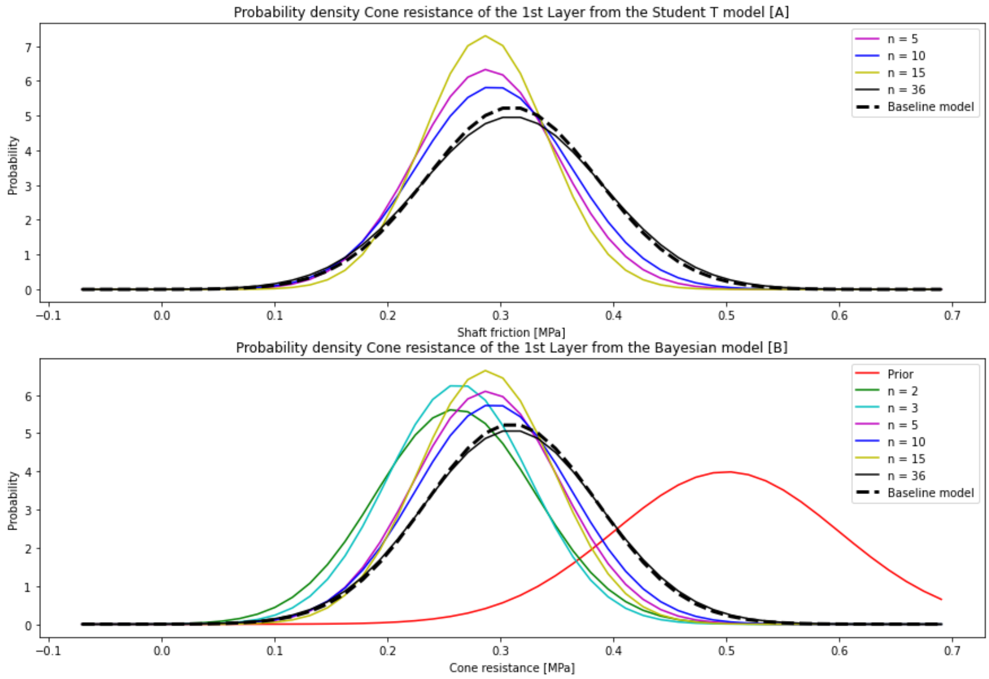

FIGURE 40 - QUANTIFICATION OF THE SHAFT FRICTION IN THE 1ST LAYER

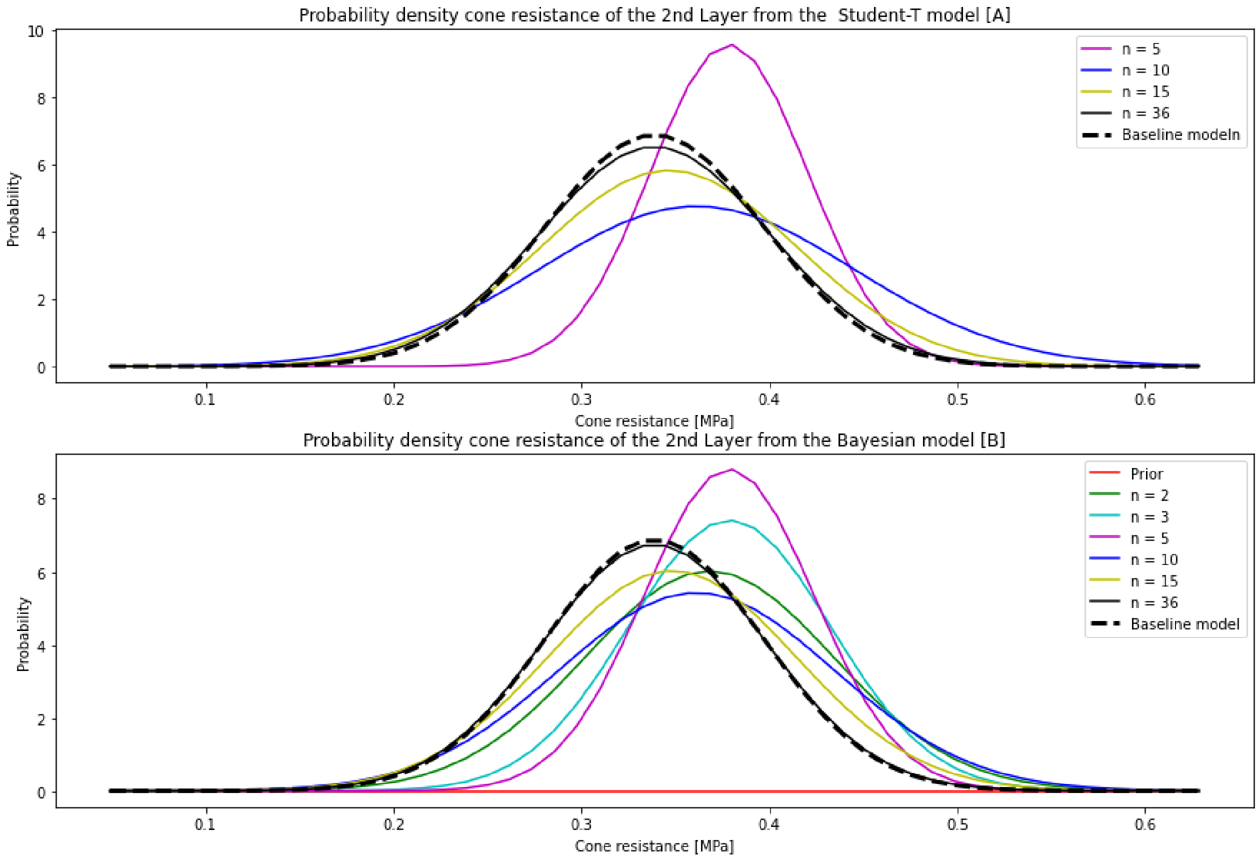

FIGURE 41 - QUANTIFICATION OF THE SHAFT FRICTION IN THE 2ND LAYER

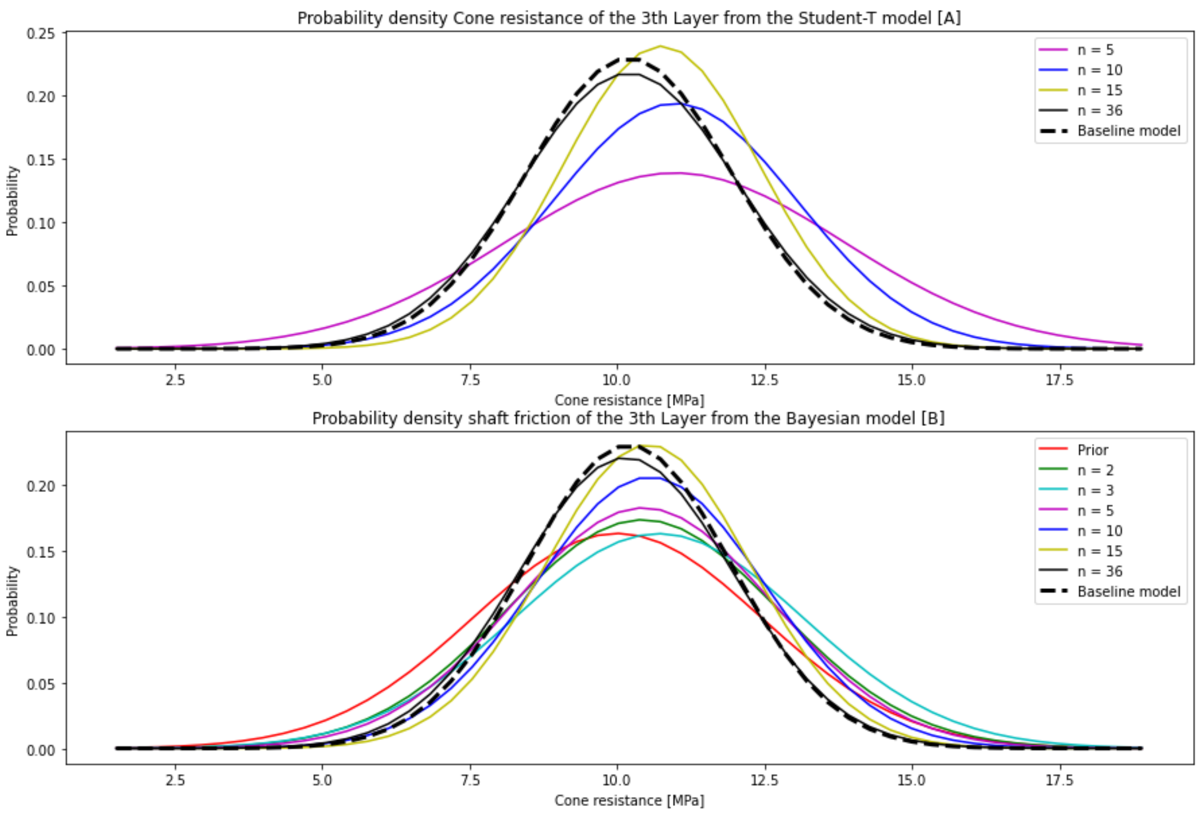

FIGURE 42 - QUANTIFICATION OF THE SHAFT RESISTANCE IN THE 3RD LAYER

APPENDIX 11 - INFLUENCE FACTOR OF THE ISOLATED RESISTANCE MODEL

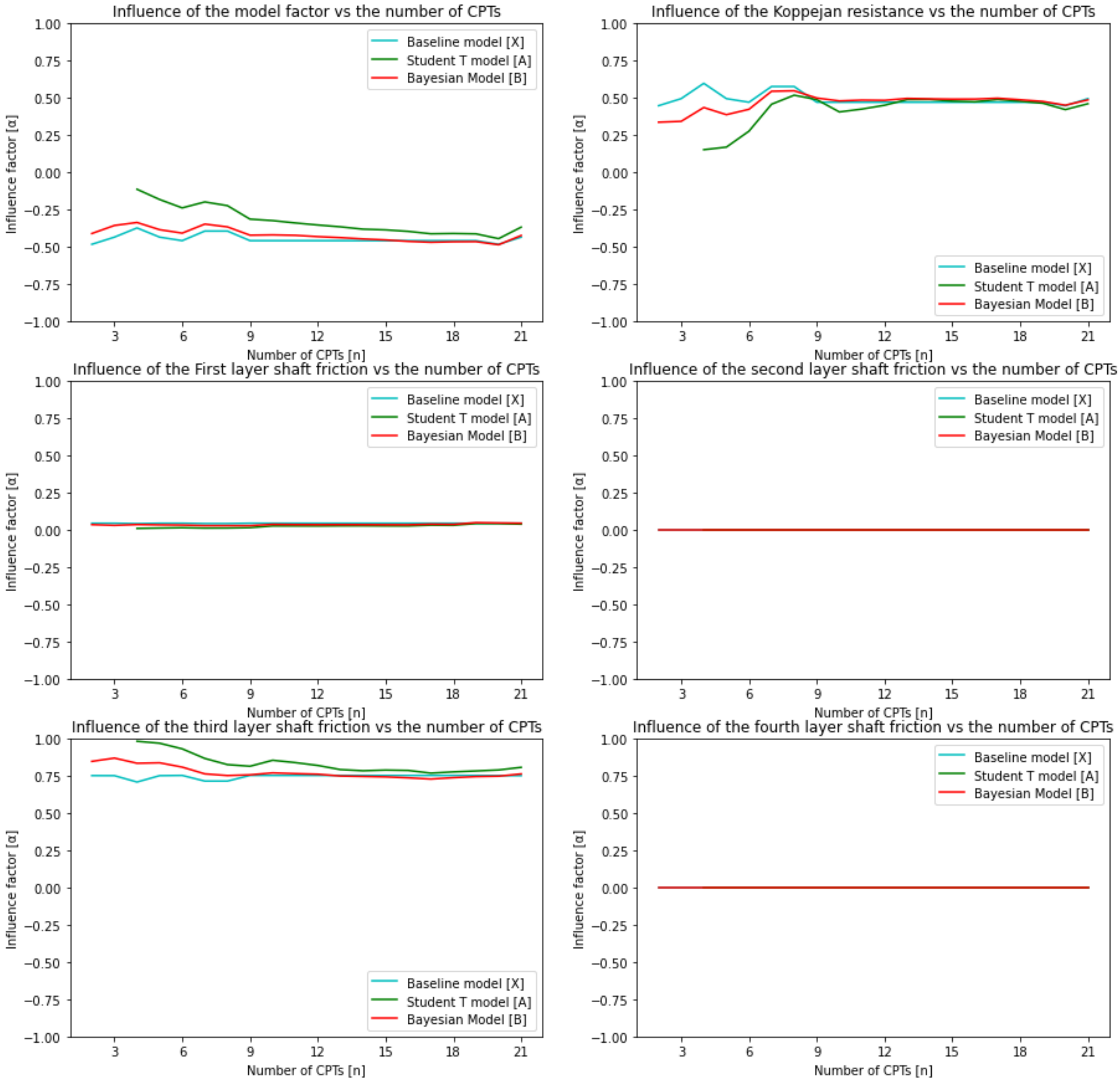

FIGURE 43 - ALPHA OF THE ISOLATED RESISTANCE MODEL